TRANSITIONS BETWEEN CIRCULATION REGIMES: THE ROLE OF TROPICAL HEATING

by

Ralph D. Getzandanner
A Dissertation
Submitted to the
Graduate Faculty
of
George Mason University
In Partial fulfillment of
The Requirements for the Degree
of
Doctor of Philosophy
Climate Dynamics

Committee:

____________________ Dr. David M. Straus, Committee Chair

____________________ Dr. Cristiana Stan, Committee Member

____________________ Dr. Kathleen Pegion, Committee Member

____________________ Dr Jim Kinter, Department Chairperson

____________________ Dr. Donna M. Fox, Associate Dean, Office of Student Affairs & Special Programs, College of Science

____________________ Dr. Ali Andalibi, Interim Dean, College of Science

Date: ____________________ Summer 2019
George Mason University
Fairfax, VA

Transitions Between Circulation Regimes: The Role of Tropical Heating

A dissertation submitted in partial fulfillment of the requirements for the degree of Doctor of Philosophy at George Mason University

By

Ralph D. Getzandanner
Master of Science
Creighton University, 1996
Bachelor of Science
University of South Carolina, 1992

Director: Dr. David M. Straus, Professor
Department of Department of Atmospheric, Oceanic, and Earth Sciences

Summer 2019
George Mason University
Fairfax, VA

Dedication

I dedicate this dissertation to my wife Rose, my sons Justin, Zachery, and Jeremy, my Mom and Dad, and Tom and Buddy who are not able to share this with me.

Acknowledgments

First, and foremost, I would like to thank my advisor Dr. David Straus. During my initial interview to apply for the Climate Dynamics program, I was impressed by his enthusiasm and passion. This along with his expertise in my area of focus, made him an easy choice as an advisor. Being retired and an older student, removed from an academic environment for almost 20 years, I presented quite a challenge. However, during my 5 years in the program, Dr. Straus showed an incredible amount of patience and always had time for even the most trivial questions. I was truly blessed to have had such an advisor and without a doubt would not have been successful in this program without him.

Next, I would like to thank Dr. Cristiana Stan. Being one of the leading scientists in the areas of tropical convection and sub-seasonal forecasting, her expertise was very much in line with the subject areas I wanted to focus my research on. Although I had some background in tropical meteorology, her class on tropical climate and her constructive feedback, aided greatly during the preparation of this dissertation.

I would also like to thank Dr. Kathy Pegion. I got to know Kathy through a class in modeling and found her to be one of those rare individuals who can take complex material and procedures and present them in such a way that allows one to easily apply. I had the pleasure to work with her to teach the introduction to climate lab and ended my coursework with her class on Air Sea Interaction. She always had time to help with any question and provided invaluable advice in the preparation of my thesis. I would also like to thank Dr. Franco Molteni and Dr. Erik Swenson for their insights and advice for this research.

I also thank Dr. Barry Klinger and Dr. Jagadish Shukla, for offering me the opportunity to study at George Mason in the department of Climate Dynamics. Many thanks to all my Professors of Climate Dynamics Program for their support and dedication. I would like to acknowledge Thomas Wakefield for his technical support and Stephanie Oneill for her outstanding administrative support.

A big thanks also goes to my cohort and other fellow students especially Dr. Mark Scafonas, Dr Priyanka Yadav, Dr. Liang Yu, Nick Lybarger, and Teresa Cicerone.

Finally, I would like to thank my family, and especially my wife Rose for her unwavering love and support.

Table of Contents

List of Tables

List of Figures

Abstract

TRANSITIONS BETWEEN CIRCULATION REGIMES: THE ROLE OF TROPICAL HEATING

Ralph D. Getzandanner, PhD

George Mason University, 2019

Dissertation Director: Dr. David M. Straus

Persistent weather patterns are responsible for much of the extreme weather experienced around the world. These persistent patterns have also been found to reoccur over certain regions including the Eastern Pacific, North America, Europe, and the North Atlantic. We term these persistent, reoccurring patterns “circulation regimes”. In this thesis we focus on regimes in the Euro-Atlantic region.

Circulation Regimes provide a single consistent framework to describe large-scale patterns in the Euro-Atlantic (EA) region such as the North Atlantic Oscillation (NAO) and European Blocking. Each individual state of the atmosphere is uniquely associated with one regime, and each regime is accompanied by distinct weather patterns, and likelihoods of extreme events. This thesis focuses on transitions between four EA regimes and precursors of such transitions. We examine the signature of tropical heating preceding transitions between each type of regime transition and identify transitions for which this forcing plays a role. We further examine the relationship of heating to the Madden-Julian Oscillation (MJO), the El-Nino Southern Oscillation, and shifts in the intertropical Convergence Zone (ITCZ). Midlatitude diabatic heating is examined to determine shifts in the storm tracks.

We use the ERA-Interim reanalysis (at full horizontal resolution, 6 hourly) to estimate

the diabatic heating as a residual in the thermodynamic equation. The same reanalysis is used to perform a k-means cluster analysis of 500 hPa geopotential height in the EA region during boreal winter, yielding the regimes of NAO+, NAO-, Scandinavian Blocking and Atlantic Ridge. We composite the vertically integrated, planetary wave diabatic heating, 300 hPa streamfunction, and Rossby wave activity. We find that the effects of Indian Ocean tropical heating are to enhance the transition from the Scandinavian Blocking EA circulation regime to the NAO+ regime, while western Pacific heating seems to force transitions from all other regimes into the NAO- regime. The flux of Rossby wave activity shows that for six transitions, mid-latitudes play a role in forcing the tropical heating. It was also found that six of the 10 transitions examined show indications of being tropically forced. Only four showed evidence that mid-latitude dynamics were the primary cause to the transition.

Only four of the transitions appeared to be related to phases of the MJO. In fact, intensification of eastern equatorial Pacific and equatorial Atlantic heating (intensification of the ITCZ) plays a role in some transitions. The role of the El-Nino Southern Oscillation is found to be only a modest factor.

Chapter 1: Introduction

Heat waves, cold snaps, rainy or snowy periods, prolonged dry periods, and even long periods of pleasant weather conditions are all the result of persistent weather patterns. These types of weather patterns are not only persistent but tend to reoccur over the same regions and can happen at any time of year and can have a dramatic impact on human and economic activity. It would be beneficial to know in advance when these recurrent, persistent patterns will occur and if occurring when these patterns will change. When we are able to identify a clear change from one persistent weather pattern to another persistent weather pattern, we refer to this change as a transition. Persistent weather patterns are embedded in particular large-scale circulation patterns, in which characteristic pressure and wind patterns steer the movement of individual weather systems. Such circulation patterns are often referred to as circulation regimes. The transitions between one persistent weather pattern to another is thus the result of a transition between one circulation regime and another. Such transitions are the subject of this thesis.

1.1 Broad Overview of Circulation Regimes

Weather and Climate in the mid-latitudes are in large part the result of transitory weather systems that can be classified into short time scale individual synoptic weather features and lower frequency large scale patterns. Low frequency patterns, which also tend be persistent, have been identified throughout the globe. Walker and Bliss (1932) were one of the first to identify correlations between pressure or geopotential heights of widely geographical separated points. Namias (1950) looked at the the configuration of large scale atmospheric flow and introduced an index that measured the degree of zonal or blocked flow in the atmoshere. Rex (1950), specifically looked at atmospheric blocking and was one of the first to describe what we now term as regimes. Weather patterns or the grosswetterlagen (German for large-scale weather pattern) have been used for many years by the German Weather Service (Straus et al., 2017) and are described by Baur (1951). A similar catalog of European weather patterns has been used by the US Air Force weather service since the 1980's. Wallace and Gutzler (1981) added to the work of Rex, futher compiling and refining relationships between seperate locations, known as teleconnections. They also presented circulation patterns based on these teleconnections. A more comprehensive review of the Northern Hemisphere circulation patterns was done by F. Panagiotopoulos et al. (2002). These patterns have been found to be associated with certain weather conditions over broad areas. Operational weather forecasters have long been aware of certain synoptic scale patterns that resulted in particular types of weather and may reoccur over a period of a week or longer. An extensive review of regime behavior is given by Hannachi et al. (2017).

Ghil and Robertson (2002) hereafter GR, put the preferred patterns and teleconnections into a broader framework. They describe two types of low frequency variability that affect the mid-latitude atmosphere. They are Planetary Flow Regimes and Intraseasonal Oscillations. Planetary Flow Regimes, referred to as "particles" by GR, are thought of as preferred patterns or regimes that have been identified on both hemispheric and regional scales. The Intraseasonal Oscillations ("waves") are periodic oscillations of the entire northern extratropical circulation that have been identified by statistical techniques, as described by Ghil and Robertson. Dynamical model results suggest that periodic solutions of simplified models (with relatively few degrees of freedom) become unstable when more waves are added to the model, but that the resulting chaotic circulation sill hovers about the original (now unstable) solution (Itoh and Kimoto, 1996).

Regimes can be useful for prediction given their persistence, (Plaut and Simonnet, 2001; Franzke et al., 2011; Straus et al., 2017), and many others, and can provide an empirical set of weather conditions to be expected when a region is being influenced by a particular regime, e.g. Cassou (2010) and Amini and Straus (2018). Understanding the dynamics involved in the development and transition of regimes is paramount in terms of their prediction and would give an understanding of the atmospheric conditions that favor a change in the planetary wave pattern. Of course, the ultimate objective would be to accurately predict a transition from one regime to another though a forecast model, an ensemble of an individual model or a collection of models.

The identification of circulation regimes via cluster analysis has been achieved in the Northern Hemisphere (Molteni et al., 1990; Kimoto and Ghil, 1993; Hannachi et al., 2017), the Pacific North American region, (Robertson and Ghil, 1999; Straus et al., 2007; Amini and Straus, 2018), and the Euro-Atlantic region, (Vautard, 1990; Plaut and Simonnet, 2001; Cassou, 2008; Straus et al., 2017). The Euro-Atlantic regimes (shown in Figure 1.1), which are of particular concern here, are often described as two phases of the North Atlantic Oscillation (NAO+, NAO-), the Scandinavian Block (SB) and the Atlantic Ridge (AR).

Since transitions between the Euro-Atlantic regimes are associated with changes in predominant weather types, they are of some importance. Transitions were addressed by Vautard (1990). Three preferred regime transitions were found: These were (in terms of our terminology) the NAO+ to Scandinavian Block, the Scandinavian Block to NAO- and NAO+ to Atlantic Ridge. Cassou (2008) also found the NAO+ to Scandinavian Block and Scandinavian Block to NAO- are preferred.

1.2 Introduction to Diabatic Heating

In the atmosphere, there are two types of heating. The first is adiabatic heating or cooling which in simple terms is due to the expansion and compression of air as it moves vertically in the atmosphere and does not exchange heat with its surroundings. Diabatic heating results when air does lose or gain heat. It is the result of many different processes which include shortwave radiation from the sun, longwave radiation emitted and absorbed by the atmosphere by clouds and aerosols like dust or pollution, heat released to the atmosphere by condensation (latent heat release), heating due to conduction of underlying surfaces such as the ocean or land, and turbulent mixing of the air by horizontal and vertical wind differences. A more technical definition of diabatic heating states that the rate of diabatic heating is proportional to the rate of change in the entropy of a parcel of air. Entropy is defined as $c_p ln\theta$, where c_p represents the specific heat of air at a constant pressure and θ represents potential temperature. We will explore diabatic heating and how it is estimated in more detail in chapter 2.

In this research, we consider diabatic heating from two different regions. We consider tropical diabatic heating which occurs near the equator between 30 degrees North and South. Sources of tropical diabatic heating are dominated by latent heat release taking place as rain showers and thunderstorms also known as convection. Convection may be associated with the Madden Julian Oscilliation (Madden and Julian, 1971), areas of tropical convergence such as the Intertropical Convergence Zone (ITCZ) and South Pacific Convergence Zone, and convection associated with displaced warm water during the El Nino and Southern Oscillation (ENSO). Air from the mid-latitudes moving into the tropics can also cause instability which in turn can lead to tropical convection and diabatic heating. Because much of the heating is latent heat released in the mid and upper troposphere, it can have an effect over large distances. In assessing the role of tropical diabatic heating on mid-latitude regimes, we refer to this heating as external or remote.

The second area of consideration for diabatic heating is in the mid-latitudes and is mostly found over the North Pacific and North Atlantic. The two main processes responsible for this heating are interaction between air and sea, and mixing and latent heating caused by small scale and high frequency disturbances, also known as eddies, that occur along the storm track. This heating is found mostly in the lower portion of the troposphere. Mid-latitude diabatic heating is an integral part of the storm tracks, and in this thesis we interpret it as an indicator of the storm tracks.

1.3 Influence of Tropical Heating

While much of the previous literature on the dynamics of regimes and their transitions has focused on mid-latitude processes (Charney and DeVore, 1979; Charney and Straus, 1980; Ghil and Mo, 1991; Itoh and Kimoto, 1996; Franzke et al., 2004; Luo and Cha, 2012; Messori et al., 2019), there is also a clear interaction between tropical diabatic heating and the circulation regimes. On seasonal to interannual time scales the heating associated with the El-Nino Southern Oscillation strongly affects the regimes in the Pacific North American region (Straus and Molteni, 2004; Straus et al., 2007). On intra-seasonal time scales, the regimes in the Euro-Atlantic sector (shown in Figure 1.1) respond to tropical heating, although this has been investigated almost exclusively in the somewhat limited context of the Madden-Julian Oscillation (Madden and Julian, 1971; Zhang, 2005; Cassou, 2008). This oscillation (referred to as the MJO), is an envelope of eastward propagating convection originating from the Indian Ocean and reaching the central Pacific with a lifecycle spanning very roughly 30 to 80 days. The MJO explains roughly 25% of the tropical variance in circulation and heating (Wheeler and Hendon, 2004). Changes in the likelihood of occurrence of regimes in the Euro-Atlantic region have been attributed to (and follow in time) the tropical diabatic heating associated with different phases of the MJO in observational and modeling studies (Cassou, 2008; Lin et al., 2009; Straus et al., 2015; Yadav and Straus, 2017; Yadav et al., 2019). But the interaction also may go the other way, with two of the circulation regimes (NAO+ and NAO-) associated with subsequent MJO phases (Lin et al., 2009), implying a mid-latitude forcing of the MJO heating.

To the extent that tropical diabatic heating in general is the physical cause of changes in the probability of occurrence of circulation regimes, this heating must affect the transition paths between regimes. This suggests that focusing on the evolution of transitions between circulation regimes, and an assessment of the diabatic heating (both tropical and extra-tropical) that precedes and interacts with these transitions, may provide a more complete picture of the full role of diabatic heating. In this study we pursue such an investigation.

1.4 Regimes in the Euro-Atlantic Region

The focus of this research covers the North Atlantic and European Region (EA) and considers regimes occurring over the domain (30-80N 100W-30E). These regimes tend to occur in conjunction with other regimes. For instance, the four Euro-Atlantic Regimes are closely related to Eddy Jet Regimes identified by Woollings et al. (2010). They also frequently occur concurrently with Regimes in the Pacific/North American regions (Straus et al., 2007; Baxter and Nigam, 2013).

Regimes in the geopotential height surfaces have been identified in the Euro-Atlantic region from reanalysis and modeling studies by (Vautard, 1990; Michelangeli et al., 1995; Cassou, 2008, 2010; Straus et al., 2015; Yadav and Straus, 2017; Yadav et al., 2019), and others. A common method for identifying these regimes is referred to as the k-means clustering method (Michelangeli et al., 1995; Straus and Molteni, 2004; Straus et al., 2017), and is described later in th:is paper. A property of this approach is that every state is assigned to one of the four regimes whose characteristic patterns are seen in Figure 1.1. The EA regimes are well established in the previously cited works, and persist longer than the typical period of baroclinic transients.

The first two regimes are highly correlated to the positive and negative phases of the well known North Atlantic Oscillation teleconnection patterns. The NAO+ is characterized by negative height anomalies centered between Greenland and Northern Europe and can be thought of as a strengthening of the semi-permanent Icelandic Low. The NAO- regime has above normal height anomalies between the North American Maritimes and Greenland with a southward shift of the North Atlantic storm track and below normal heights over the Central Atlantic and Western Europe.

The last two regimes are the Atlantic Ridge, which exhibits above normal height anomalies across the entire North Atlantic and the Scandinavian Blocking which is characterized by a positive height anomaly centered over the Scandinavian region of Northern Europe. It should be noted that the NAO teleconnection pattern is often based on an index which is

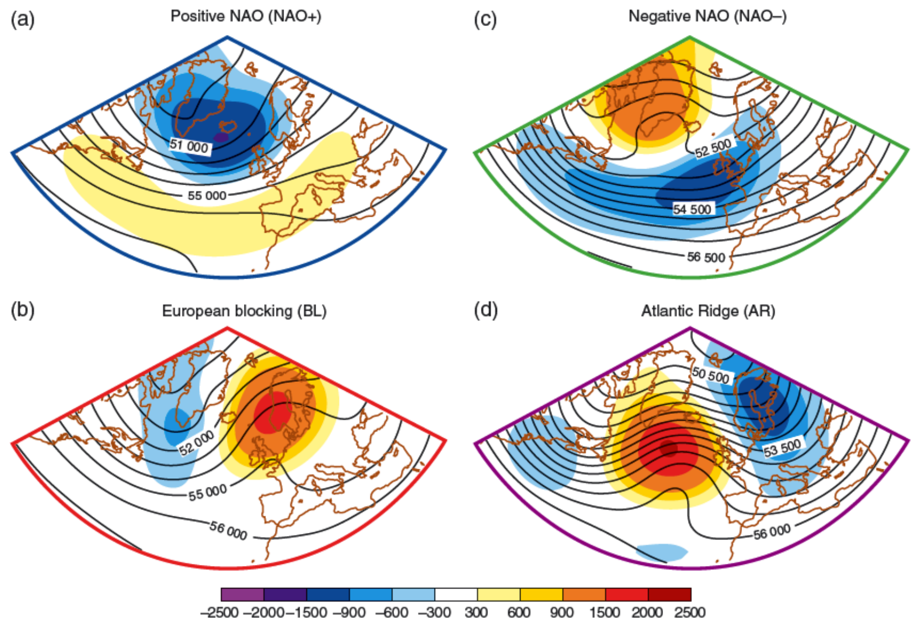

Figure 1.1: Euro-Atlantic Regimes at 500hPa (Ferranti et al., 2015), shown are geopotential anomalies (color shading) and geopotential (contours) in ms^{-2}. Note, the regime labeled European blocking is the same as Scandinavian blocking regime in this research.

simply the sea level pressure difference between a point in the vicinity of the Subtropical High centered near the Azores and a point near the Subpolar Low in the area near Iceland (Walker and Bliss, 1932). Because the points do not change, there is, by definition, a symmetry between the two. As mentioned in the previous paragraph, the NAO+/NAO- regimes are similar to the NAO index patterns but are determined at the 500hPa level and do not show the same symmetry (see Figure 1.1).

Some of the weather associated with each regime is as follows (Cassou, 2008):

- NAO- Below normal temperatures Eastern N. America, Northern Europe. Above normal precipitation over Europe (e.g. Winter of 2009/2010).
- NAO+ Above normal temperatures. Extreme precipitation events possible
- Atlantic Ridge Possible cold outbreaks over the Iberian Peninsula.

- Scandinavian Blocking Dry conditions over Northern Europe. Above normal Precipitation along the Mediterranean coast of Spain.

Each of the Euro-Atlantic Regimes can be associated with extreme weather conditions. This is shown in term of minimum temperature and rainfall in Figure 1.2 which uses station data of temperature and precipitation to relate weather to Euro-Atlantic regimes..

Vautard (1990) using similar Euro-Atlantic regimes, except on a 700hPa surface, found three preferred regime transitions. These were the Zonal (NAO+) to Blocking (Scandinavian Block), Blocking to Greenland Block (NAO-) and Zonal (NAO+) to Atlantic Ridge. Cassou (2008) also found the NAO+ to Scandinavian Block and Scandinavian Block to NAO- are preferred. They also determined that some of these transitions were related to phases of the MJO.

1.4.1 The Role of Mid-latitude Dynamics

Since it is natural to seek local causes for the formation of circulation regimes and their transitions, many studies have examined the role of mid-latitude dynamics in this context. That the changing configuration of mid-latitude waves and jet streams are the primary cause of regime transitons constitutes a null hypothesis, against which the role of remote tropical heating may be compared.

The midlatitude forcing of the NAO teleconnection pattern has been studied extensively (see review of Song (2016)) with several variations in approach. One school of thought is that the eddies play a dominant role in the forcing and maintenance of the NAO. In particular, transient eddy vorticity forcing (Barnes and Hartmann, 2010), and Rossby wave breaking (Franzke et al., 2004; Rivière and Orlanski, 2007; Michel and Rivière, 2011) are important. Both wave breaking and vorticity forcing are related to the poleward flux of zonal momentum, and their forcing of circulation changes underlies the role of changing intensity and position of the storm tracks.

Another school of though posits that NAO development is a response to the pre-existing configuration of eddies. Song (2016) found that the phase speed of the eddies leads to the

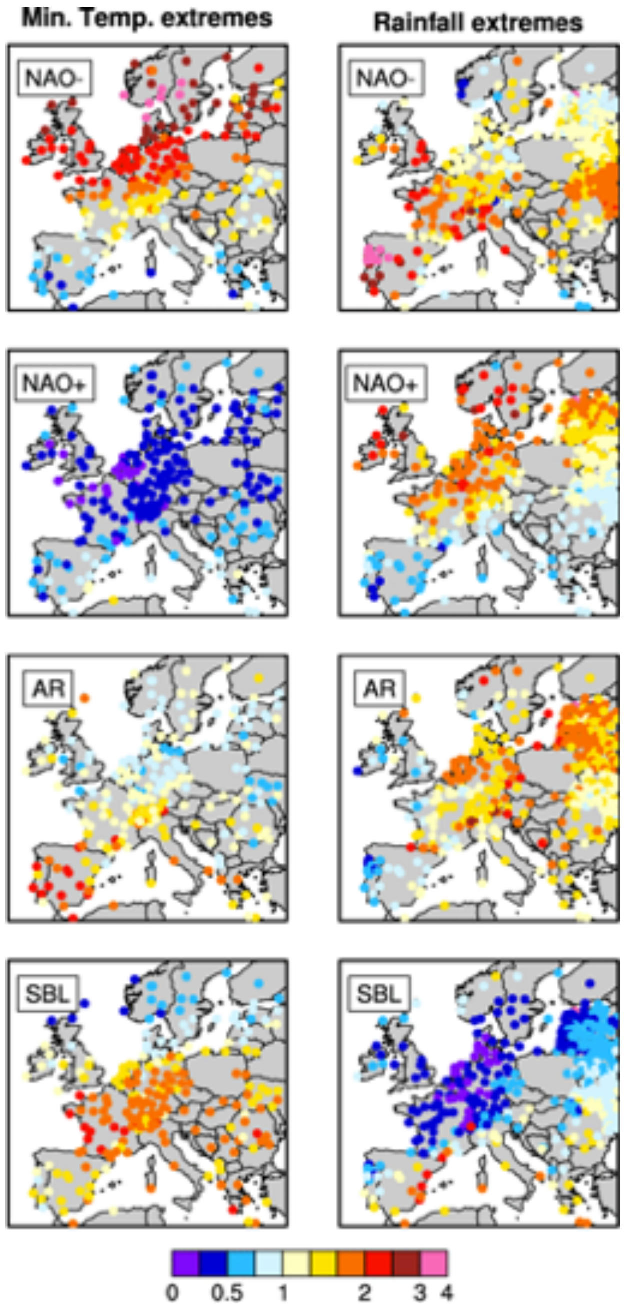

Figure 1.2: Shown are the relative changes during each of the four boreal winter Euro-Atlantic regimes based on data from the European Climate Assessment dataset. The maps on the left are the frequency of extreme cold days and the maps on the right are are the frequency of extreme wet days. The values are significant at the 95 percent level for each station (dots). The blue shades represent a low chance of extreme low temperature or rainfall. The orange and red shades represent increased probability of occurrence. A value of 0 means there is no chance of the extreme to occur. A value of 2 or 3 indicates that there is double or triple the chance of the extreme to occur from Cassou (2008).

development of the NAO (faster phase speed leads to NAO+), and that the eddy vorticity forcing from high and low frequency eddies act differently.

Atmospheric blocking accounts for two of our four Euro-Atlantic regimes, NAO- and Scandinavian Block. Because of the processes involved in the life-cycle of blocking and its inherent persistence and relationship to extreme weather, it is one of the more studied atmospheric phenomena (Molteni et al., 1990; Rex, 1950; Nakamura et al., 1997; Michelangeli and Vautard, 1998). A good review of blocking is provided by Huang et al. (2007). Rex (1950) was one of the first to identify blocking and defined it as a dipole pattern associated with the breakdown in the prevailing westerly flow at midlatitudes, often associated with a split in the zonal jet and with a persistent high pressure ridge typically poleward of the jet stream. As with the NAO, the role of transient eddy forcing is very prominent (Nakamura et al., 1997). The strength of the background mean westerly wind is of great importance to the life cycle of blocking with weak flow aiding the maintenance and strong flow leading to its destruction (Huang et al., 2007). Studies of the decay of blocking focus on energy conversions (Ma and San Liang, 2017) and the role of the decay of blocking in forcing the stratospheric circulation has been discussed by Attard and Lang (2019). Much of the previously quoted work on blocking addresses local blocking patterns following a large number of blocking definitions (Nakamura et al., 1997; Michelangeli and Vautard, 1998; Straus and Molteni, 2004; Huang et al., 2007; Henderson et al., 2016; Ma and San Liang, 2017; Henderson and Maloney, 2018; Attard and Lang, 2019) . Little work has been done specifically in the context of the Atlantic Ridge and Scandinavian blocking regimes.

1.4.2 The Role of Tropical Forcing

The role of forcing of the Euro-Atlantic regimes by tropical diabatic heating has more recently been considered as an alternative to the local mid-latitude dynamics hypothesis described in the previous section. In this point of view, mid-latitude dynamics is still important but changes are ultimately a response to tropical heating.

Many have suggested a link between the mid-latitudes and the MJO. Figure 1.3 from

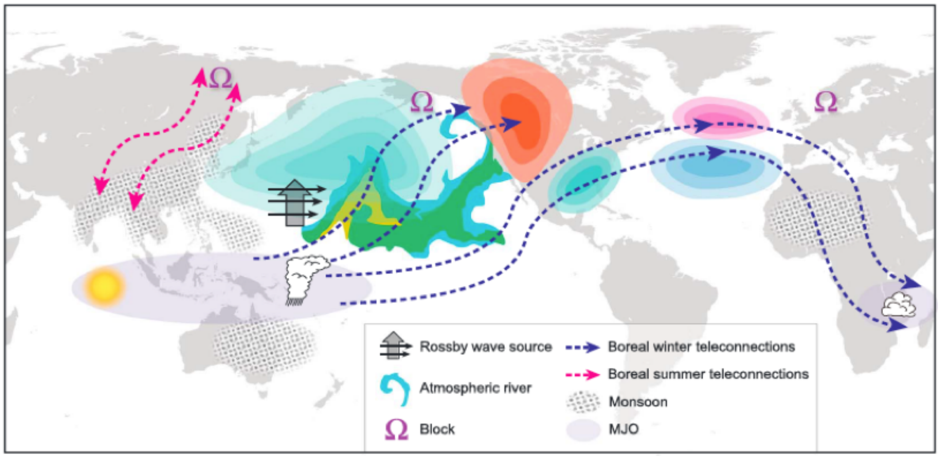

Figure 1.3: Shows the interaction of tropical and Northern Hemisphere interactions. Green and blue areas represent atmospheric rivers, the omegas represent areas of blocking patterns, and the grey shaded areas with the cloud symbol in the Indian and W. Pacific Ocean is a representation of the MJO (Stan et al., 2017)

Stan et al. (2017) provides a general depiction of some of the interactions between the tropics and the mid-latitudes. The schematic shows how the convection associated with the MJO in the W. Pacific Ocean can help generate a Rossby Wave source (Sardeshmukh and Hoskins, 1988) which in turn can affect variability in the mid-latitudes. The figure also shows how, in the case of the NAO, mid-latitude energy fluxes can intrude into the tropics by creating instability and forcing circulations and convection in those regions (Stan et al., 2017).

In terms of the response of the Euro-Atlantic circulation more specifically to the MJO, Lin et al. (2009) studied the relationship between the MJO and the NAO patterns as defined by an emperical orthogonal function analysis, (not to be confused with the NAO+ and NAO- regimes.) They found that significant increases of the occurrence of the NAO+ often occur 5 to 15 days after MJO-related enhanced convection in the Indian Ocean and a decrease when it is not present. They also found a decrease in the index 5-15 days after the MJO convection reaches the tropical central Pacific.

It has also been established by Cassou (2008) that a relationship exists between the MJO and Euro-Atlantic regimes. In this paper, MJO phases are defined as the 8 phases identified by Wheeler and Hendon (2004). It was found by Cassou (2008) that the NAO+ is more likely following phase 2 and 3 (convection over the Indian Ocean) and that the Scandinavian Blocking is more likely at short lags following Phase 6 (convection over the western and central Pacific). He suggests that the NAO- may not be directly related to the MJO but may be more a consequence of the preferred transition sequence of NAO+ to Scandinavian Block and then to NAO- following phase 6 and 7. Yadav and Straus (2017) took the research by Cassou (2008) further and found that there were fast and slow modes of the MJO and that the relationship between the Euro-Atlantic regimes depended on the speed of the oscillation. They define fast episodes as those taking 10 days or less to propagate from the Indian Ocean to the Western Pacific (MJO phase 6) and the slow episodes taking 20 days or more to reach phase 6. They also found that the NAO+ and the NAO- response was greater during slow episodes.

In terms of blocking, Henderson and Maloney (2018) show that high-latitude blocking was related to the MJO. Baxter and Nigam (2013) determined that the Pacific North American pattern (PNA) interacts with the MJO. They found that the NAO led the PNA of the opposite sign. The PNA pattern is defined by an index similar to the NAO but found over the Pacific and North America. It's positive phase is characterized by above normal height anomalies over western North America and below normal heights in southeastern North America with the negative phase being the opposite (Wallace and Gutzler, 1981). Baxter and Nigam (2013) used an analysis of the simple barotropic vorticity equation to show how the NAO may be forcing the PNA. They found that the total advection term shows the vorticity forcing from the NAO results in both westward propagation of the longwave pattern across North America and in energy propagation to the Arabian Peninsula and through southern and eastern Asia, culminating in the Pacific.

1.5 Goals

As a forecaster, it would be useful to have a general model that would indicate when a change in regime might occur. As shown in the introduction, many have found a relationship between tropical diabatic heating, mainly in the form of the MJO, and the onset of regimes in the Euro-Atlantic domain. Relating remote tropical heating to regime transitions has the added benefit of potentially extending the limit of predictably. Therefore the role of tropical heating needs to be examined in the framework of regime transitions. This research seeks to develop a comprehensive framework of regime transitions in order to systematically determine their association with tropical heating.

In other words we seek to better quantify the influence tropical forcing and mid-latitude dynamics have on Euro-Atlantic regimes prior to transitions and also to examine if the transitions have any effect on initiating convection in the tropics. We assume that all transitions are related to mid-latitude dynamics, but seek to quantify those that are also related to tropical heating. We also explore the possibility that mid-latitude dynamics may be involved in influencing the tropical heating.

By using composites prior to each regime transition of diabatic heating, circulation (streamfunction), and Rossby wave activity we seek to:

1. Assess which transitions are related to tropical heating, including the location of the heating.

2. Assess the role of MJO tropical heating vs. non-MJO related tropical heating.

3. Assess whether the regime themselves or their transitions play a role in stimulating tropical heating.

Chapter 2: Data and Methods

2.1 How Are Regimes Identified?

Regimes are identified by cluster analysis (k-means method) applied to 500hPa height fields (Z500) for boreal winter. The k-means clustering is a method to take the set of states in a reduced dimensional phase space and cluster these states around k centroids. The algorithm iteratively re-positions the centroids until the following variance ratio R is maximized: R is the ratio between the variance of the cluster centroids (weighted by the cluster population) divided by the sum of the Euclidean squared distance between each state and the centroid to which is assigned. See Michelangeli et al. (1995) and Straus et al. (2007), as well as the Appendix, in which the method of assessing statistical significance is given.

In order to apply the cluster analysis to boreal winter fields of Z500, the following steps are taken: The data is filtered using 5-day running means to remove the most rapidly evolving synoptic systems. The seasonal cycle is estimated by fitting the evolution of Z500 at each grid point with a parabola in time, followed by an average of the parabola over all years considered (Straus, 1983). (We will consistently refer to the 5-day running means as days, with the understanding that each day refers to the middle day of a running 5-day mean.) Following this, a principle component analysis is applied to the un-normalized data. The resulting variates (principal component time series) form the coordinates in an N-dimensional phase space, where N is the number of modes retained. N is chosen to capture about 80 percent of the spacetime variance, which led to a choice of N =12.

The k-means clustering method is one of a class of partitioning methods in which all states (days) are assigned to a unique cluster. Since k must be chosen a priori, there is some ambiguity in its choice. We limit the choice of k by requiring a high degree of significance (see Appendix A), but yet low enough to provide robust statistics. The choice of k=4 is consistent with much previous literature, for example Cassou (2008) and Ferranti and Corti (2011).

Two data sets were used to analyze and evaluate. The two are obtained from reanalysis covering different periods.

The first set of analyses used the European Centre for Medium-Range Weather Forecasts (ERA-Interim, hereafter ERAI) reanalysis (Dee et al., 2011) for the 35 boreal winters of 1980/81 through 2014/15. The winter season was defined as the 132 days starting from 16 November.

The second set was compiled from the National Centers for Environmental Prediction Reanalysis data set (hereafter NCEP) for the 63 boreal winters of 1948/49 to 2010/11. The definition of winter (132 days commencing 16 November) is the same as for ERAI.

2.2 How Are Regime Transitions Defined?

In order to provide consistent results, we must establish a systematic set of rules to determine when a transition has occurred. It is also important that we consider only those transitions that are highly correlated with the regimes and are persistent enough to provide reliable results.

The criterion used by the k-means algorithm for assigning a state to a particular cluster (regime) is based on Euclidian distance in PC-space, corresponding to mean-squared error. In order to focus on states closest to the cluster centroid, we focus only on those states whose pattern correlation with the regime centroid is high. (Pattern correlation corresponds to angular distance in PC-space.)

The specific method used for determining regime transitions is based on persistence of the regime and the pattern correlations between states prior to the transition to the regime centroid to which they are assigned. Regime transitions in this research are defined using the following criteria referring to Figure 2.1. The prior regime must persist for at least 5 days and be correlated to the centroid by a predetermined correlation coefficient threshold

<table>
<tr><td colspan="11">Daily regime index is found by taking the observed regime index over a 5-day period centered on the day (it)</td></tr>
<tr><td>it-5</td><td>it-4</td><td>it-3</td><td>it-2</td><td>it-1</td><td>it</td><td>it+1</td><td>it+2</td><td>it+3</td><td>it+4</td><td>it+5</td></tr>
<tr><td>old regime</td><td>old regime</td><td>old regime</td><td>old regime</td><td>old regime</td><td>*transiton</td><td>new regime</td><td>new regime</td><td>new regime</td><td>new regime</td><td>new regime</td></tr>
<tr><td colspan="5">Pattern correlation of each old regime day > cor* (*cor is a predetermined pattern correlation ranging from 0.0 to 0.6)</td><td>*regime index is in new regime</td><td colspan="5">Any correlation as long as index is in new regime</td></tr>
<tr><td colspan="11">The variable composites (i.e. velocity potential) are taken from daily data and averaged over the period. In the example of 1 to 5 days prior to the transition, the average is calculated taking the sum of the variable from it-1 to it-5 and dividing the sum by 5.</td></tr>
</table>

Figure 2.1: Rules used in this research to determine regime transitions The prior regime must persist for at least 5 days (green boxes) and be correlated to the centroid by a predetermined correlation coefficient threshold ranging from 0.0 to 0.6. Transition occurs over a 1-day period (red box). Once a transition has occurred and the atmosphere is in a new regime, it must persist in that regime for at least 5 days (blue boxes)

.

ranging from 0.0 to 0.6 (green boxes). Most of results we will present meet a threshold of 0.4 or greater. Once a transition has occurred and the atmosphere is in a new regime (red box), it must persist in that regime for at least 5 days (blue boxes). Note that we have not put a requirement on the pattern correlation threshold for the new regime; we have verified that a requirement of 0.4 pattern correlation with the new centroid for the first five days of the new regime does not markedly reduce the number of transitions considered.

Although the requirement is for the previous regime to have a threshold correlation with the cluster centroid for five days, the actual average correlation for that period is higher than the minimum threshold. (For a threshold of 0.4, the average correlation is over 0.6 usually.)

This method of identifying regime transitions focuses on states which correspond fairly closely to one of the patterns shown in Figure 1.1, and so would be readily identified by a forecaster. Even though we will take composites of heating and streamfunction as far as 20 days prior to the transition in the following sections, we do not insist that the system be in a single regime for the entire time span as this would drastically reduce the number of transition episodes and so severely restrict significance.

2.3 How Do We Estimate Diabatic Heating?

The diabatic heating is estimated from four times daily circulation and thermodynamic fields from the ERAI reanalysis at full horizontal resolution (512 × 256 Gaussian grid) and at 37 pressure levels, using a residual method similar to that of Hagos et al. (2010). Specifically the heating rate Q is obtained from:

$$c_p \frac{1}{\Pi} \left(\frac{\partial \theta}{\partial t} + \vec{\nabla} \cdot (\vec{v}\theta) - \theta(\vec{\nabla} \cdot \vec{v}) + \omega \frac{\partial \theta}{\partial p} \right) = Q \tag{2.1}$$

Here θ is potential temperature, p is pressure, $\omega = dp/dt$, c_p the specific heat at constant pressure, $\vec{v}$ the horizontal velocity, and $\Pi = \left(\frac{p}{p_0}\right)^{R/c_p}$ is the Exner function, where $p_0 = 1000$ hPa and R is the gas constant. The heating was vertically integrated over the atmospheric column from 1000 hPa to 50 hPa. In order to focus on the large-scale component of diabatic heating, the vertically integrated heating is filtered to retain only zonal waves 0-3. This planetary wave heating is denoted by PW.

2.4 Composites of Diabatic Heating and Streamfunction Preceding the Regime Transitions

In order to determine the change in diabatic heating prior to a regime transition from regime A to regime B, the difference between the vertically integrated, PW diabatic heating (hereafter referred to as simply the heating) averaged over the period 1-5 days prior to the transition, and the climatological mean of the heating in regime A, is formed. This difference is a type of anomaly, but taken with respect to the average conditions in regime A. Thus, if the transition in question on the pentad starting on day d is from Scandinavian Blocking to NAO-, the difference formed is the heating averaged 1-5 days prior to the transition, minus the average of Scandinavian Blocking heating over the whole record. This procedure is repeated for the periods 6-10 days prior to the transition, 11-15 days prior to the transition, and 16-20 days prior to the transition. It may happen that for the larger leads (e.g. 16-20 days), the system might be in a regime other than Scandinavian Blocking in the example. For clarity we also show the anomaly of PW heating in the regime being transitioned from, where the anomaly is constructed with respect to the climatological heating.

Anomalies of the streamfunction at 300 hPa are also presented in exactly the same format, as anomalies from the current regime, and as anomalies from climatology. We compute the flux of Rossby wave activity associated with the first type of anomaly, based on the formulation of Takaya and Nakamura (2001) in order to assess the mutual influence of the tropics and extratropics through wave propagation.

2.5 Assignment of MJO Phases Prior to Transitions

We compute the average of the MJO indices (RMM1 and RMM2) for each of the 5-day periods prior to a transition (1-5 days, 6-10 days, 11-15 days, 16-20 days). These indices are taken from the Australian Bureau of Meteorology Website (`http://www.bom.gov.au/climate/mjo/graphics/rmm.74toRealtime.txt`), and correspond to the leading two principal components of combined outgoing long-wave radiation and zonal winds at 850 and 200 hPa, following Wheeler and Hendon (2004). An average value of RMM1 and RMM2 was determined for each 5-day period, and from that the average amplitude and phase of the MJO computed. Then for each regime transition we construct a histogram of the frequency of occurrence of each phase prior to a particular regime transition.

2.6 Determination of Warm and Cold ENSO Events

The determination of warm and cold event is taken from the Nino 3.4 anomalies of sea surface temperature (SST). This index represents SST anomalies near the equator ($5^o N$ to $5^o S$) from near the dateline ($170^o W$ to $120^o W$) and is widely considered the area of the Eastern Pacific that determines if a warm or cold event is occurring. The index was taken from the HadlSST1 dataset (Rayner et al., 2003) `https://www.esrl.noaa.gov/psd/gcos_` wgsp/Timeseries/Data/nino34.long.anom.data. We consider values of -1.0 or less to be moderate cold events and +1.0 or greater, to be moderate warm events. Values in between are considered neutral. Strong warm (cold) events are associated with a value of the index greater than +1.5 (less than -1.5).

Chapter 3: Results

3.1 What are the Regimes and How Often Do They Occur?

The results of the k-means cluster analysis for 500 hPa geopotential height (for four cluster) in EA region are shown in Figure 3.1 for both ERA-Interim and the NCEP-Reanalysis. The figure shows the composites of the height field for all days assigned to a particular regime. Table 3.1 shows the percentage of occurrence of each regime, where a regime is assigned to each day based on the least mean square distance to the centroid of one of the four regimes. In the ERA-Interim database the most frequent regime is NAO+ at 33.77 percent followed by Scandinavian Blocking 23.75 percent, Atlantic Ridge 22.97 percent, and finally NAO- at 19.51 percent. The percent of occurrences are consistent with Cassou (2008), Ferranti et al. (2015), Swenson and Straus (2017), and others. It should be noted that these percentages can vary widely from winter to winter as seen in Table 3.4. For example, there were 9 winters when the NAO- occurred 10 days or less and 6 winters when it did not occur at all. The widely varying regime occurrences can also mean there are less opportunities for certain transitions. Looking at the winter of 1999-2000, the Scandinavian Block regime did not occur at all and the NAO- regime only occurred 5 times, meaning all the transitions that winter were between the NAO+ and Atlantic Ridge.

Looking at the total number of regime events during El-Nino (warm) and La-Nina (cold) winters (based on the Nino3.4 index) there does not appear to be a strong relationship of one regime versus another (see tables 3.1 and 3.2 and Table 3.4). However, we see that during very strong and strong El Nino events, the NAO- occurs less often. For example, during the very strong 1982/83 and the strong 1991/92 El Nino events, there were no occurrences of NAO-. During the 1997/98 warn event, NAO- occurred less that the other 3 events. La Nina or cold ENSO events do not seem to have a preferred regime pattern although Table

Table 3.1: Statistics for each of the four Euro-Atlantic regimes. The percentage of the total Winter days along with the mean number of days for each winter. The bottom two rows are for the variance and standard deviation. In the ERA-Interim database the most frequent regime is NAO+ at 33.77 percent followed by Scandinavian Blocking 23.75 percent, Atlantic Ridge 22.97 percent, and finally NAO- at 19.51 percent. The percent of occurrences are consistent with (Cassou, 2008; Ferranti et al., 2015; Swenson and Straus, 2017), and others.

	Scan Block	**Atl Rdg**	**NAO-**	**NAO+**
% of Occurrence	23.75%	22.97%	19.51%	33.77%
Mean	31.3	30.3	25.7	44.6
Variance	183.11	254.34	451.14	435.02
Std Dev	13.53	15.95	21.24	20.86

Table 3.2: The correlation between each regime and Nino 3.4 for the Boreal Winter period from 1980-2015.

	Scan Blk	Atl Rdg	NAO-	NAO+
Nino 3.4	0.04	-0.02	-0.13	-0.29

3.2, which shows the correlation between each regime and the Nino 3.4 index, seems to suggest the NAO- is more associated with cold events where the NAO+ is associated with warm events. We look at warm and cold events and how they relate to individual regime transitions in more detail in section 3.5.

3.2 How Persistent are the Euro-Atlantic Regimes?

Another important question is how persistent are these regimes. NAO- was found to be the most persistent regime lasting an average of 12.77 days and the Scandinavian Block was the least persistent regime lasting an average of 9.58 days. Table 3.3 shows the average and maximum persistence for each regime. All four regimes have persisted for 4 weeks or more at least once over the 35-year period. The NAO+ and NAO- regimes have the longest periods of persistence.

Table 3.3: Average and maximum persistence for each of the 4 Euro-Atlantic Regimes. NAO- was found to be the most persistent lasting an average of 12.77 days and the Scandinavian Block was the least persistent 9.58 days. All four regimes have persisted for 4 weeks or more at least once over the 35-year period.

	Scan Blk	Atl Ridge	NAO-	NAO+
Average	9.58	10.45	12.77	12.36
Max	27	33	46	56

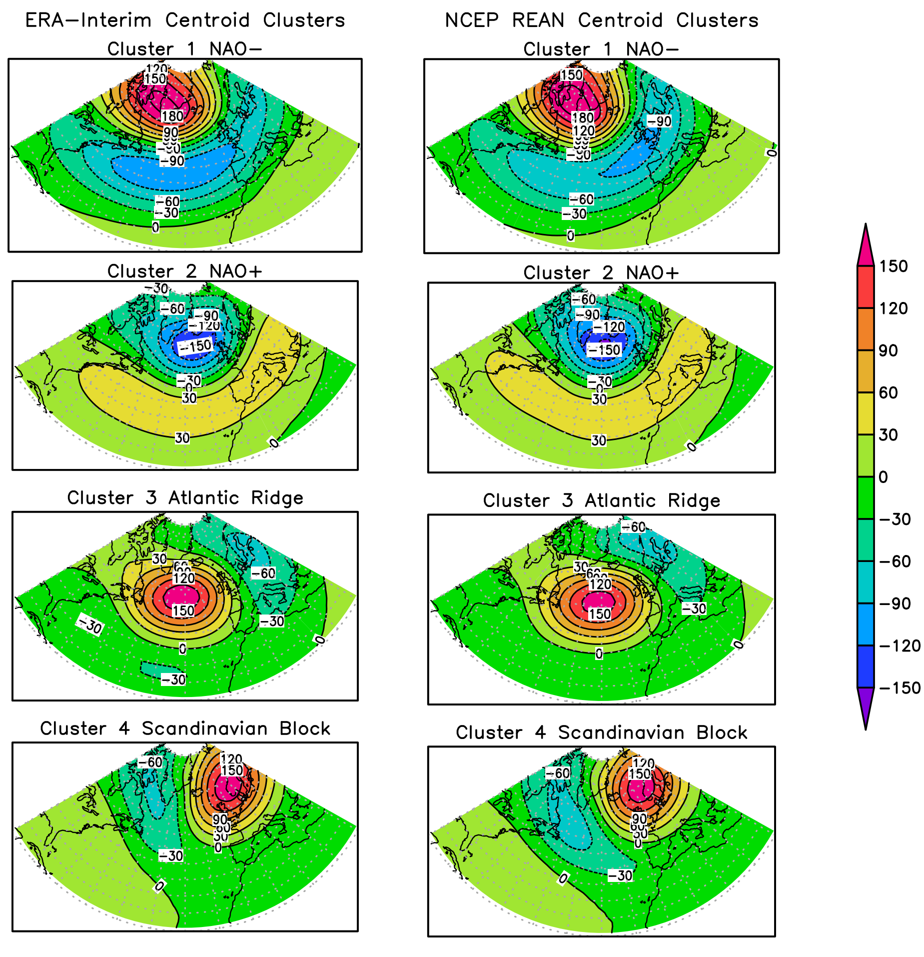

Figure 3.1: Regimes obtained from k-means cluster analysis for running 5-day means: 16 Nov to 31 Mar (NCEP 1 Nov to 31 Mar).

Table 3.4: the total number of days (5-day running means) in each regime for all 35 winters examined in the ERA-I dataset . Blue shading represents less than 10 occurrences. Orange shading is 80 or more occurrences. The last two columns indicate the seasonal average the Nino 3.4 index and the intensity of the warm or cold event with weak event less than 1, moderate between 1 and 1.5, strong between 1.5 and 2.0 and very strong greater that 2.0. Cold events are the same values except negative.

Winter	Scan Block	Atl Ridge	NAO-	NAO+	avg Nino3.4	
1980-1981	10	59	30	32	-0.092	
1981-1982	32	26	35	39	-0.078	
1982-1983	28	51	0	52	2.148	Very Strong
1983-1984	31	33	16	53	-0.778	Weak
1984-1985	48	10	53	21	-1.094	Moderate
1985-1986	29	15	44	44	-0.554	Weak
1986-1987	26	28	34	44	1.124	Moderate
1987-1988	24	29	23	56	0.734	Weak
1988-1989	18	22	10	82	-1.762	Strong
1989-1990	24	2	22	84	0.03	
1990-1991	51	30	16	35	0.266	
1991-1992	52	38	0	42	1.498	Moderate
1992-1993	38	33	0	61	0.445	
1993-1994	28	20	13	71	0.056	
1994-1995	16	35	12	69	0.962	Weak
1995-1996	53	30	43	6	0.192	
1996-1997	34	18	41	39	-0.292	
1997-1998	37	32	28	35	2.142	Very Strong
1998-1999	24	43	14	51	-1.32	Moderate
1999-2000	0	68	5	59	-1.506	Strong
2000-2001	35	8	58	31	-0.916	Weak
2001-2002	40	18	21	53	-0.154	
2002-2003	63	16	34	19	0.984	Weak
2003-2004	30	53	23	26	0.208	
2004-2005	19	58	30	25	0.486	
2005-2006	52	41	29	10	-0.722	Weak
2006-2007	29	14	27	62	0.528	Weak
2007-2008	33	27	3	69	-1.57	Strong
2008-2009	29	45	25	33	-0.74	Weak
2009-2010	18	5	88	21	1.396	Moderate
2010-2011	19	20	64	29	-1.428	Moderate
2011-2012	48	37	0	47	-0.832	Weak
2012-2013	26	25	60	21	-0.152	
2013-2014	18	24	0	90	-0.21	
2014-2015	35	48	0	49	0.66	Weak

3.3 What are the Observed Transitions?

Regime transitions are the primary purpose of this research. First, it should be noted that there are frequent times when a regime persists for less than 5 days and may transition to another regime which may also persist for less than 5 days. (Recall that the day in question is the middle-day of a running 5-day mean.) We will term these episodes chaotic regimes. There are also many scenarios where there is a transition from a chaotic regime to a regular regime or when a regular regime may transition to a chaotic regime. Finally, there are situations where a regime lasts for 5 or more days, transitions to a new regime for less than 5 days then returns to the original regime. In the ERAI data (1980-2015), these chaotic situations account for 20.56 percent of all episodes or a total of 950 days.

Preferred transitions have been identified in the literature by (Vautard, 1990; Cassou, 2008) and others. The ERA-I and NCEP reanalysis regime transitions for correlations greater 0.4 were tested for significance using the bootstrap method described in Appendix B. As shown in Table 3.5 only three of the possible 12 transitions achieved 95 percent significance. Most of the results presented later in this thesis are from the ERA-I reanalysis but we show the NCEP reanalysis to show the robustness of the regimes.

The following are the ERA-I significant transitions:

- NAO+ to Scandinavian Block
- Scandinavian block to NAO-
- Scandinavian Block to Atlantic Ridge

The NCEP-Reananalysis transitions had a total of 5 transitions which were significant. The following are the significant NCEP-Reanalysis transitions:

- NAO+ to Scandinavian Block
- Scandinavian block to NAO-
- Scandinavian Block to NAO+

- NAO- to Scandinavian Block

- Atlantic Ridge to NAO+

Table 3.5: The total number of occurrences for each transition for the ERA-I reanalysis, The table on top is for pattern correlations of greater than 0.0 and on the bottom for correlations of greater than 0.4 on the bottom. The top figure is all transitions with a positive pattern correlation and the bottom figure is for all transitions with a pattern correlation greater than 0.4. The rows are the previous regime and the columns are the regime transitioned to. Using the top figure as an example, Scandinavian Block remains in the same regime 907 times for the ERA-I dataset (1st row, 1st column). The Scandinavian Block transitioned to the NAO+ 20 times for the ERA-I (1st row, 4th column). However if we look at the opposite transition, NAO+ to Scandinavian Block (4th row, 1st column) we see that the numbers are higher and seem to favor this transition, 29 for the ERA-I. Note that the ERA-I dataset is based on 35 years.

	Scan Block	Atlantic Rdg	NAO-	NAO+
Scandinavian Block	907	13	20	20
Atlantic Ridge	14	875	9	19
NAO-	14	0	797	7
NAO+	29	23	6	1361

	Scan Block	Atlantic Rdg	NAO-	NAO+
Scandinavian Block	727	10	9	10
Atlantic Ridge	7	700	6	6
NAO-	5	0	745	7
NAO+	17	10	0	1053

Table 3.5 shows all transitions with a positive pattern correlation and the bottom figure is for all transitions with a pattern correlation greater than 0.4. The rows are the previous regime and the columns are the regime transitioned to. Using the top figure as an example, Scandinavian Block remain in the same regime 907 time for the ERA-I dataset, 1907 for the NCEP-Reanalysis. The Scandinavian Block transitioned to the NAO+ 20 times for the ERA-I, 44 for the NCEP-Reanalysis. However if we look at the opposite transition, NAO+

to Scandinavian Block (4th row, 1st column) we see that the numbers are higher and seem to favor this transition, 29 for the ERA-I, 54 for the NCEP-Reanalysis.

Our research confirms some of these preferred paths but also some of the opposite transitions occur almost as often (see Table 3.5). The two preferred paths most widely acknowledged are the NAO+ to Scandinavian Block and the Scandinavian Block to NAO-, Vautard (1990), Cassou (2008). It should be noted that the NAO+ to NAO- transition does occur but only at correlations below 0.3. Unless noted all pre-transition heating was done for transitions with pattern correlations greater than 0.4 using the ERAI dataset. In this dataset there were no NAO- to Atlantic Ridge transitions.

3.4 What is the Regime Climatology?

In this section we look at composites of PW diabatic heating and streamfunction by comparing climatology and each of the four regimes. The purpose is to show large scale changes prior to each transition. First, we look at climatology of diabatic heating for November through March. We then show the diabatic heating signature associated with each regime compared to the other three regimes for times ranging from 20 days prior to 20 days following each regime. These maps provide a base-line heating for each regime. Just prior to each transition we will later evaluate the heating compared to the base-line for the appropriate regime. The last climatology map, shown in Figure 3.6, is for the streamfunction.

Figure 3.2 shows the climatology for the boreal winter (NDJFM) vertically integrated planetary wave diabatic heating. The majority of the diabatic heating in the tropics is at the mid and upper levels mainly due to convection and in the higher latitudes the heating is confined mainly to the lower troposphere mostly due to eddy fluxes of latent heat as seen in the Pacific and Atlantic storm tracks.

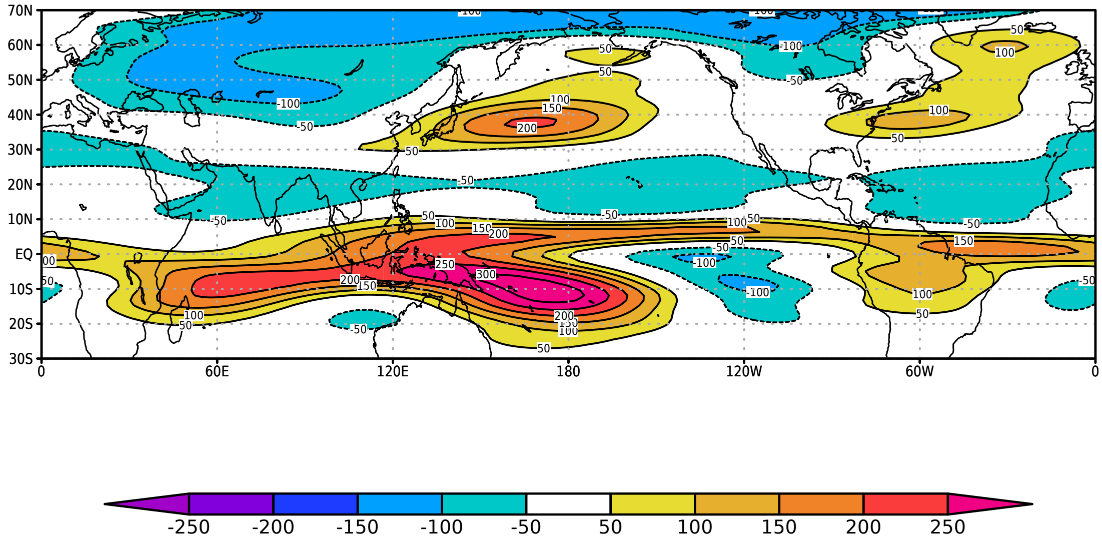

Figure 3.2: Climatology for the Total Planetary Wave Diabatic Heating for 16 Nov to 27 March, 1980 to 2015 from ERA-I Dataset. Note that the majority of the diabatic heating in the tropics is at the mid and upper levels mainly due to convection and in the higher latitudes the heating is confined mainly to the lower troposphere due to eddy fluxes of latent heat (as seen in the Pacific and Atlantic storm tracks).

Figure 3.3 shows the PW diabatic heating at 10 days (right panel) and 20 days (left panel) prior to each of the four regimes. Note that for less lag there is also less heating. Figure 3.4 is for no lag. The heating shown in Figures 3.3 and 3.4 is the heating one would expect knowing only that the system is in a particular regime. In order to determine changes in heating prior to regime transitions, we seek changes from the regime-based climatologies shown. Finally, Figure 3.5 shows the PW diabatic heating for 10 days (left panel) and 20 days (right panel) following each regime.

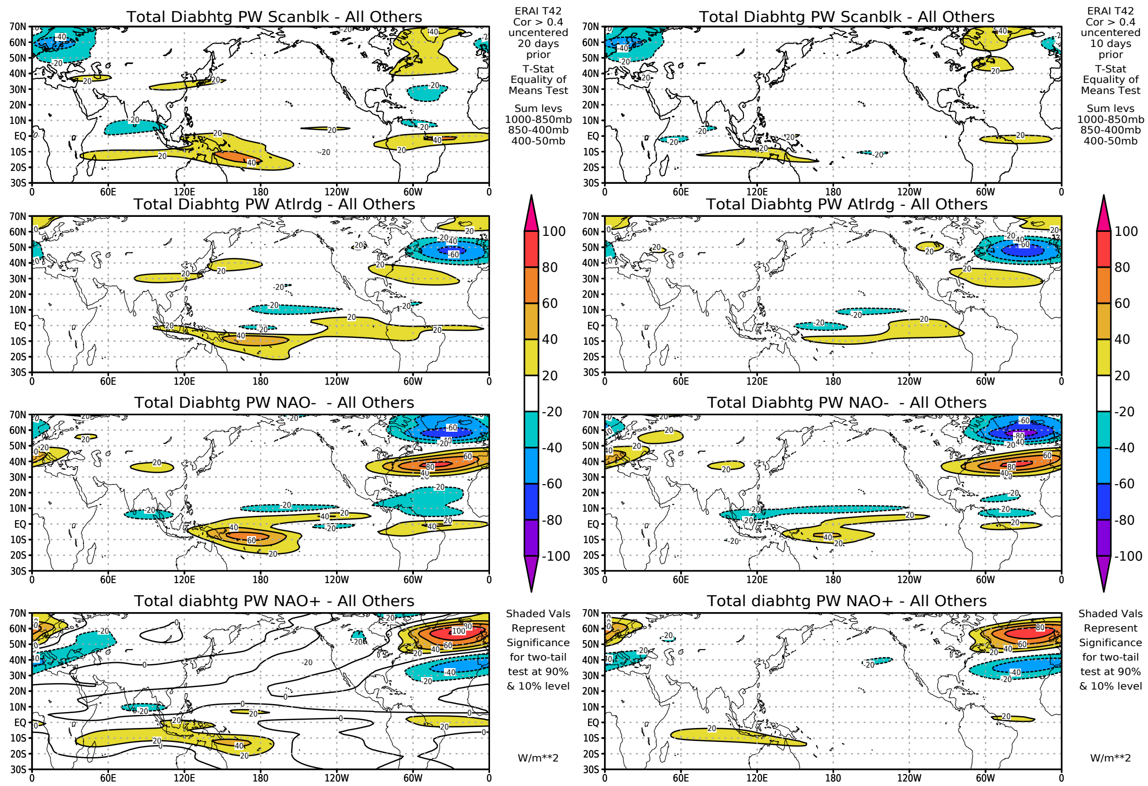

Figure 3.3: Total Planetary Wave Diabatic heating for each regime minus the total of all the others for 10 and 20 days prior to the regime. The heating is based on regime pattern correlations of greater than 0.4.

Figure 3.6 shows the streamfunction anomalies for each regime with respect to the climatology of the other regimes. Nearly all of the strong anomalies are confined to the EA region.

3.5 Anomalies Associated With Individual Regimes Transitions

The following figures are the composites for each individual transition to show changes prior to the transition from one regime to another. Ideally these maps will show large differences which will allow us to differentiate between each transition. These results will also allow us

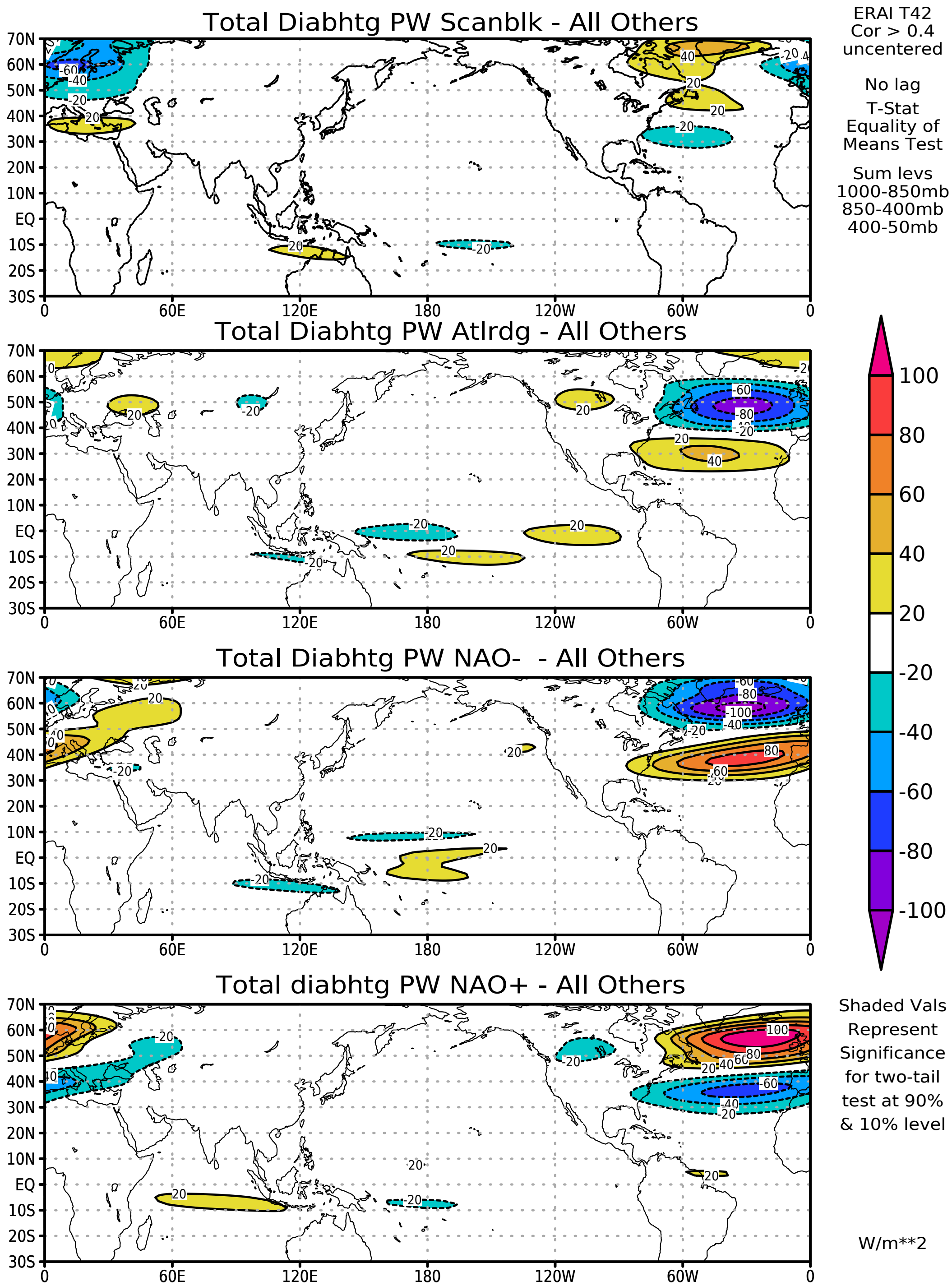

Figure 3.4: Total Planetary Wave Diabatic heating for each regime minus the total of all the others. The heating is based on regime pattern correlations of greater than 0.4.

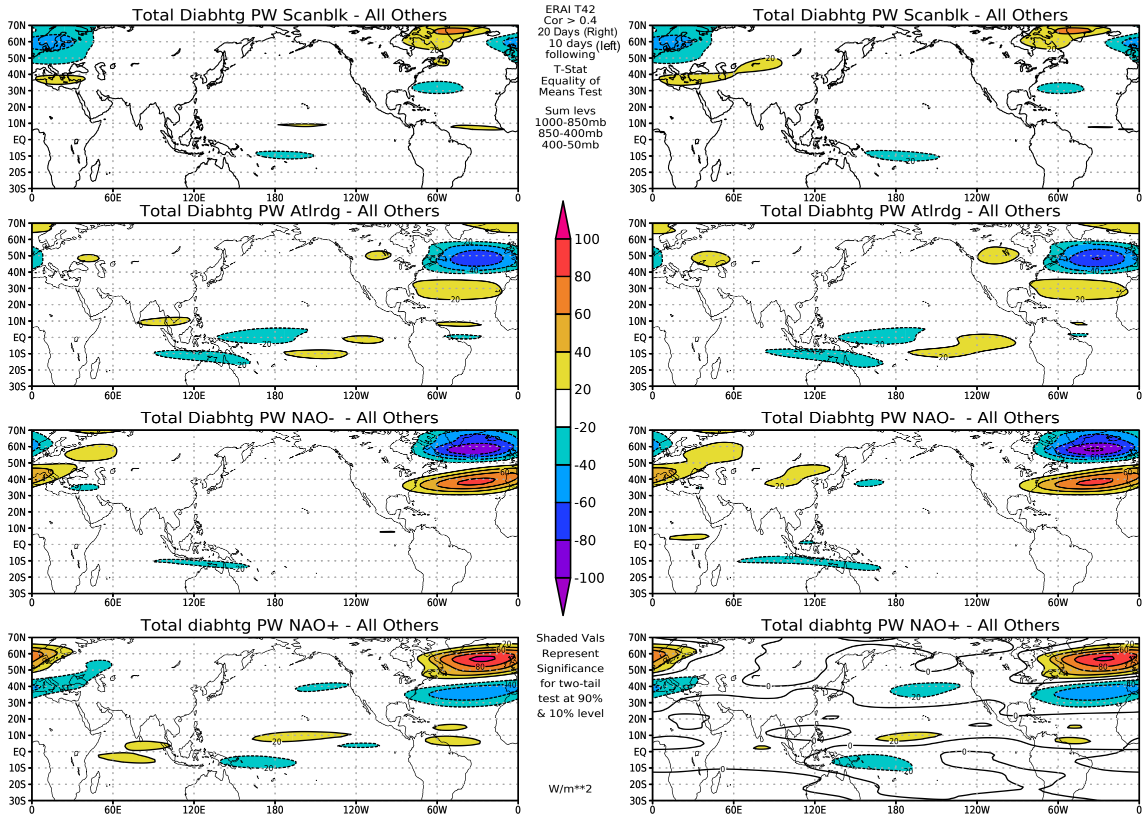

Figure 3.5: Total Planetary Wave Diabatic heating for each regime minus the total of all the others for 10 and 20 days after the regime. The heating is based on regime pattern correlations of greater than 0.4.

to determine the role of tropical heating, MJO, and ENSO. For each of the 10 transitions examined, we show composites of diabatic heating, streamfuction and Rossby wave activity. We also show a MJO phase histogram and relationship to warm and cold ENSO events for each transition. The first set of figures shows differences in vertically integrated heating prior to the transition (1-5days, 6-10 days, 11-15 days, 16-20 days) minus the climatological heating in the regime being transitioned from. Such differences are called pre-transition anomalies. For each figure, the left hand set of panels are the pre-transition anomalies, while the right hand set of panels show the anomalies of heating with respect to the full climatology. In addition, the same format is used to display the 300 hPa streamfunction. Note that in general, the full anomalies of streamfunction with respect to the regime being

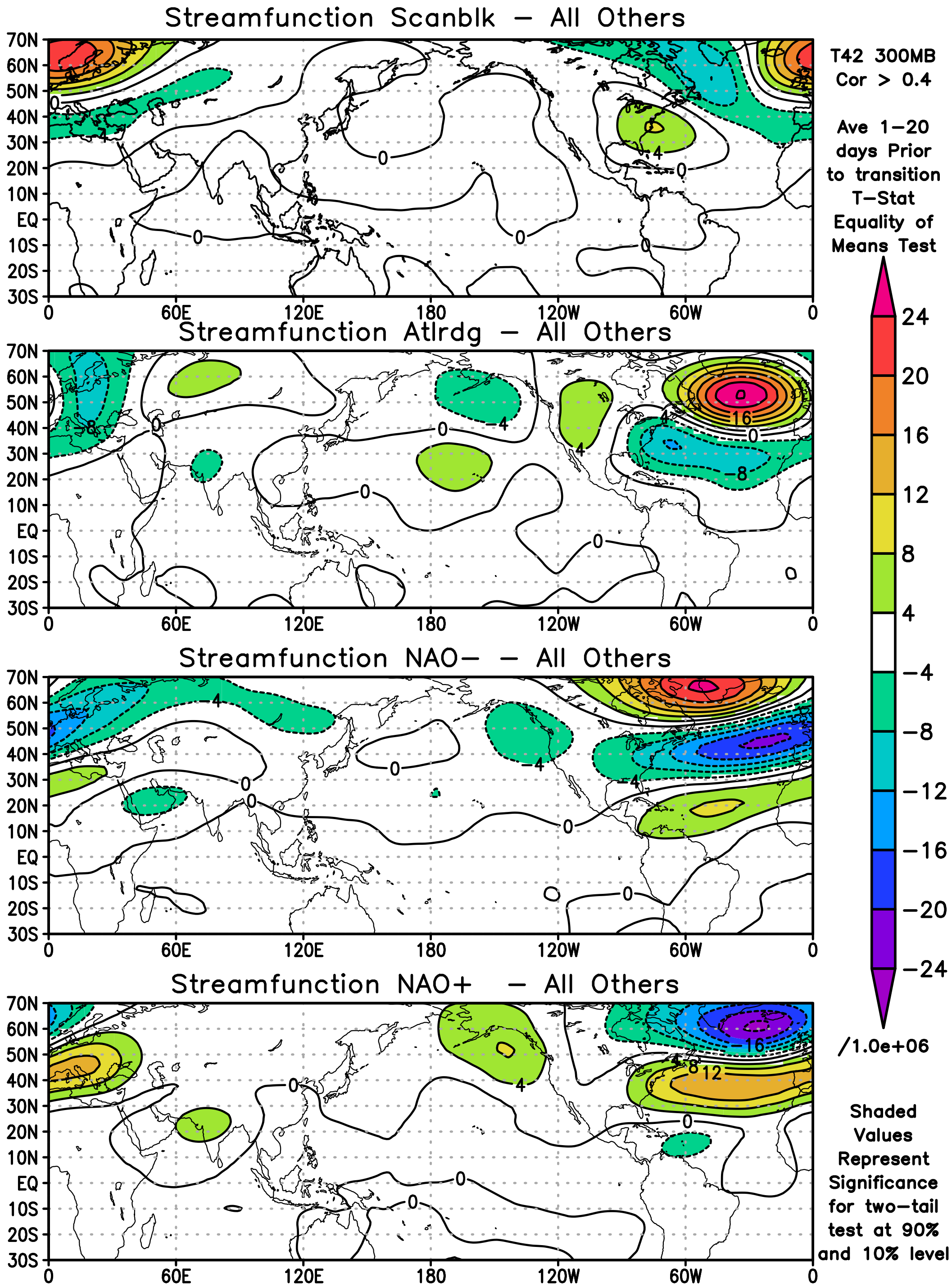

Figure 3.6: Streamfunction at 300hPa for each regime minus the climatology of all the regimes. The streamfunction is based on regime and transition pattern correlations of greater than 0.4.

transitioned from (left column) are quite similar to the full anomalies (right column) outside of the EA region. We also show the flux of Rossby wave activity in the left-hand column. For each transition, we also show histograms of the relative frequency of MJO for different periods preceding the transitions, as well as histogram of the frequency of warm and cold ENSO events. The heating is integrated from 1000 hPa to 50hPa in Watts per meter squared. The solid lines are the heating difference between the previous regime and the transition. The shading is significance at the 90 percent level based on the equality of means student t test.

3.5.1 Transitions from the Scandinavian Block

We start by looking at transitions from the Scandinavian Block regime. For each transition we first examine the diabatic heating which will help identify areas of tropical heating and changes in the storm track intensity and location. We then examine the streamfunction and Rossby wave activity which indicates atmospheric circulation and areas of Rossby wave propagation into and out of the tropics. We then look at each transition to determine if there is a relationship to phases of the MJO. Finally we look at ENSO based on the Nino 3.4 index to determine if a regime transition is related to a warm or cold event more than 50 percent of the time.

Scandinavian Block to Atlantic Ridge Transition

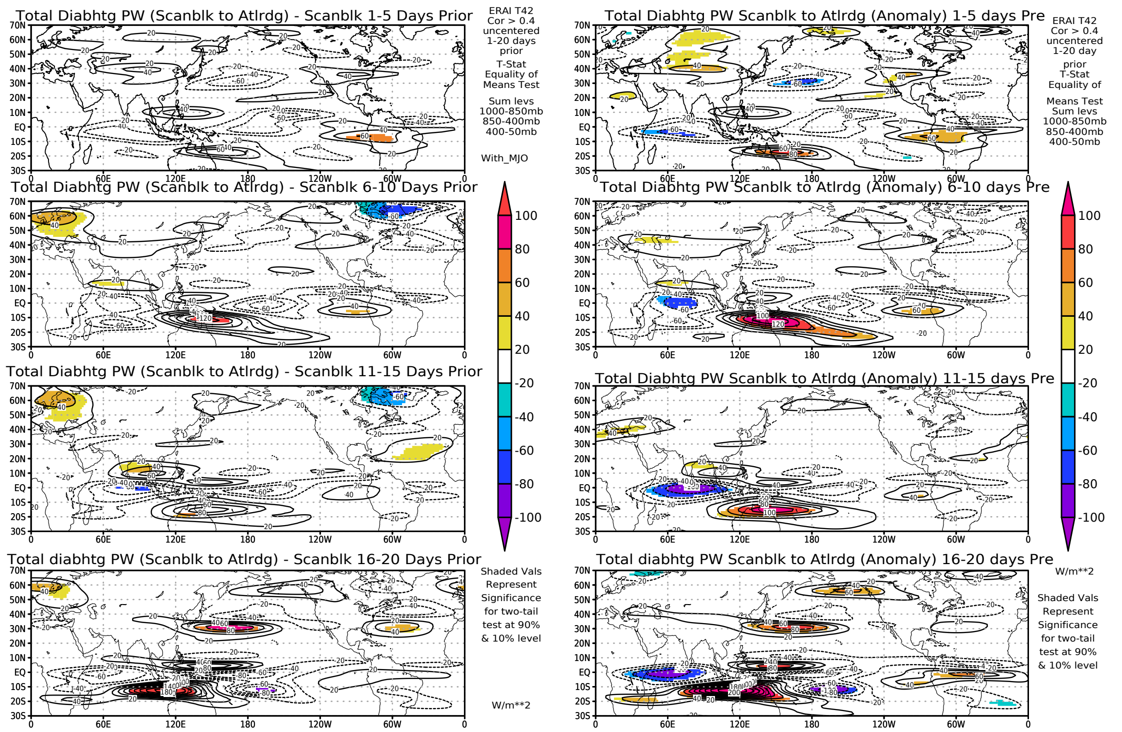

Figure 3.7: The planetary wave heating for the transition from Scandinavian Block to Atlantic Ridge. The panels on the left show the diabatic heating difference 1-20 days prior to the transition and the composite of the previous regime. The right figure show the anomaly of the days prior to the transition compared to the climatology. Shaded areas are significant at the 90 percent level.

In the heating difference and anomaly maps shown in Figure 3.7, a region of heating in the western Pacific at about $15^{o}S$ is seen for all lags, although it becomes less significant as you get closer to the transition. In the high latitudes, looking at the difference pattern, we see heating over Northern Europe and cooling off the coast of Newfoundland. This is just the opposite of the climatological pattern of heating prior to the Scandinavian Block regime.

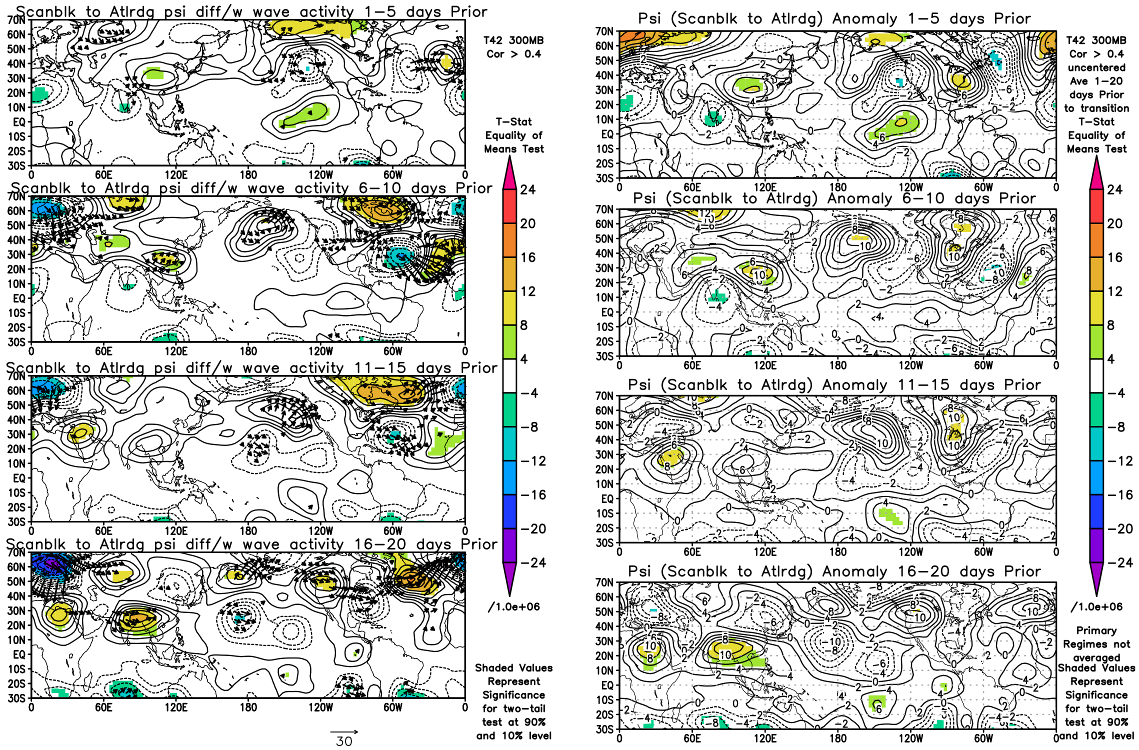

Figure 3.8: The streamfunction and Rossby wave activity for the transition from Scandinavian Block to Atlantic Ridge. The panels on the left are the Rossby wave activity and difference between the days prior to the transition and the Scandinavian Block regime. Shaded areas are significant at the 90 percent level. The right panel is the anomaly between the days prior to the transition and the climatology.

The corresponding streamfunction difference and anomaly maps along with the Rossby wave activity for the Scandinavian Block to Atlantic Ridge transition are seen in Figure 3.8. With the exception of the North Atlantic, the difference between the pre-transition days and the normal Scandinavian Block has a pattern very similar to the anomalies (right figure). The difference plots show the dissipation of the Scandinavian Block (20 to 6 days prior), and then the beginning of the formation of the Atlantic Ridge at 1-5 days prior to the transition. The decay of the Scandinavian Block 16-20 days is associated with strong wave activity from Northern Canada. Looking at the anomaly 1-5 days prior to the transition, it is somewhat more diffuse than total Scandinavian Block anomaly. Wave activity is seen propagating from Northern Europe eastward and equatorward towards mid-latitudes, but does not reach the subtropics. This is consistent with little diabatic heating seen north of the equator.

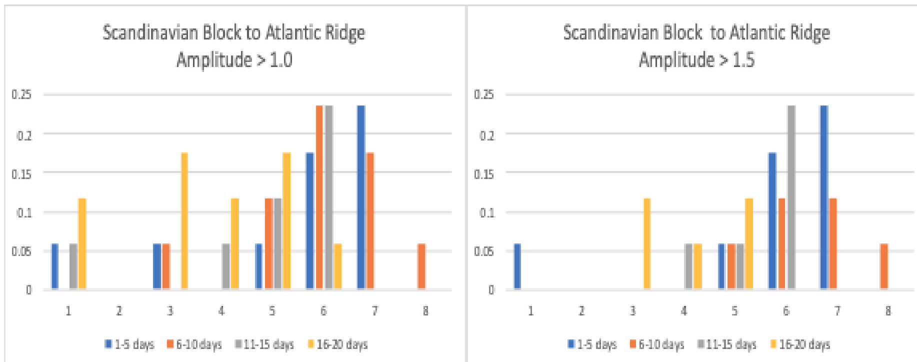

Figure 3.9: Scandinavian Block to Atlantic Ridge. The Graph on left is for MJO amplitudes greater the 1.0, right is greater than 1.5.

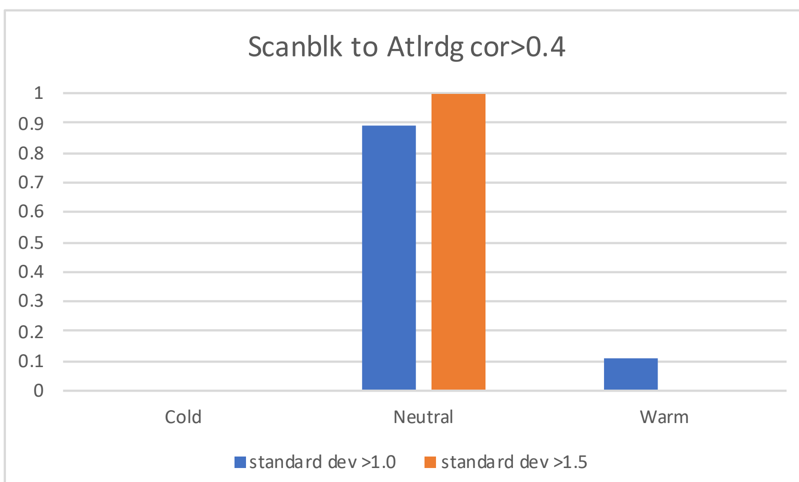

Figure 3.10: Scandinavian Block to Atlantic Ridge transitions occurrences during cold, neutral, and warm events based on the SST standard deviation of the Nino34 index. The blue bar represents standard deviations greater than 1.0 and the orange bar represents standard deviations greater than 1.5

The MJO histogams shown in Figure 3.9 shows all phases of the MJO are represented in this transition, although there is some preference for the later phases (5-7). Figure 3.10

shows that most of these transitions occur during neutral ENSO years.

Scandinavian Block to NAO- Transition

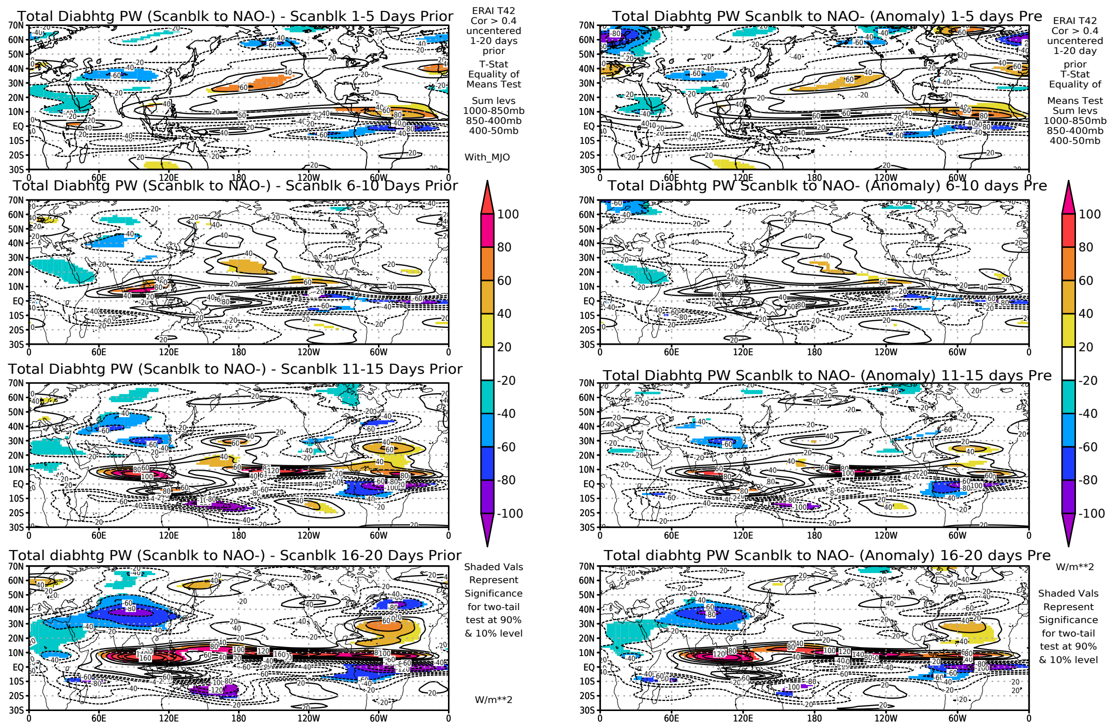

Figure 3.11: Pre-transition planetary scale diabatic heating for transitions from the Scandinavian Block to NAO-. The panels on the left show the diabatic heating difference 1-20 days prior to the transition and the composite of the previous regime (Scandinavian Block). The right figure shows the anomaly of the days prior to the transition compared to the climatology. Shaded areas are significant at the 90 percent level.

Figure 3.11 shows strong tropical heating in the Indian and Atlantic Oceans in both the difference and anomaly plots 1-5 days prior to the transition. Very strong heating is seen in the Indian, Pacific and Atlantic Oceans 10-20 days prior. The heating over the eastern Pacific is seen in 7 out of the 9 episodes that go into these composites, including neutral and cold ENSO years (not shown).

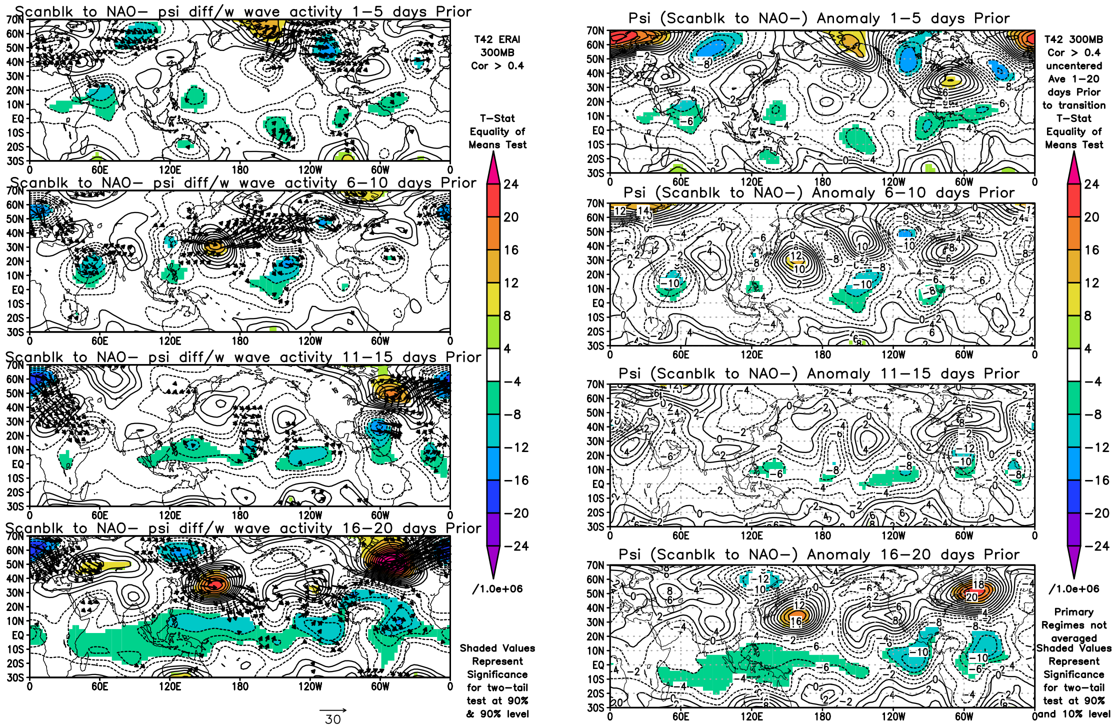

Figure 3.12: The streamfunction and Rossby wave activity for the for transition from Scandinavian Block to NAO-. The panels on the left are the Rossby wave activity and difference between the days prior to the transition and the Scandinavian Block regime. Shaded areas are significant at the 90 percent level. The right panel is the anomaly between the days prior to the transition and the climatology.

Looking at Figure 3.12, the streamfunction anomalies show the Scandinavian Block in place 1-5 days prior and 6-10 days prior to the transition. The streamfunction differences and associated wave activity show a strong eastward and equatorward propagation into the northern tropics 6-15 days prior, and strong wave activity emanating from the mid-Pacific at around $35^o N$ over the North America into the Atlantic at 1-10 days prior to the transition.

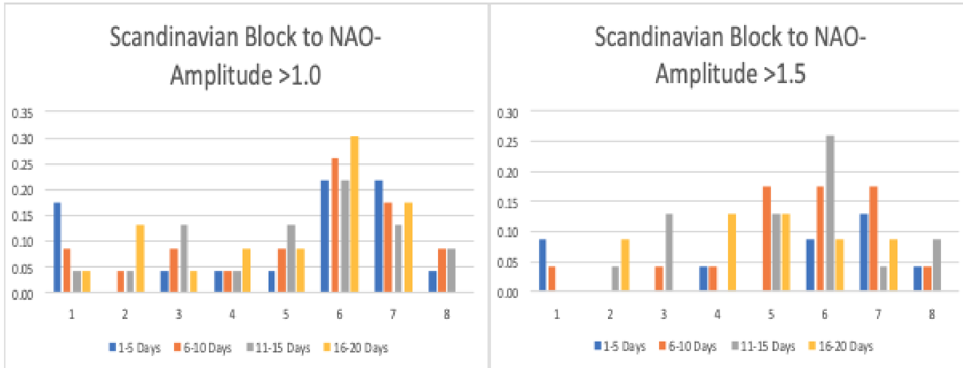

Figure 3.13: Scandinavian Block to NAO-. The Graph on left is for MJO amplitudes greater the 1.0, right is greater than 1.5. Note the increases prior to MJO phase 6 and 7.

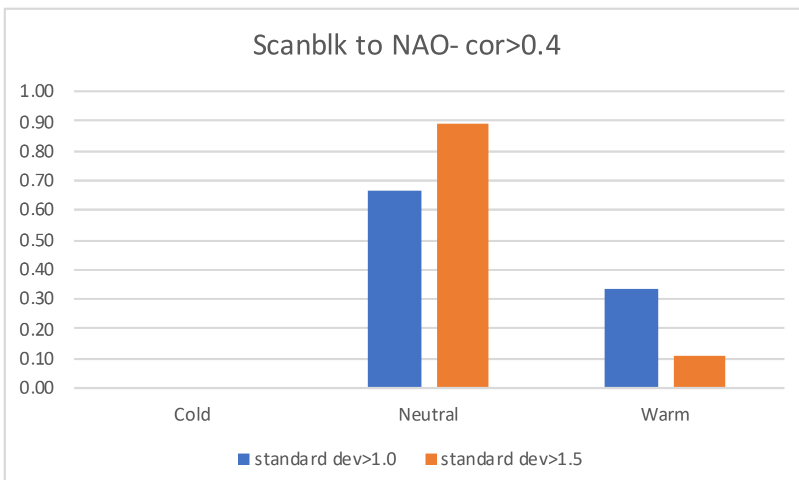

Figure 3.14: Scandinavian Block to NAO- transitions occurrences during cold, neutral, and warm events based on the SST standard deviation of the Nino34 index. The blue bar represents standard deviations greater than 1.0 and the orange bar represents standard deviations greater than 1.5

Figure 3.13 shows all phases of the MJO participate, but there is some preference for later phases. Most of the transitions occur during ENSO neutral years, with only a few occurring during warm years as shown in Figure 3.14.

Scandinavian Block to NAO+ Transition

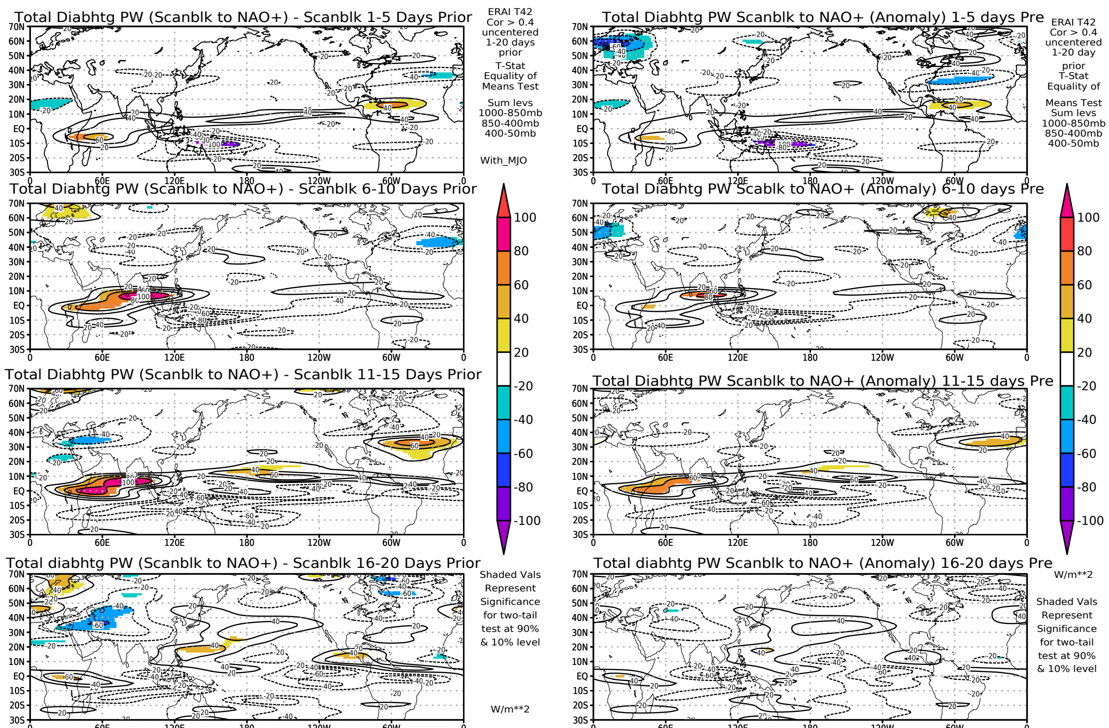

Figure 3.15: Pre-transition planetary scale diabatic heating for transitions from the Scandinavian Block to NAO+. The panels on the left show the diabatic heating difference 1-20 days prior to the transition and the composite of the Scandinavian block regime. The right figure shows the anomaly of the days prior to the transition compared to the climatology. Shaded areas are significant at the 90 percent level.

Figure 3.15 is the transition into the NAO+ from the Scandinavian Block and shows there is strong heating over the Indian Ocean seen at 6-10 and 10-15 days prior to the transition, with some seen 1-5 days prior to the transition.

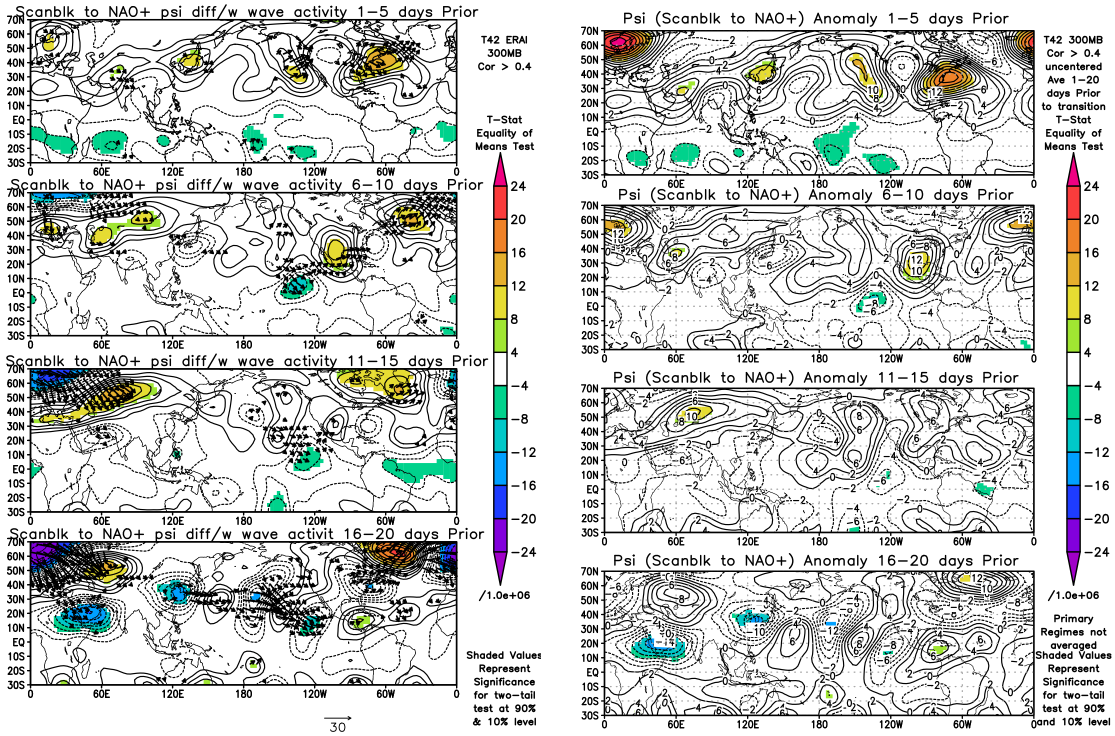

Figure 3.16: The streamfunction and Rossby wave activity for the for transition from Scandinavian Block to NAO+. The panels on the left are the Rossby wave activity and difference between the days prior to the transition and the Scandinavian Block regime. Shaded areas are significant at the 90 percent level. The right panel is the anomaly between the days prior to the transition and the climatology.

The Streamfunction differences given in Figure 3.16 show wave activity propagating from the North Atlantic eastward and southward into the tropics 16-20 days prior, consistent with tropical heating 11 to 15 days prior to the transition. Anomalies at 16-20 days prior show strong cyclonic values around $20^o N$ over the Indian Ocean.

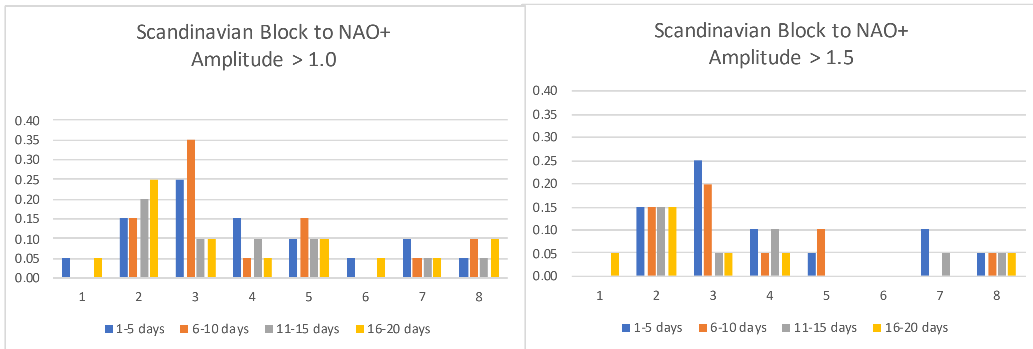

Figure 3.17: Histogram for the 20 day period prior to the transition from Scandinavian Block to NAO+. The Graph on left is for MJO amplitudes greater the 1.0, right is greater than 1.5.

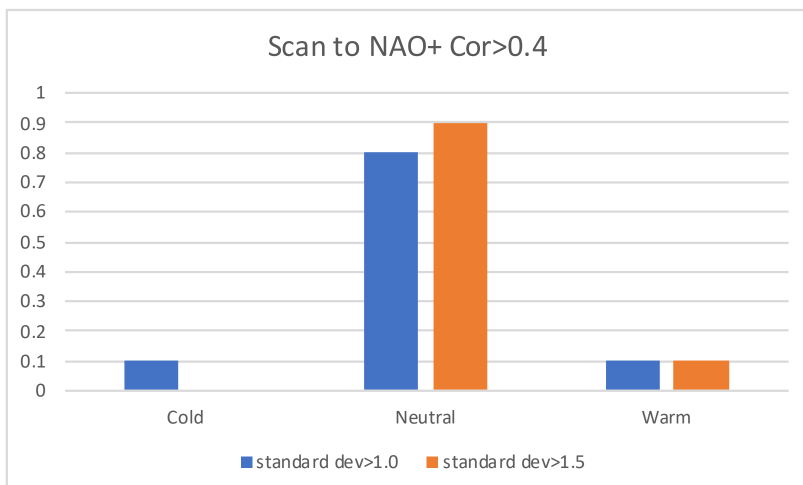

Figure 3.18: Scandinavian Block to NAO+ transitions occurrences during cold, neutral, and warm events based on the SST standard deviation of the Nino34 index. The blue bar represents standard deviations greater than 1.0 and the orange bar represents standard deviations greater than 1.5.

Figure 3.17 shows a preference for MJO in phases 2-3, although all phases are seen. The vast majority of transitions occur during neutral ENSO years as seen in Figure 3.18.

3.5.2 Transitions from the Atlantic Ridge

Atlantic Ridge to Scandinavian Block Transition

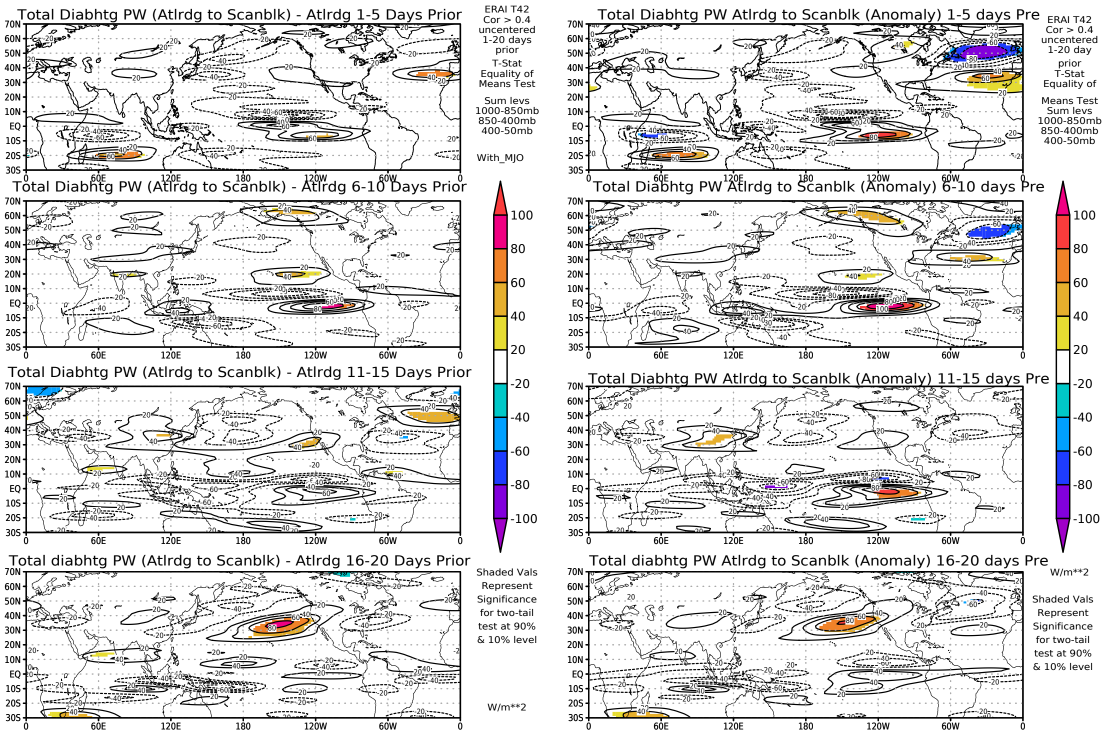

Figure 3.19: The planetary wave heating for the transition from Atlantic Ridge to Scandinavian Block. The panels on the left show the diabatic heating difference 1-20 days prior to the transition and the composite of the previous regime. The right figure shows the anomaly of the days prior to the transition compared to the climatology. Shaded areas are significant at the 90 percent level.

Figure 3.19 shows the pre-transition diabatic heating for the Atlantic Ridge to the Scandinavian Block transition. There is very little evidence of tropical heating but subtropical heating is seen around 30^oN in the eastern Pacific 11-20 days prior to the transition. An enhancement of North Atlantic storm track is seen around 50^oN at 11-15 days prior to the transition.

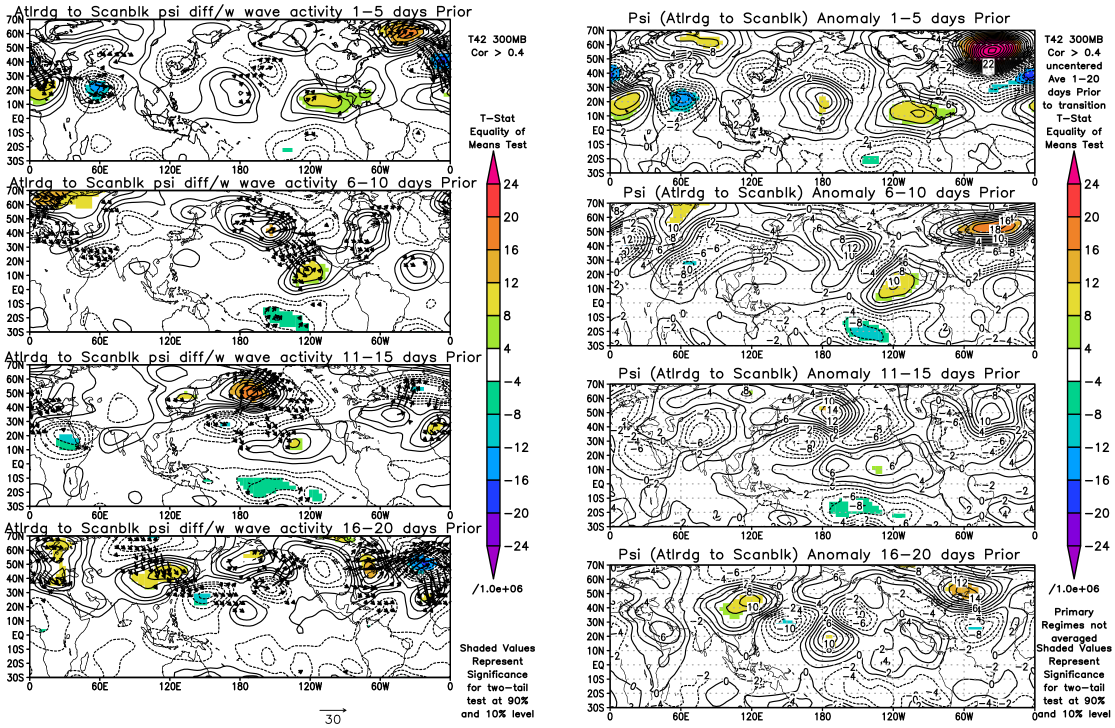

Figure 3.20: The streamfunction and Rossby wave activity for the for transition from Atlantic Ridge to Scandinavian Block. The panels on the left are the Rossby wave activity and streamfunction difference between the days prior to the transition and the Atlantic Ridge regime. Shaded areas are significant at the 90 percent level. The right panel is the anomaly between the days prior to the transition and the climatology.

Figure 3.20 shows that 6-10 days prior to the transition, wave activity is seen propagating southward and eastward into subtropics around 60 degrees East and tropics around 150 degrees West, but no indication of associated diabatic heating (Figure 3.19).

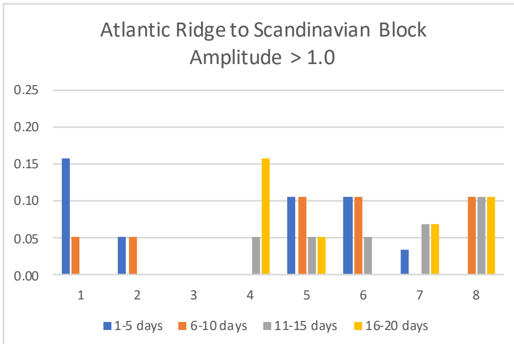

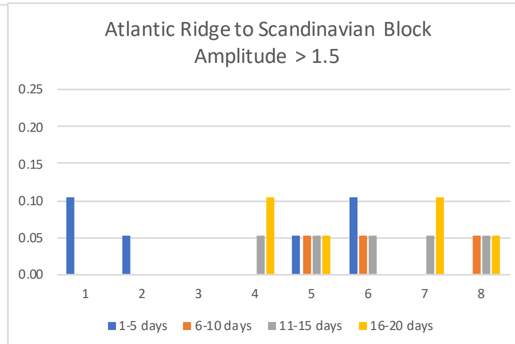

Figure 3.21: Atlantic Ridge to Scandinavian Block. The Graph on left is for MJO amplitudes greater the 1.0, right is greater than 1.5.

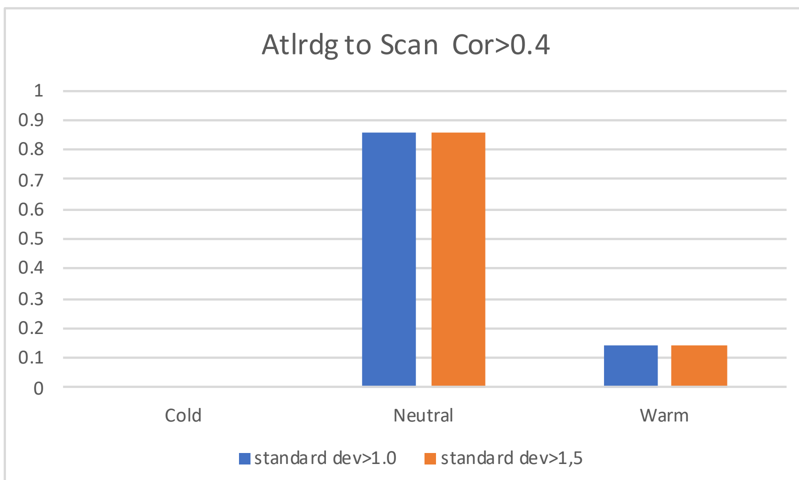

Figure 3.22: Atlantic Ridge to Scandinavian Block transitions occurrences during cold, neutral, and warm events based on the SST standard deviation of the Nino34 index. The blue bar represents standard deviations greater than 1.0 and the orange bar represents standard deviations greater than 1.5

From Figure 3.21 we see that most MJO phases participate in this transition, (except phase 3), but further back than 5 days only phases 4-8 participate. Most episodes occur during neutral ENSO years as seen from Figure 3.22.

Atlantic Ridge to NAO-

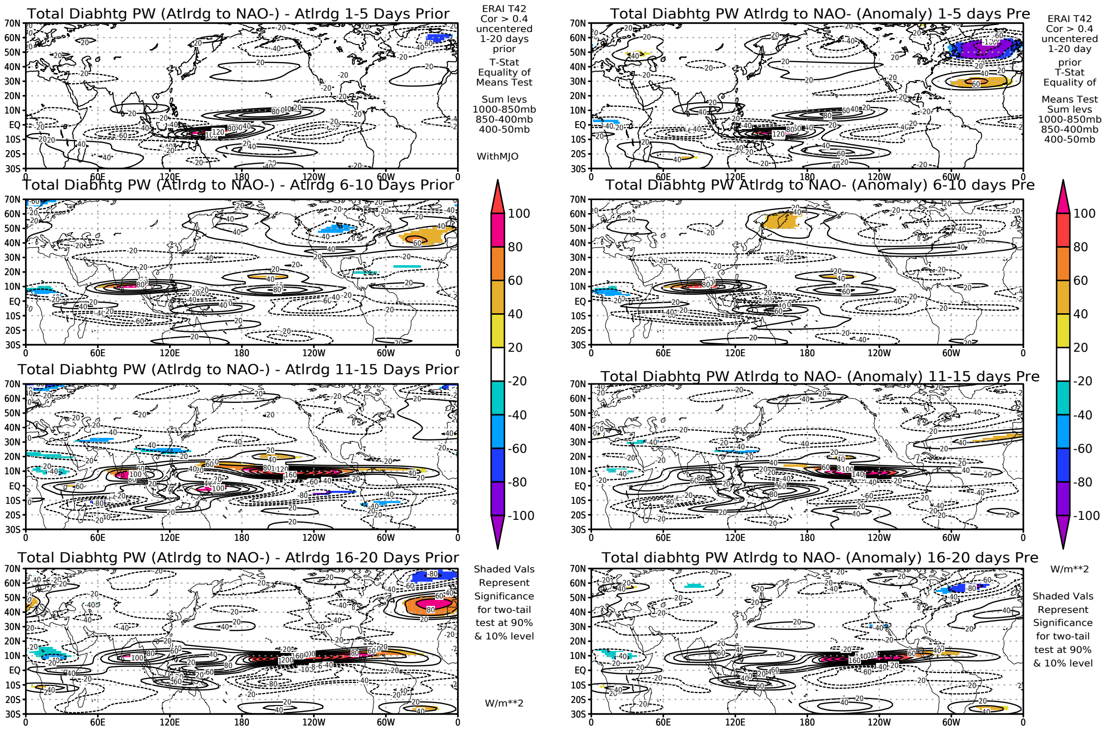

Figure 3.23: The planetary wave heating for the transition from the Atlantic Ridge to NAO-. The panels on the left show the diabatic heating difference 1-20 days prior to the transition and the composite of the previous regime. The right figure show the anomaly of the days prior to the transition compared to the climatology. Shaded areas are significant at the 90 percent level.

Figure 3.23 shows the pre-transition heating for the Atlantic Ridge to NAO- transition. Indian Ocean heating is seen at 11-15, 6-10, and 1-5 days prior to the transition (propagating eastward), also in the eastern Pacific heating seen 11-20 days prior to the transition. At 16-20 days prior to the transition there is evidence of a southward shift in Atlantic storm track consistent with the NAO- regime.

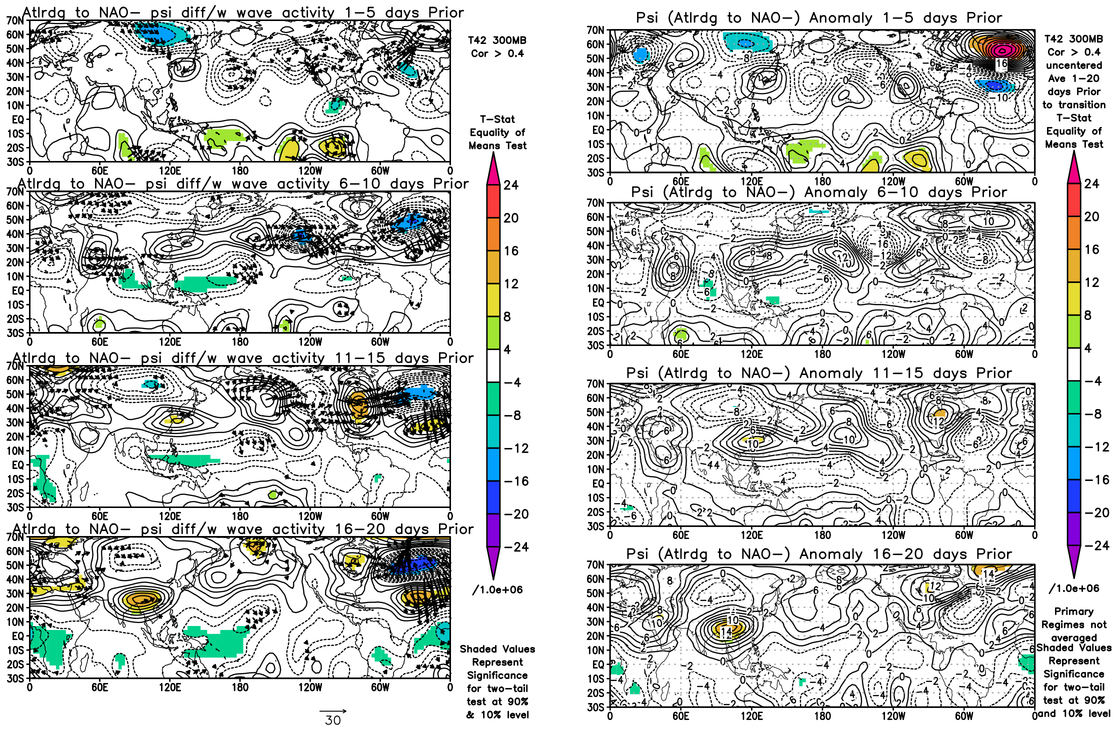

Figure 3.24: The streamfunction and Rossby wave activity for the for transition from Atlantic Ridge to NAO-. The panels on the left are the Rossby wave activity and difference between the days prior to the transition and the Atlantic Ridge regime. Shaded areas are significant at the 90 percent level. The right panel is the anomaly between the days prior to the transition and the climatology.

From Figure 3.24 we see evidence of the Pacific North America pattern as a source of wave activity into Atlantic region prior to day 6 based on the wave activity vectors.

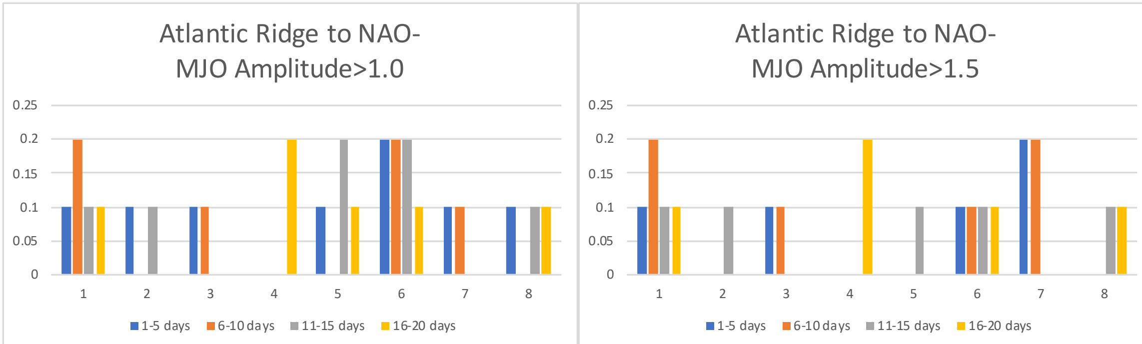

Figure 3.25: Atlantic Ridge to NAO-. The Graph on left is for MJO amplitudes greater the 1.0, right is greater than 1.5.

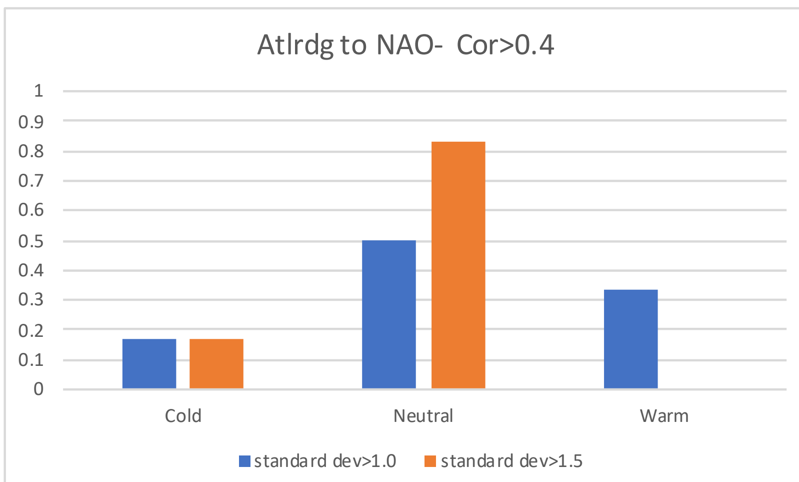

Figure 3.26: Atlantic Ridge to NAO- transitions occurrences during cold, neutral, and warm events based on the SST standard deviation of the Nino34 index. The blue bar represents standard deviations greater than 1.0 and the orange bar represents standard deviations greater than 1.5

From Figures 3.25 and 3.26 we see no preference for any phase of MJO. Figure 3.26 shows no preference for warm or cold events.

Atlantic Ridge to NAO+

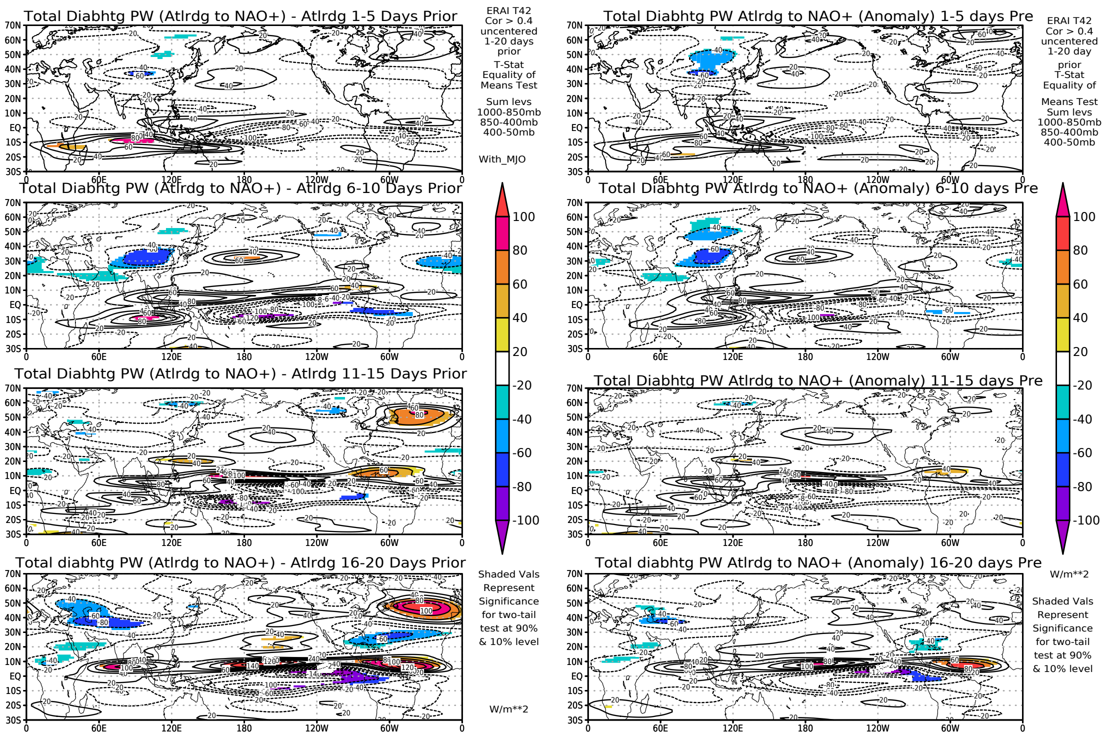

Figure 3.27: Pre-transition planetary scale diabatic heating for transitions from the Atlantic Ridge to NAO+. The panels on the left show the diabatic heating difference 1-20 days prior to the transition and the composite of the previous regime. The right figure shows the anomaly of the days prior to the transition compared to the climatology. Shaded areas are significant at the 90 percent level.

Figure 3.27 shows the pre-transition heating for the Atlantic Ridge to NAO+ transition. Significant tropical heating is seen in the central Pacific and Atlantic Oceans 10-20 days prior. Tropical Indian Ocean heating is also seen at 16-20 days prior to the transition and moves into the southern tropics at 6-10 days and 1-5 days prior to the transition. Also, the beginning of NAO+ storm track development seen around $45^o N - 55^o N$ at 10-20 days prior but not closer to the transition. Cooling over Asia, and in the southern tropical Pacific is seen at up to 20 days prior to the transition.

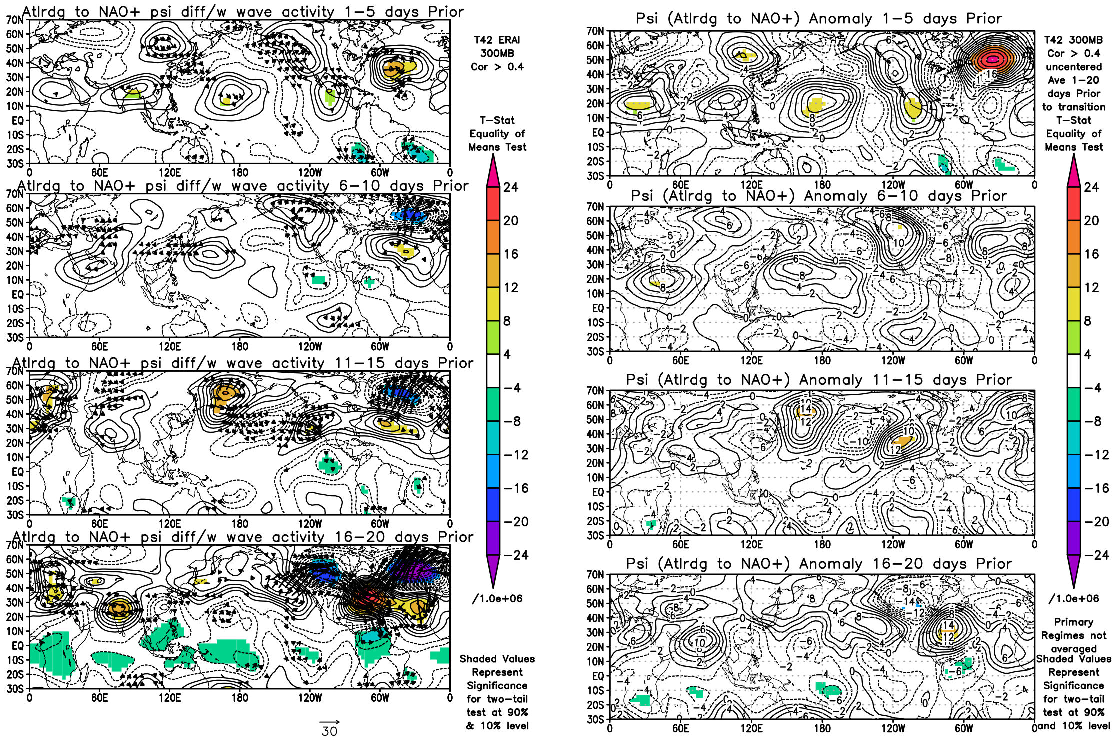

Figure 3.28: The streamfunction and Rossby wave activity for the transition from Atlantic Ridge to NAO+. The panels on the left are the Rossby wave activity and difference between the days prior to the transition and the Atlantic Ridge regime. Shaded areas are significant at the 90 percent level. The right panel is the anomaly between the days prior to the transition and the climatology.

In Figure 3.28 we see a very strong streamfunction response in the difference plots in Atlantic sector consisting of meridional dipole which is consistent with decay of Atlantic Ridge and positioning of the Atlantic storm tracks into NAO+ configuration. There is also a Mid-latitude wave train seen from the north Pacific propagating eastward and equatorward into the eastern Pacific for 10-15 days, also seen in wave activity flux. At 16-20 days prior to the transition, there is a strong mid-latitude response to Pacific heating (Figure 3.27) as seen in wave activity.

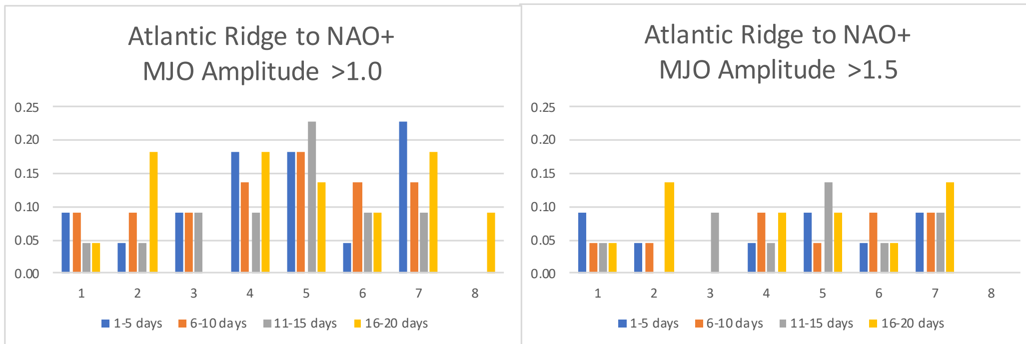

Figure 3.29: Histogram for the 20 day period prior to the transition from Atlantic Ridge to NAO+. The Graph on left is for MJO amplitudes greater the 1.0, right is greater than 1.5.

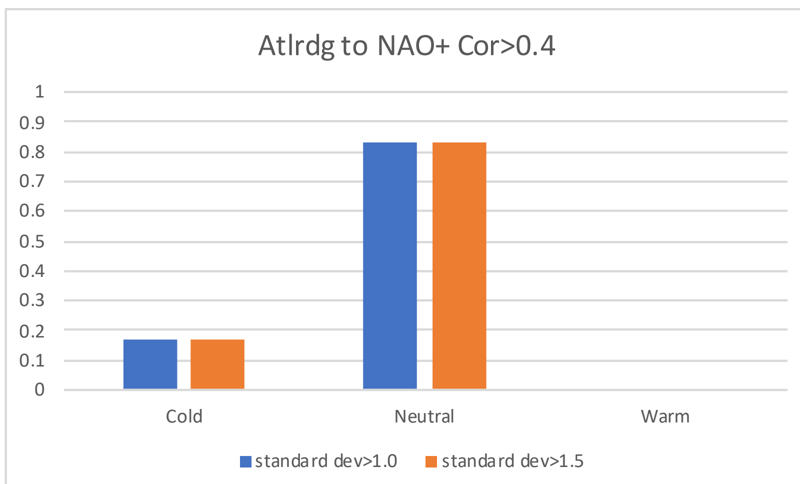

Figure 3.30: Atlantic Ridge to NAO+ transitions occurrences during cold, neutral, and warm events based on the SST standard deviation of the Nino34 index. Blue bar represents standard deviations greater than 1.0 and the orange bar represents standard deviations greater than 1.5

Figure 3.30 virtually every MJO phase participates with no preference. Only a few cold ENSO events and no warm ENSO events participate as shown in Figure 3.30. The vast majority are neutral and therefore shows no preference for warm or cold events.

3.5.3 Transitions from the NAO-

NAO- to Scandinavian Block Transition

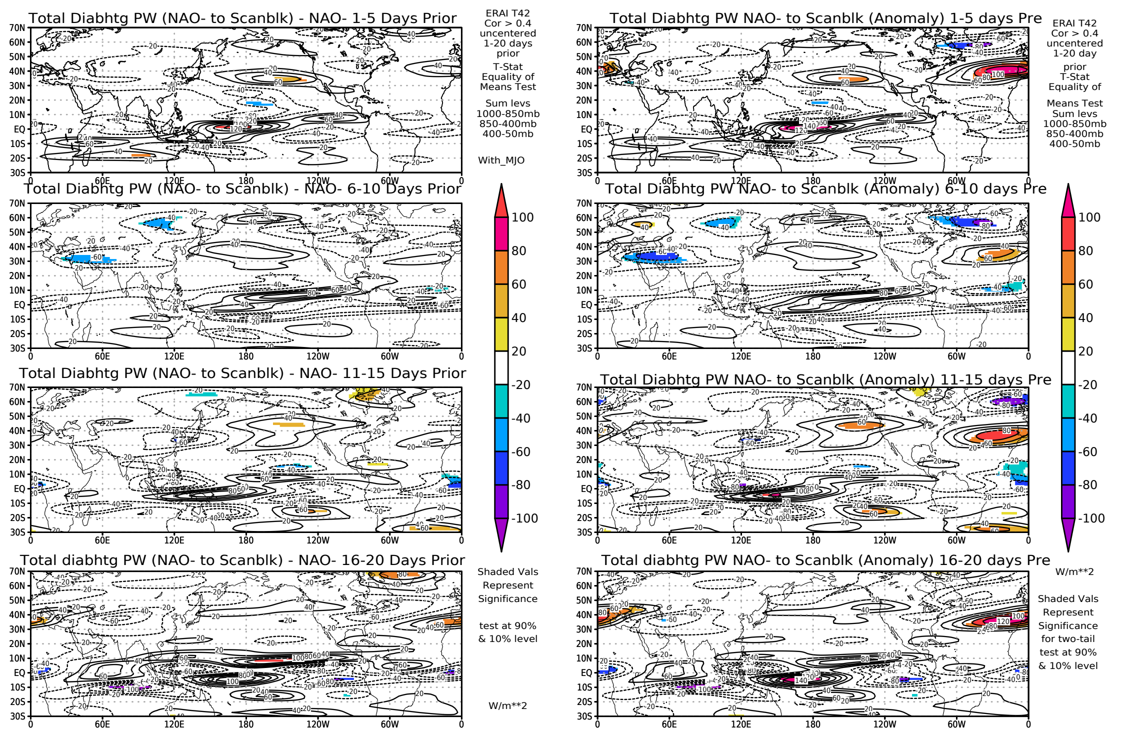

Figure 3.31: The planetary wave heating for the for transition from NAO- to Scandinavian Blocking. The panels on the left show the diabatic heating difference 1-20 days prior to the transition and the composite of the previous regime. The right figure show the anomaly of the days prior to the transition compared to the climatology. Shaded areas are significant at the 90 percent.

The next transition, seen in Figure 3.31, is the NAO- to Scandinavian Blocking transition. A small area of significant tropical heating is seen in the western Pacific at 1-5 days and in the central Pacific days 16-20 days prior to the transition.

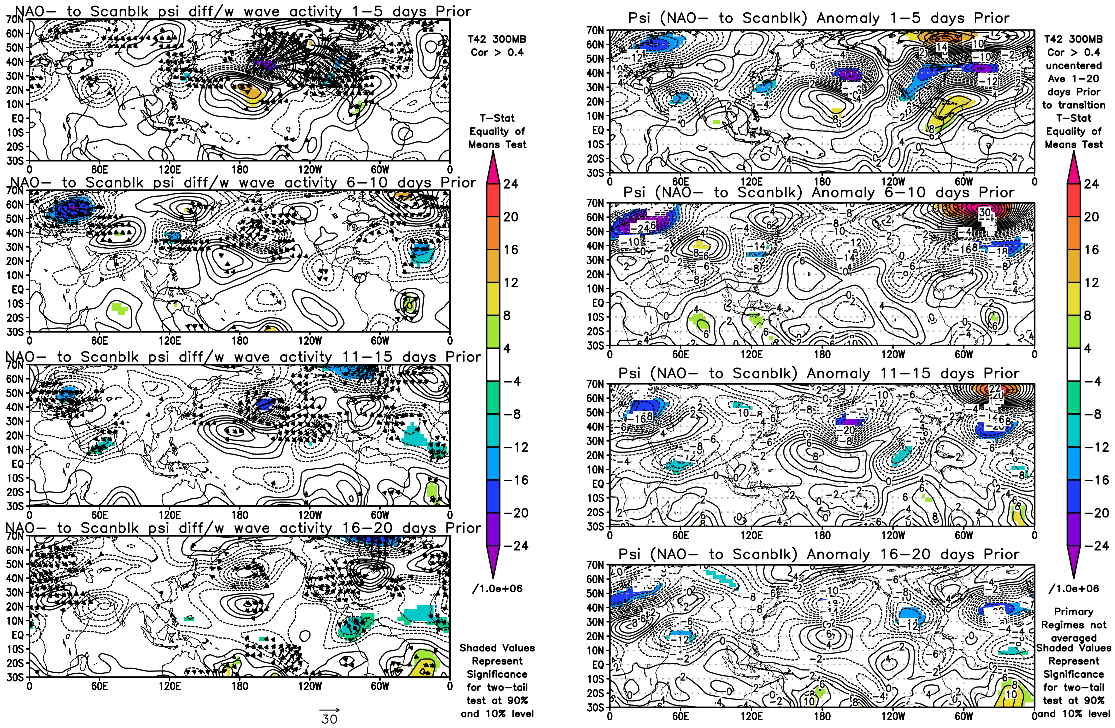

Figure 3.32: The streamfunction and Rossby wave activity for the transition from Atlantic Ridge to Scandinavian Block. The panels on the left are the Rossby wave activity and difference between the days prior to the transition and the Atlantic Ridge regime. Shaded areas are significant at the 90 percent level. The right panel is the anomaly between the days prior to the transition and climatology.

In Figure 3.40, streamfunction differences and streamfunction anomalies both show a very strong mid-latitude wave-train seemingly emanating from tropics into Euro-Atlantic region. Mid-latitude wave trains are also seen emanating from $50^o N$ into tropics near the Indian Ocean 11-20 days prior to the transition.

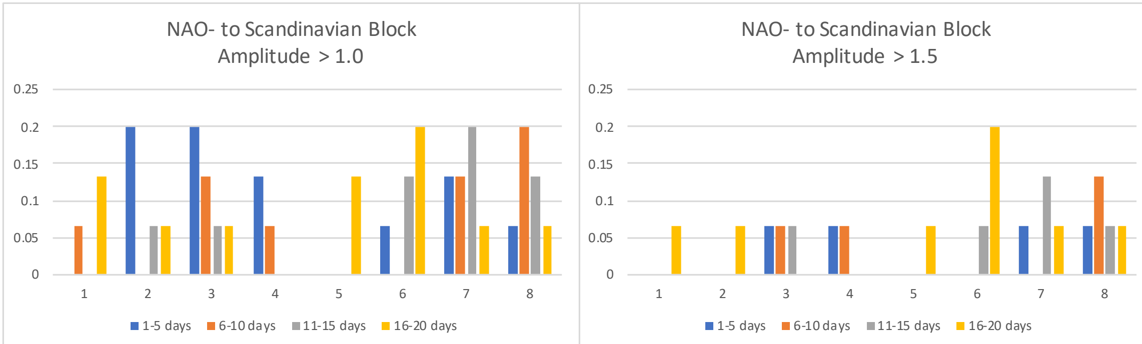

Figure 3.33: NAO- to Scandinavian Block The Graph on left is for MJO amplitudes greater the 1.0, right is greater than 1.5.

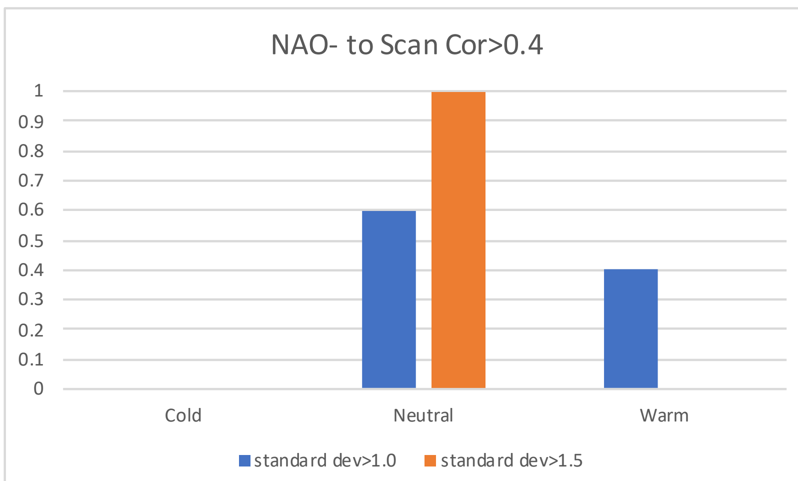

Figure 3.34: NAO- to Scandinavian Block transitions occurrences during cold, neutral, and warm events based on the SST standard deviation of the Nino34 index. Blue bar represents standard deviations greater than 1.0 and the orange bar represents standard deviations greater than 1.5

Figure 3.33 shows that all MJO phases participate, but for strong MJO episodes there is a preference for Phase 6 (heating over central/western Pacific). A little more than a third of the episodes are moderate warm ENSO events (none are strong), with no cold ENSO events as seen in Figure 3.34, however, the majority occur during neutral events with no preference of warm or cold events.

NAO- to NAO+ Transition

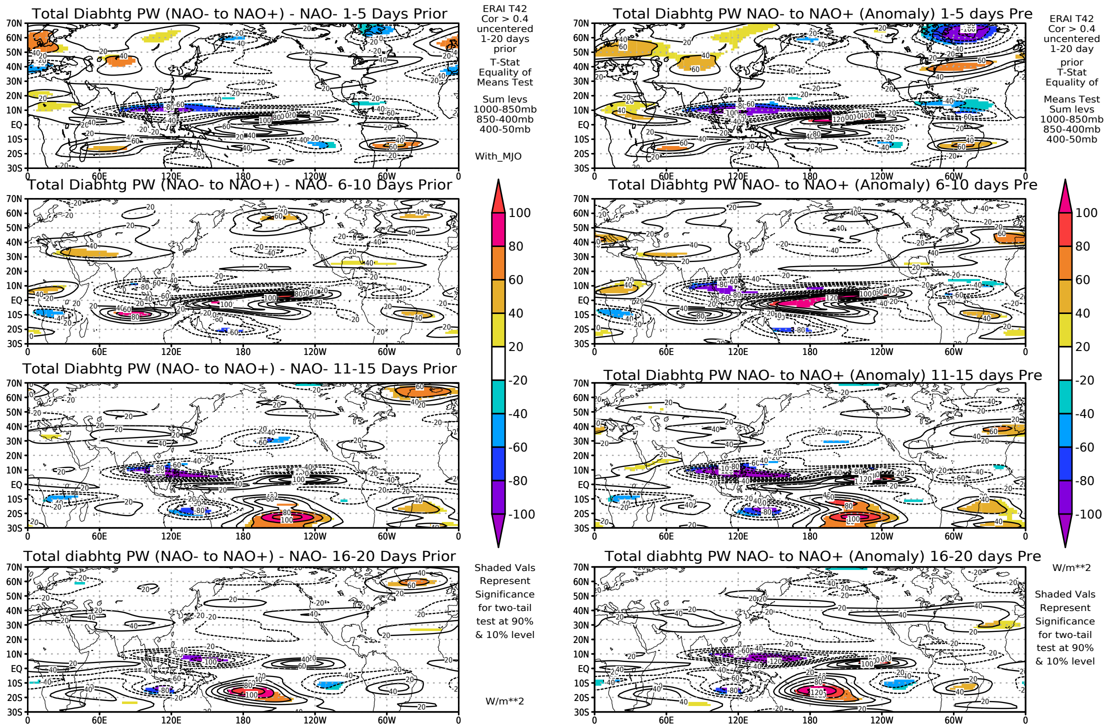

Figure 3.35: Pre-transition planetary scale diabatic heating for transitions from the NAO- to NAO+. The panels on the left show the diabatic heating difference 1-20 days prior to the transition and the composite of the previous regime. The right figure show the anomaly of the days prior to the transition compared to the climatology. Shaded areas are significant at the 90 percent level.

Looking at the NAO- to NAO+ transition in Figure 3.35, Tropical central Pacific heating is seen 1-5 days prior and 6-10 days prior to the transition, but only a small area of significance. Indian Ocean and western Pacific cooling is seen throughout in the tropics. Note at days 1-5 days prior to the transition, the setting up of storm track heating in the North Atlantic is consistent with the formation of the NAO+.

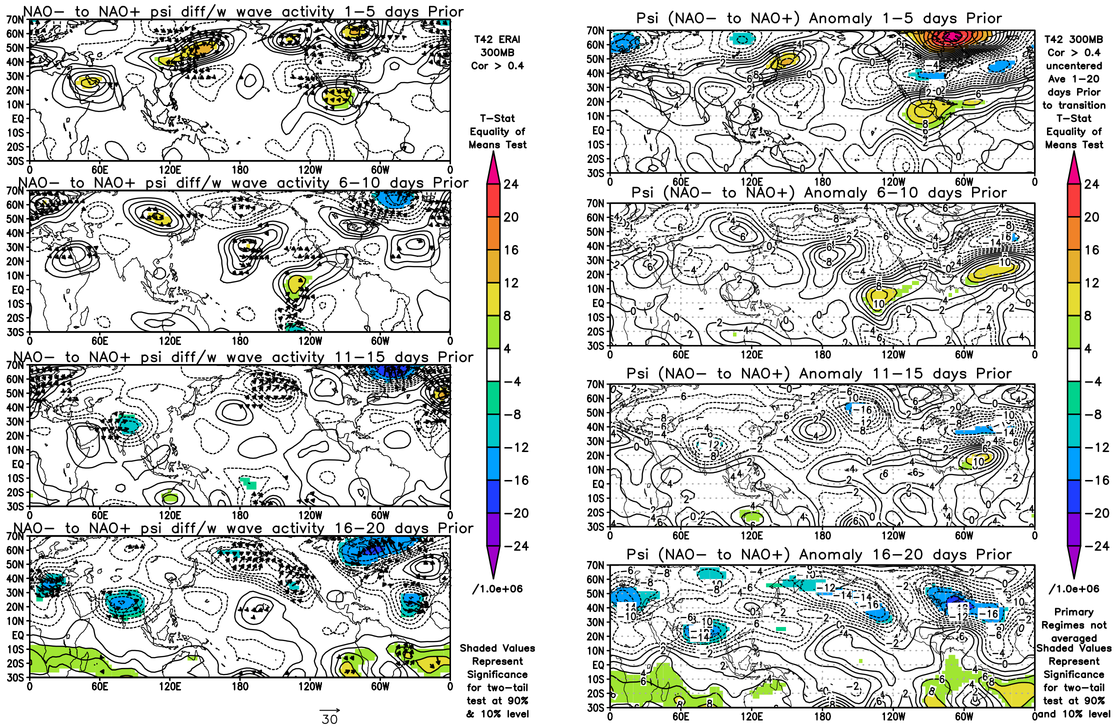

Figure 3.36: The streamfunction and Rossby wave activity for the transition from NAO- to NAO+. The panels on the left are the Rossby wave activity and difference between the days prior to the transition and the NAO- regime. Shaded areas are significant at the 90 percent level. The right panel is the anomaly between the days prior to the transition and the climatology.

From Figure 3.36 the streamfunction difference and anomaly plots for 6-10 days prior show a weak but distinct wave train extending from north-central Asia (55^oN, 120^oE) southeastward all the way to the equator around 140^oW.

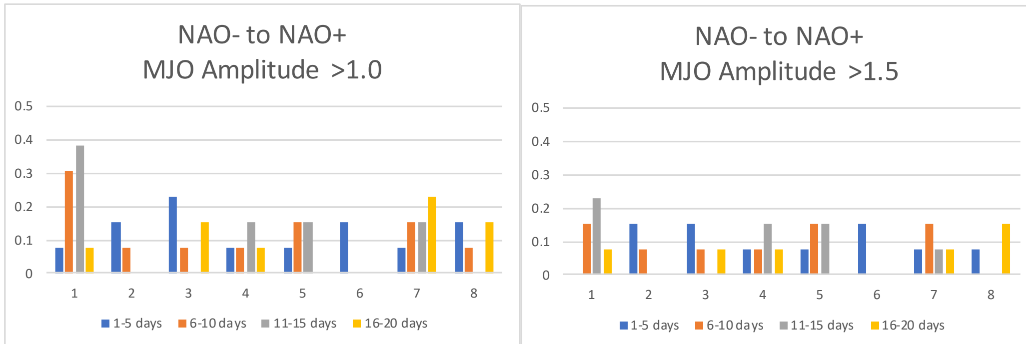

Figure 3.37: Histogram for the 20 day period prior to the transition from NAO- to NAO+. The Graph on left is for MJO amplitudes greater the 1.0, right is greater than 1.5.

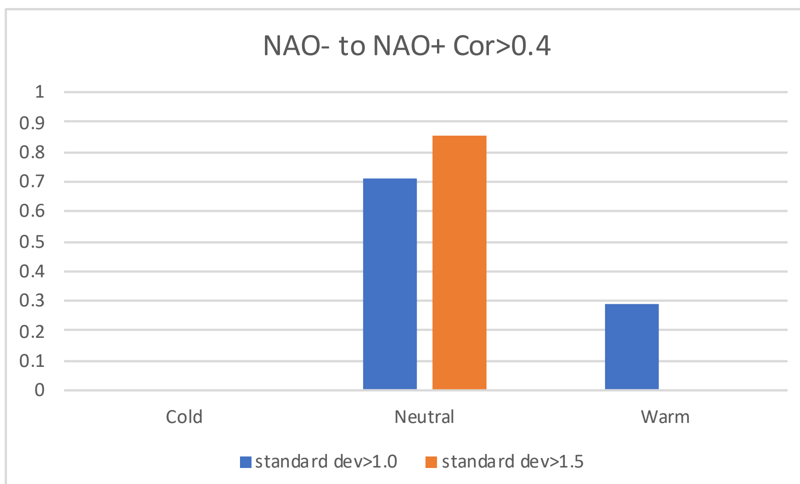

Figure 3.38: NAO- to NAO+ transitions occurrences during cold, neutral, and warm events based on the SST standard deviation of the Nino34 index. Blue bar represents standard deviations greater than 1.0 and the orange bar represents standard deviations greater than 1.5

Figure 3.37 shows that MJO participation in these episodes is quite uniform with respect to phase. Figure 3.38 shows that less than one-third of the episodes occur during a moderate warm ENSO event (none during a strong ENSO event or a cold ENSO event). The vast majority show no preference for warm or cold events.

3.5.4 Transitions from the NAO+

NAO+ to Scandinavian Block Transition

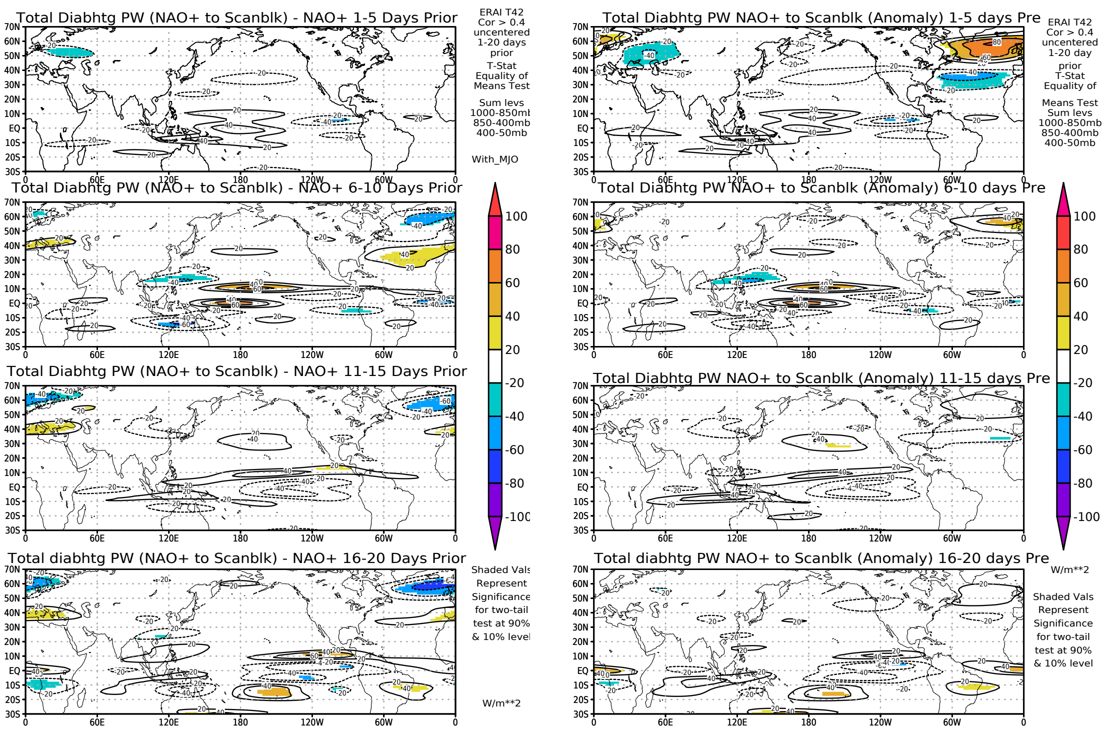

Figure 3.39: Pre-transition planetary scale diabatic heating for transitions from the NAO+ to Scandinavian Blocking. The panels on the left show the diabatic heating difference 1-20 days prior to the transition and the composite of the previous regime. The right figure show the anomaly of the days prior to the transition compared to the climatology. Shaded areas are significant at the 90 percent level.

Figure 3.39 shows the pre-transition heating for the NAO+ to Scandinavian Blocking transition. This is one of the transitions identified by as preferred by Cassou (2008). Small areas of heating in central Pacific, mostly north of the equator, but significance is achieved only at 6-10 days prior. Heating in the storm track regions of the North Atlantic show decay of storm track in preparation for blocking.

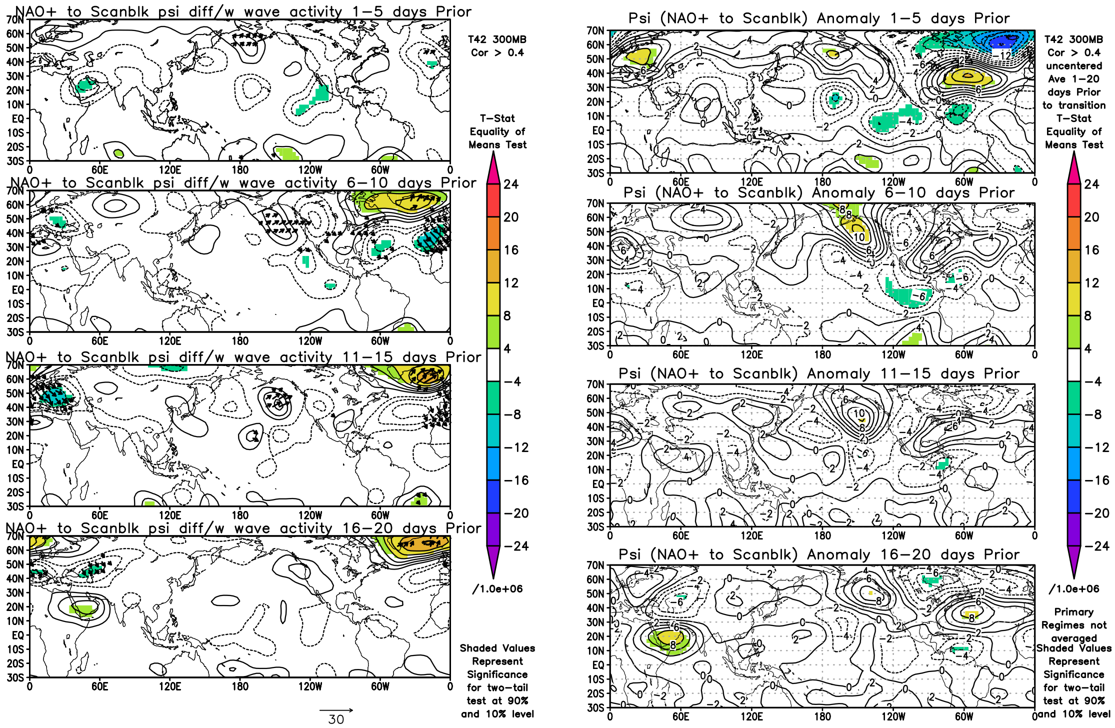

Figure 3.40: The streamfunction and Rossby wave activity for the transition from NAO+ to Scandinavian Block. The panels on the left are the Rossby wave activity and difference between the days prior to the transition and the NAO- regime. Shaded areas are significant at the 90 percent level. The right panel is the anomaly between the days prior to the transition and the climatology.

The maps shown in Figure 3.40 are very quiescent in the tropics in terms of stream function and wave activity. Note that the anomaly 1-5 days prior is weaker than the overall NAO+ anomaly (Figure 3.6), indicating the weakening of the NAO+.

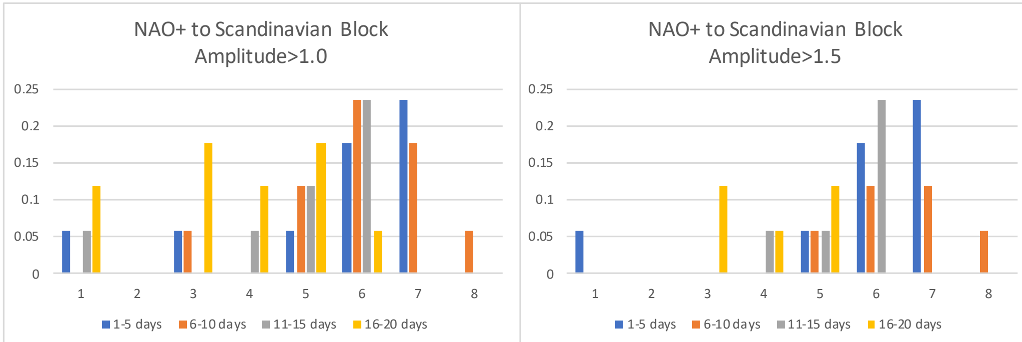

Figure 3.41: The percentage of time in each phase for each 5-day period prior to the regime transition The Graph on left is for MJO amplitudes greater the 1.0, right is greater than 1.5.

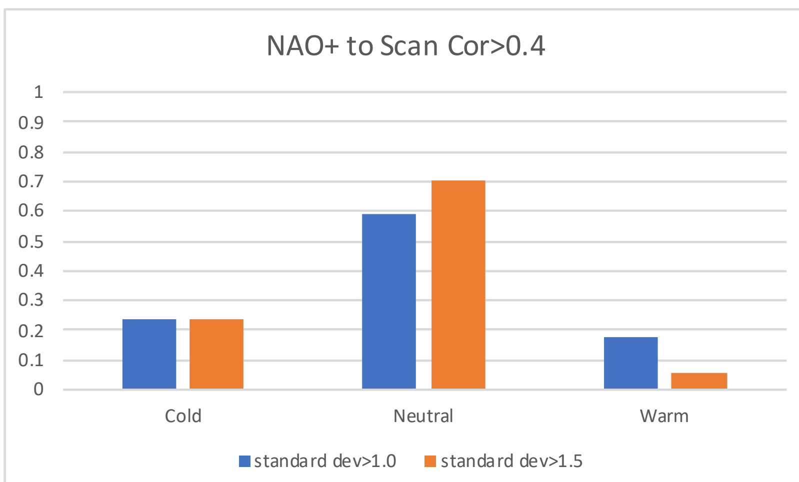

Figure 3.42: NAO+ to Scandinavian Block transitions occurrences during cold, neutral, and warm events based on the SST standard deviation of the Nino34 index. The blue bar represents standard deviations greater than 1.0 and the orange bar represents standard deviations greater than 1.5

Figure 3.41 and 3.42 indicate that all phases of MJO participate with some preference for later phases, and all phases of ENSO (although more than half are neutral) but show no preference for warm or cold events.

NAO+ to Atlantic Ridge Transition

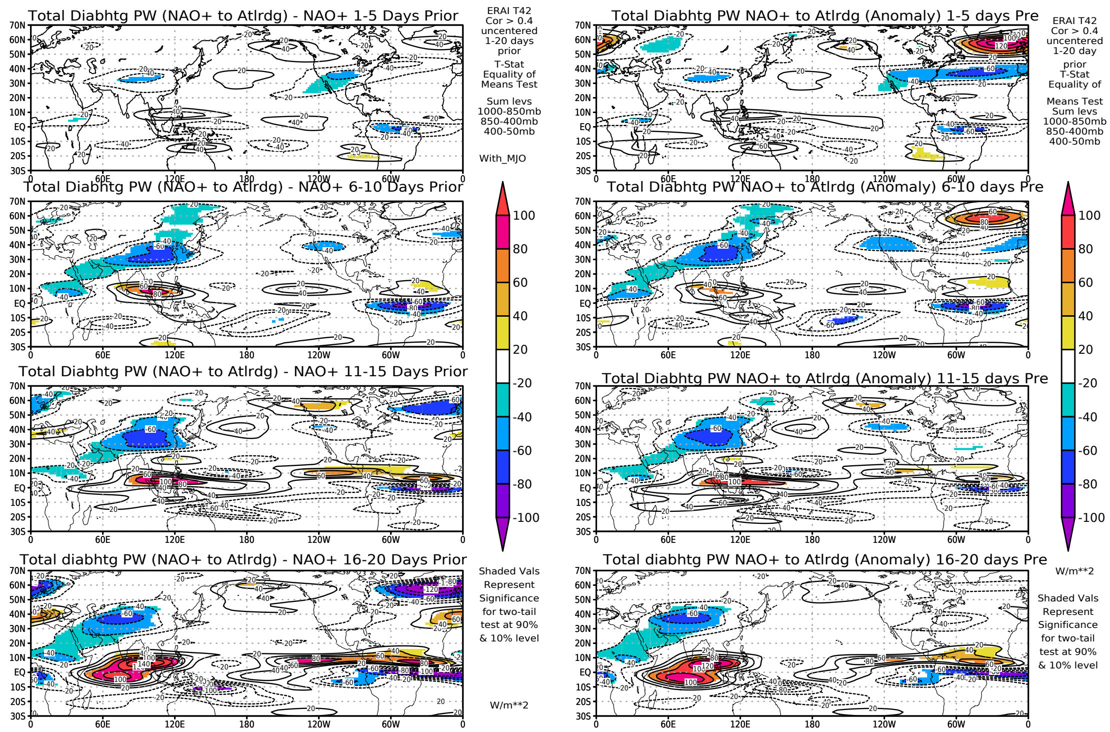

Figure 3.43: The planetary wave heating for the transition from NAO+ to Atlantic Ridge. The panels on the left show the diabatic heating difference 1-20 days prior to the transition and the composite of the previous regime. The right figure show the anomaly of the days prior to the transition compared to the climatology. Shaded areas are significant at the 90 percent level.

Figure 3.43 shows the pre-transiton heating for the NAO+ to the Atlantic Ridge transition. Tropical heating is seen in the Indian Ocean for prior days 6-20. Heating is also evident in the eastern Pacific Ocean (and Atlantic) for days 11-20. Also indicated is the decay of NAO+ storm track heating anomalies up to 6 days prior to the transition.

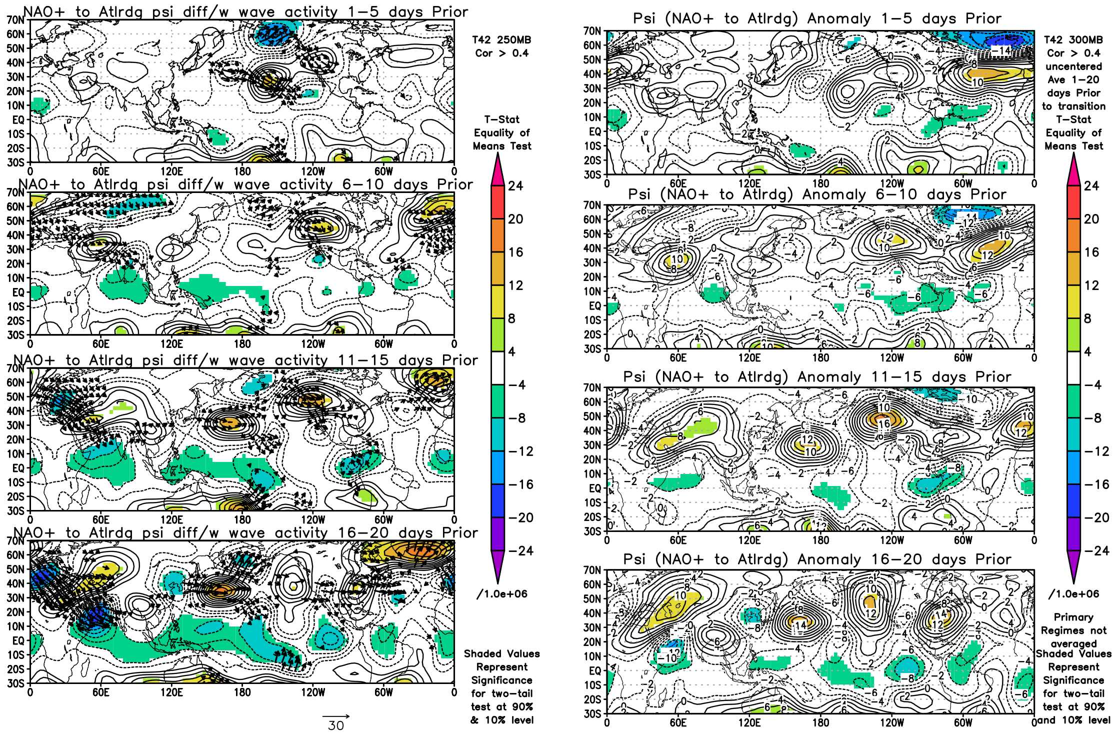

Figure 3.44: The streamfunction and Rossby wave activity for the transition from NAO+ to Atlantic Ridge. The panels on the left are the Rossby wave activity and difference between the days prior to the transition and the NAO- regime. Shaded areas are significant at the 90 percent level. The right panel is the anomaly between the days prior to the transition and the climatology.

Figure 3.44 shows a very strong indication of wave train activity from Euro-Atlantic region southwards and eastwards into tropical Pacific Ocean up to 6 days prior to the transiton. The anomaly of streamfunction 1-5 days prior is weaker than the NAO+ overall streamfunction anomaly which is an indication the NAO+ regime is decaying prior to transition.

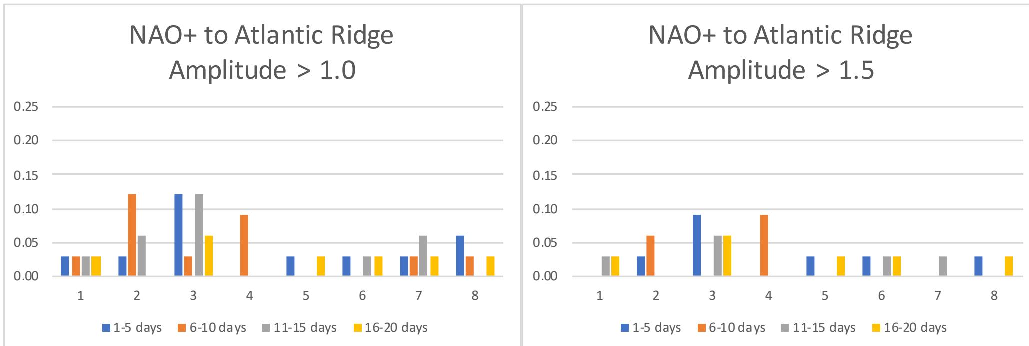

Figure 3.45: NAO+ to Atlantic Ridge transition. The Graph on left is for MJO amplitudes greater the 1.0, right is greater than 1.5.

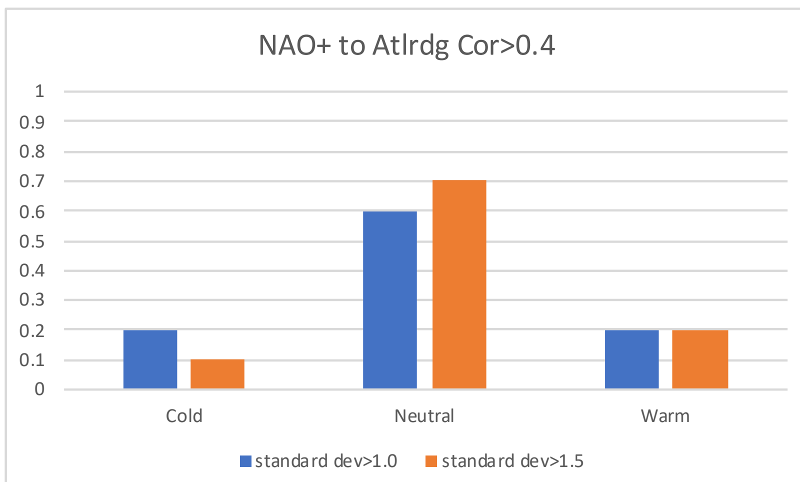

Figure 3.46: NAO+ to Atlantic Ridge transitions occurrences during cold, neutral, and warm events based on the SST standard deviation of the Nino34 index. The blue bar represents standard deviations greater than 1.0 and the orange bar represents standard deviations greater than 1.5

Figure 3.45 shows some indication of a preference for MJO phases 2-4, consistent with Indian Ocean heating. Figure 3.46 shows no preference for warm or cold events.

Chapter 4: Disscussion

During this research, the preferred transitions found were in agreement with previous work by Vautard (1990) and Cassou (2008). The term ”preferred” in this context means that the transitions occur more ofter than would be expected on the basis of the frequency of occurrence of the regimes. Using the ERAI dataset only three regime transitions were found significant at the 95 percent level. They were the two transitions we term ”Cassou transitions”, (NAO+ to Scandinavian Block and Scandinavian Block to NAO-), and the Scandinavian Block to Atlantic Ridge. Using the NCEP-Reananalysis, we found the same two Cassou transitions significant and in addition 3 others. The newly found transitions include the Scandinavian Block to NAO+, NAO- to Scandinavian Block, and Atlantic Ridge to NAO+. Other transitions (non-preferred) did not occur more ofter than would be expected on the basis of the frequency of occurrence of the regimes. Nevertheless these transitions often occur as seen in chapter 3 and can also be preceded by tropical heating.

As presented in Section 1, prior research has indicated that there appears to be a strong relationship between some Euro-Atlantic regimes and the MJO (Cassou, 2008; Lin et al., 2009; Yadav and Straus, 2017; Stan et al., 2017), and others. We determined the MJO relationship in two ways:

- Histograms of phase using the real-time multivariate index of Wheeler and Hendon (2004) to determine the phase and amplitude of the MJO.

- Subtracting the first two principal components of tropical heating and zonal wind for 850hPa and 200hPa that represent the MJO (see appendix B).

The latter method shows almost no change in tropical heating preceding any transition. The difference between the two methods lies in the fact that the use of the index takes into account all states in a given MJO phase.

Considering all the transitions, only the transitions to NAO+ (specifically Scan Block to NAO+), the transitions to NAO-, and the NAO+ to Atlantic Ridge transition, showed any coherent MJO signal. For the transition to NAO+ we see increase just prior to phase 2 and 3. For the NAO- transitions, we see increases prior to phases 6-7. It should also be noted that despite the an apparent relationship in the histograms, the percentages of frequency occurrence of any one phase does not exceed 30 percent in almost all cases.

We examine the two transitions discussed in detail by Cassou (2008), namely NAO+ to Scandinavian Block (SB), and SB to NAO-. in terms of tropical heating generally and specifically to see if there was a relationship with the MJO. The NAO+ to Scandinavian Block transition (Figure 3.39), shows some areas of diabatic heating in the central Pacific that don't seem to be moving in an eastward direction as would be expected if associated with the MJO. This transition seems to be forced from mid-Pacific, (starting 6 to 10 days prior), but perhaps this is partly due to Indian Ocean heating that forced the NAO+ propagating eastward.

Finding that the MJO influence on midlatitude blocking (Scandinavian Block and NAO-) is relatively weak on interannual time scales, Gollan and Greatbatch (2017) point out that on shorter time scales, early MJO phases are associated with weakened blocking over Europe and late phases are associate with strengthened blocking over Europe, in agreement with Cassou (2008) and Henderson et al. (2016).

When we look at the Scandinavian Block to NAO- transition, Figure 3.11, we see large area of significant heating covering a great deal of the tropics. A shift in Atlantic Intertropical Tropical Convergence Zone (ITCZ) is indicated 1-5 days prior to transition. Perhaps this northward shift plays a role in increased moisture in the Atlantic Storm Track. Cassou (2008) found evidence that this increased moisture helped destabilize the atmosphere upstream from the North Atlantic storm track. They found that this destabilized atmosphere favors CWB (Cyclonic Wave Breaking) and could thus be an additional factor to the increased occurrence of the NAO- regime.

In addition to Cassou, Henderson et al. (2016) found that prior to phase 6, a negative

PNA pattern may serve as a wave guide that redirects Rossby wave energy toward Europe (also see Branstator (2002)). The presence of significant heating 11-15 days prior to the transition shows that tropical forcing in the eastern Pacific is involved. This is completely consistent with the Rossby wave source seen in Cassou (2008) Figure 6b (Supplementary Figure) seen an 25^oN 110^oW. The second mechanism proposed by Cassou (2008) to explain the teleconnection between MJO and NAO- depends on direct tropical forcings originating from the eastern Pacific. Despite weak anomalous convection just prior to the transition, phase 6 is associated with tropical upper-level divergence in the eastern Pacific around 120W. This leads to advection of absolute vorticity by the divergent outflow from the MJO and to enhanced momentum convergence to the north around 30N. This is consistent with a Rossby wave source around 20N, 110W. This forcing initiates a downstream northeastward propagating wave train towards the EA region.

Chapter 5: Summary and Conclusion

5.1 Summary

We have investigated the interactions between the tropics and extratropics in the context of the Euro-Atlantic (EA) circulation regimes and their transitions during boreal winter. The background tropical (planetary wave) diabatic heating anomalies, defined as the heating associated with any one of the four EA regimes minus the average heating in all other regimes, lie in in the range of $40 - 60\,Wm^{-2}$ in the the central Pacific. For transitions from each regime, we form one type of anomaly by taking the difference between the heating prior to the transition and the background heating of the regime being transitioned from. We restrict the analysis to transitions which occur when the atmospheric circulation anomaly has a pattern correlation of at least 0.40 (and on average over 0.60) with one regime for the 5 days prior to a transition into a second regime, in which the atmosphere remains for at least 5 days. The sequence of heating anomalies depends on the particular group of trajectories. The following summary is organized by which regime is being transitioned from, that is from the point of view of making a forecast transition from a known regime:

- *Scan Block to NAO- transitions:* Strong, statistically significant, heating anomalies appear in the central and eastern Pacific 11-20 days prior to the transition, with less heating in the equatorial Atlantic and Indian Oceans just north of the equator for 11-20 days prior to the transition, but diminish in size and scope as the transition is approached. A significant dipole of Atlantic diabatic heating/cooling at around $30^oN/50^oN$, is seen 11-20 days prior to the transition. Wave activity flux vectors for ranges of 6-15 days prior show strong propagation from high latitudes equatorward into the Indian Ocean, indicating that the mid-latitude dynamics preceding these transitions contributes to the Indian Ocean equatorial heating. While all phases of the MJO (as defined by the conventional Wheeler-Hendon index) may be found in examples of this transition, there is a preponderance of Phases 5 to 7 (heating in the Pacific Ocean). The apparent role of Pacific Ocean heating anomalies 6-15 days ahead of these transitions is consistent with previous MJO-focused studies showing the NAO- occurrence peaking after Pacific Ocean convection. The involvement of the equatorial and mid-latitude Atlantic heating is new.

- *Scan Block to NAO+ transitions:* The areas of strong and significant heating anomalies prior to this transition are confined to the equatorial Indian Ocean at lags of 6-15 days, with diminishing strength 1-5 day prior. There is a strong indication of wave activity propagating from mid-latitudes towards the equatorial Indian Ocean from 20 up to 6 days prior, suggesting that the Indian Ocean heating and NAO+ development for the trajectories undergoing this transition are coupled. The presence of strong Indian Ocean heating and weaker heating elsewhere is consistent with the preference for phases 2 and 3 seen in the Wheeler-Hendon indices.

- *Scan Block to Atlantic Ridge transitions:* A region of heating in the western Pacific at about $15^o S$ is seen for all lags, although it becomes less significant as the lag decreases. In high latitudes looking at the difference pattern, there is heating over Northern Europe and cooling off the coast of Newfoundland and is just the opposite of the climatological pattern of heating prior to the Scandianvian Block (SB), as would be expected (Figure 3.7). The difference between the pre-transition days and the normal SB has a pattern very similar to the anomalies from climatology except in the EA regions. The difference plots show the dissolution of the SB (days 20 to 6 prior), and then the beginning of the formation of the Atlantic Ridge at 1-5 days prior. The decay of the Scandinavian Block at 16-20 days is associated with strong wave activity from Northern Canada. The anomaly 1-5 days prior is some what more diffuse than the total Scandinavian Block anomaly. Wave activity is seen propagating from Northern Europe eastward and equatorward towards mid-latitudes, but does not reach the subtropics, consistent with little heating north of the equator. All phases of the MJO are represented, although some preference for the later phases (5-7). Most of these transitions occur during neutral ENSO years.

- *NAO+ to Scan Block transitions:* Small areas of heating in central Pacific, mostly north of the equator, but significance is achieved only at 6-10 days prior. Heating in storm track regions in North Atlantic show decay of storm track in preparation for blocking. The tropics are very quiescent in terms of stream function and wave activity. It should be noted that the anomaly 1-5 days prior is weaker than overall NAO+ anomaly, so that NAO+ weakens. All phases of MJO participate, and all phases of ENSO (although more than half are neutral). Local dynamics (including synoptic eddy fluxes) may play a role in this path to blocking onset, but tropical forcing does not.

- *NAO+ to Atlantic Ridge:* Tropical heating is seen in the Indian Ocean for days 6-20 days prior to the transition and also in eastern Pacific Ocean (and Atlantic) for days 11-20. There is a decay of NAO+ storm track heating anomalies up to 6 days prior. There is a very strong indication of wave train activity from Euro-Atlantic region southwards and eastwards into tropical Pacific Ocean up to 6 days prior. The anomaly of streamfunction 1-5 days prior is weaker than the NAO+ overall streamfunction anomaly, so NAO+ is decaying prior to transition. A clear indication of preference for MJO phases 2-4 is seen, consistent with Indian Ocean heating. Very few episodes during warm ENSO events, about 20 percent for cold ENSO events, so the heating in the eastern Pacific is NOT due to ENSO.

- *NAO- to Scan Block transitions:* Small area of significant tropical heating in western Pacific days 1-5 and central Pacific days 16-20. Streamfunction differences and anomalies both show very strong mid-latitude wave-trains seemingly emanating from tropics into Euro-Atlantic region. We see mid-latitude wave trains emanate from

$50^o N$ into tropics near the Indian Ocean earlier on (days 16-20, 11-15). The 1-5 day prior anomaly is very similar to the overall NAO- anomaly, but shifted westward. This change may signal this transition. All MJO phases participate, but for strong MJO episodes there is a preference for Phase 6 (heating over central/western Pacific). About a third of the episodes are moderate warm ENSO events (none are strong), with no cold ENSO events.

- *NAO- to NAO+ transitions:* Contrary to the other transitions into the NAO+, this one is preceded by significant Northern equatorial Indian Ocean cooling from 15 days prior forward, with significant central Pacific equatorial heating (6-10 days prior), which may be partly stimulated by equatorial wave activity originating from the subtropics. There is a slight preference for phase 1 of the MJO, although every phase of the MJO is seen at each lag.

- *Atlantic Ridge to Scan Block transitions:* Very little evidence of tropical heating is seen, but heating is seen around $30^o N$ in eastern Pacific 11-20 days prior. Also, enhancement of North Atlantic storm track is evident around $50^o N$ 11-15 days prior. Wave activity is seen propagating southward and eastward into the subtropics 6-10 days prior around $60^o E$ and into the tropics around $150^o W$, but with no indication of associated diabatic heating. Most MJO phases participate in this transition, (except phase 3), but further back than 5 days only phases 4-8 participate. Most episodes occur during neutral ENSO years

- *Atl Ridge to NAO- transitions:* Strong, statistically significant, heating anomalies appear in the Indian, Pacific and Atlantic Oceans just north of the equator for 11-20 days prior to the transition, but as the transition is approached (6-10 days prior) the heating is more confined to the Indian Ocean and even closer to the transition to the western Pacific. There is little indication of equatorward propagation of wave activity vectors. A significant dipole of Atlantic diabatic heating/cooling at around $50^o N/70^o N$ 11-20 days prior to the transition is entirely consistent with the southward shift of storm tracks associated with NAO-, although this is strongest 15-20 days prior to the transition, indicating an in situ role for diabatic heating. Contrary to the Scan Block to NAO- transitions, there are no preferred phases of the MJO.

- *Atl Ridge to NAO+ transitions:* Strong heating just north of the equator extending from the central Pacific and across the Atlantic is accompanied by cooling along the equator for days 16-20 prior to the transition, along with strong Indian Ocean heating. As the lag lessens, the heating anomalies diminish, with the Indian Ocean heating essentially disappearing 11-15 days prior, and then reappearing in a modest way at $10^o S$ 1-5 days prior to the transition. There is no evidence of mid or high-latitude Rossby wave forcing of equatorial disturbances, and no particular MJO phase is preferred. Of interest is the appearance of significant diabatic heating in the Atlantic at mid-latitudes ($50^o N$) 11-20 days prior to the transition. The high-latitude circulation is affected by this heating as seen in the strong poleward fluxes of wave activity.

5.2 Conclusions

A substantial amount of previous work has been focused on the MJO-related forcing of the NAO-related Euro-Atlantic regimes, while the processes leading to transitions between regimes have been largely studied from a mid-latitude point of view. Almost no connection has been made between these two schools of thought. We have shown that the overall composites of tropical planetary wave diabatic heating vary from regime to regime and so we measure anomalies of heating prior to transitions as differences with respect to these regime-specific composites.

We have examined the large-scale tropical and extra-tropical heating along particular sets of trajectories (evolutions) which undergo clear transitions between states in one regime to those in another, and found that different transition paths to the same regime are associated with different evolutions of diabatic heating, both tropical and mid-latitude. In some cases the tropical heating (e.g. Atlantic heating prior to the Scan Block to NAO- transition) is itself influenced by the Rossby wave activity originating from the Euro-Atlantic region, while the involvement of mid-latitude heating (presumably related to storm track shifts) is seen up to 20 days prior to some of the transitions.

We have found that for most of transitions examined, there is not a clear preference for any specific traditional MJO phase prior to the transition, nor does subtracting the diabatic heating specifically related to the MJO make a large difference. From this we conclude not that the MJO is unimportant, for it is possible that existing diagnostics of the MJO are likely too restrictive. In any case, the emphasis in using heating to predict transitions should be on the complete structure of heating. The detailed mechanisms behind the tropical-extratropical interactions (for example the Scan Blocking to NAO- transition), and the role of mid-latitude heating (in for example the Atlantic Ridge to NAO+ transition) should be studied in the future using large ensembles of simulations and forecasts.

We have shown tropical heating almost certainly plays a role in the transition of some of the Euro-Atlantic regimes. Of course, this is not a new finding, Cassou (2008); Henderson et al. (2016); Yadav and Straus (2017); Gollan and Greatbatch (2017); Henderson and Maloney (2018) and others have established that certain phases of the MJO can lead to an increase in transitions to the NAO+, Scandinavian Block, and NAO-.

What is new is that we show when heating in the tropics plays a role in the transition of Euro-Atlantic Regimes, a preferred phase of the MJO is typically present in no more than 30 percent of the episodes. This is not to say previous work on the relationship between the MJO and Euro-Atlantic Regimes is not valid, we are simply saying the MJO is not required. This was seen in the Scandinavian Block to NAO- transitions where we found similar results to Cassou (2008) and Yadav and Straus (2017) that an increase is seen following MJO phase 6-7. However, we also found that in more that 70 percent of the episodes during the boreal winter, it did not follow the MJO. Most importantly in 7 of the 9 cases of the Scandinavian Block to the NAO- transition, tropical Pacific heating is present prior to transition suggesting this heating is a probable prerequisite regardless of the cause of the heating. We also found that tropical Atlantic heating was evident in some of the transitions. Grimm (2019) found that South American and south Atlantic convection may play a role in MJO initiation in the Indian Ocean but may also serve as a Rossby wave source affecting the Euro-Atlantic region.

We have shown that warm and cold events ENSO do not play much of a role in regime transitons. This can be understood in the context of what Swenson and Straus (2015) found, that even during warm or cold events, the tropical diabatic heating is highly variable. We have also shown that prior to some of the transitions, there is a tropical response to the mid-latitude forcing.

The goal of this thesis was to answer the following questions:

1. Assess which transitions are related to tropical heating, including the location of the heating:

    - We show that in terms of transitions into Scan Block, of the three, only the NAO- to Scandinavian Block seems to involve tropical forcing, especially from the eastern Pacific and the tropical Atlantic.
    - Both transitions to the NAO- involve tropical heating.
    - NAO+ to Atlantic Ridge show tropical heating including the eastern Indian Ocean and tropical Atlantic.
    - Scandinavian Block to NAO+ shows heating particularly in the Indian Ocean.

2. Assess the role of MJO tropical heating vs. non-MJO related tropical heating:

    - Only four transitions clearly involved MJO related heating, Scandinavian Blocking to NAO- (following MJO phases 5-7), SB to NAO+ (phases 3-4), NAO- to NAO+ (phase 1), NAO+ to Atlantic Ridge (phase 2-4).
    - The majority of these transitions were not associated with a particular phase of the MJO.

3. Assess whether the regime themselves or their transitions play a role in stimulating tropical heating.

    - Six of the 10 transitions appear to stimulate tropical heating. Atlantic Ridge to Scan Block, Scan Block to Atlantic Ridge, Scan Block to NAO-, Atlantic Ridge to NAO-, Scan Block to NAO+, and the Atlantic Ridge to NAO+ transition.

5.3 Unanswered Questions and Future Research

Our results have raised several questions regarding the origin of the precursor tropical heating, and the physical mechanisms by which tropical heating affects the regimes. In particular, does the Atlantic heating seen prior to some of the transitions result from a shift of the ITCZ or an overall strengthening of the ITCZ? Does the Atlantic tropical heating influence the regime transitions indirectly via the storm tracks? We also have no explanation for the remarkable result that tropical heating throughout the Pacific and Atlantic regions is consistently seen far in advance of the Scandinavian Block to NAO- transition.?

Looking forward to the possible application of these findings to forecasting regime transitions, our results can be used to construct indices based on tropical heating (or outgoing long-wave radiation) and test the usefulness of such indices in forecasts. One area of concern is the role of the systematic model error in the basic state in distorting the regime transition response to tropical heating. Investigation of this awaits the future.

Appendix A: Statistical Significance of k-means clusters

The k-means algorithm will almost always converge to a set of clusters for any value of k, independent of the number of distinct maxima in the multi-dimensional probability distribution function (pdf). It is therefore necessary to have a procedure for distinguishing the results of a cluster analysis from the results that would have been obtained had the Principal Components been truly independent of each other, thereby precluding multiple local maxima in the pdf. This can be achieved by defining a distinct stochastic process *for each PC* in such a way that (i) the synthetic data sets generated from these processes capture some desired property of the PC time series, and (ii) the synthetic data sets generated using the processes for distinct PCs are statistically independent. Using realizations of each process for each PC, a large number N_s of synthetic data sets, each with the same number of points (times) and the same dimension (number of PCs) as the original data set are generated, and cluster analysis applied to each. The percentage of these N_s cluster analyses for which the ratio variance is less than that of the original data yields a confidence level, which in our case exceed 99%. The approach used to generate the synthetic series for each individual PC aims at approximating the auto-correlation at all time lags computed from the observed PC time series. This "random phase approximation" was introduced by Christiansen (2007) , and modified for use of seasonal data by Straus (2010) and Straus et al. (2017).

Appendix B: Significance Testing

B.1 Significance Testing

For the heating anomaly and difference maps shown in the next section, significance was found using the statistic equality of means test. To determine the significance of the frequency of transitions, a bootstrap with replacement method was applied 1000 times. In this context, significance measures whether the frequency of a particular transition is higher than would be expected based on the overall frequency of regimes and thus identifying "preferred" regimes. In the bootstrap procedure, a large number of synthetic data sets of cluster assignments is generated. Each synthetic data set has 132 daily entries for each of 35 years each corresponding to a 5-day running mean in the original data set. For each daily entry (for day d), the cluster assignment used is the ERAI cluster assignment for a randomly chosen pentad and year. However, if that ERAI cluster assignment is the first of N five-day running means assigned to the same cluster (say cluster m) in the ERAI record, the entire block of d to d+N-1 in the synthetic data set is assigned to cluster m. This method uses replacement meaning that the same randomly chosen ERAI dates may be selected multiple times.

The next step is to determine regime transitions. The technique for finding synthetic transitions is the same set of rules used to compute the significance of the real data. The data must remain in the regime for at least 5 consecutive 5-day running mean and must have a positive correlation to the current regime. The day of transition is considered the day the data goes into a new regime. Once in the new regime, the data must remain in that new regime for at least 5 running 5-day means. If the number of transitions between cluster A and cluster B is NAB in the real (reanalysis or reforecast) record, this is considered significant if the same number exceeds NAB for only 5 percent or fewer of the synthetic data sets.

Appendix C: MJO Calculation Based on Diabatic Heating

In order to obtain the manifestation of the MJO we use a process similar to that of Wheeler and Hendon (2004) , in which the the (tropically averaged 15^oN to 15^oS) outgoing longwave radiation (OLR) and zonal wind at 850hPa and 200hPa are used as input to principal component analysis. In our calculation OLR is replaced by the vertically integrated diabatic heating. We then apply a regression of the full vertically integrated heating maps on to the two leading PCs (shown in Figure C.2). The regression patterns of the heating on the leading two PCs are shown in Figure C.1 These two EOFS explain about 34 percent of the total variance, while the lag-correlation between the leading two modes indicates eastward propagation (shown in Figure C.2).

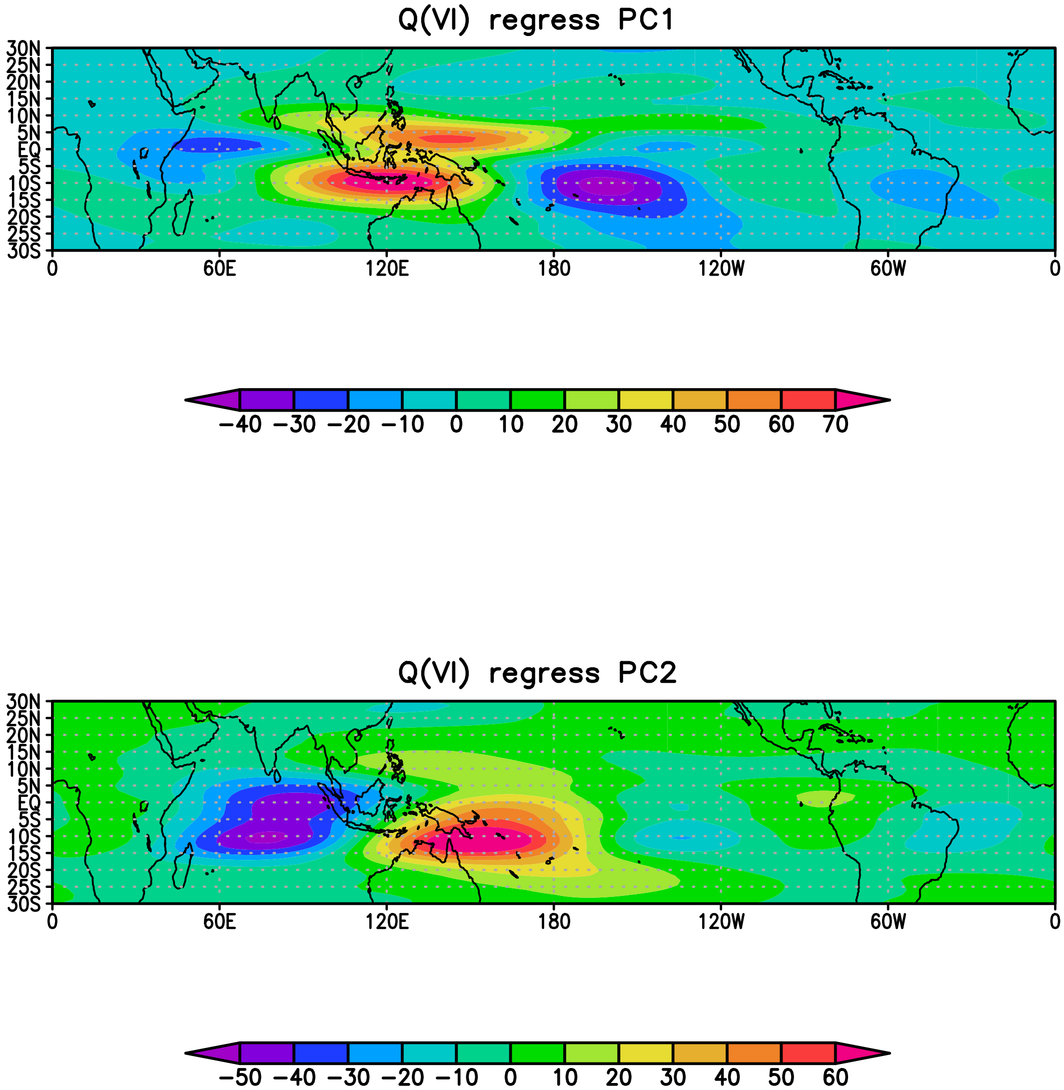

Figure C.1: Regression of the vertically integrated heating on each PC (The units are Watts/m**2 per standard deviation of the PC).

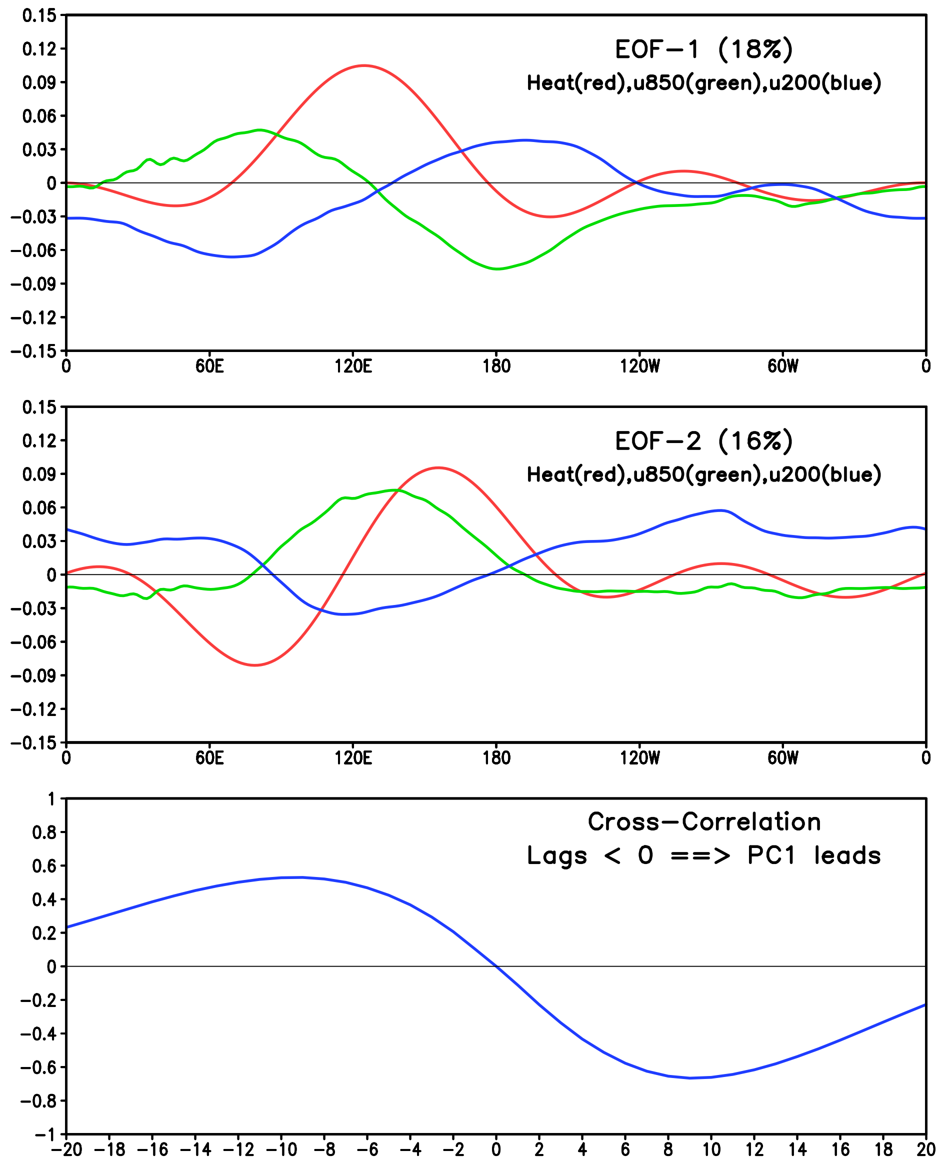

Figure C.2: First two EOFs of the diabatic heating, u850, and u200. The bottom panel show the Lag correlation between pc1/pc2 of heating. The lag-correlation between the leading two modes indicates eastward propagation

Bibliography

Amini, S. and D. M. Straus, 2018: Control of storminess over the pacific and north america by circulation regimes. *Climate Dynamics*.

Attard, H. E. and A. L. Lang, 2019: Troposphere-stratosphere coupling following tropospheric blocking and extratropical cyclones. *Monthly Weather Review*, **147 (5)**, 1781–1804, doi:{10.1175/MWR-D-18-0335.1}.

Barnes, E. A. and D. L. Hartmann, 2010: Dynamical feedbacks and the persistence of the nao. *Journal of the Atmospheric Sciences*, **67 (3)**, 851–865, doi:10.1175/2009JAS3193.1, URL `https://doi.org/10.1175/2009JAS3193.1`.

Baur, F., 1951: *Compendium of Meteorology*, chap. Extended-Range Weather Forecasting, 814–833. American Meteorological Society, Boston, MA.

Baxter, S. and S. Nigam, 2013: A subseasonal teleconnection analysis: PNA development and its relationship to the NAO. *Journal of Climate*, **26 (18)**, 6733–6741, doi:10.1175/JCLI-D-12-00426.1, URL `https://doi.org/10.1175/JCLI-D-12-00426.1`, `https://doi.org/10.1175/JCLI-D-12-00426.1`.

Branstator, G., 2002: Circumglobal teleconnections, the jet stream waveguide, and the north atlantic oscillation. *Journal of Climate*, **15 (14)**, 1893–1910, doi:10.1175/1520-0442(2002)015⟨1893:CTTJSW⟩2.0.CO;2, URL `https://doi.org/10.1175/1520-0442(2002)015<1893:CTTJSW>2.0.CO;2`.

Cassou, C., 2008: Intraseasonal interaction between the Madden-Julian Oscillation and the North Atlantic Oscillation. *Nature*, **455 (7212)**, 523–527, doi:{10.1038/nature07286}.

Cassou, C., 2010: Euro-atlantic regimes and their teleconnections ECMWF. seminar on predictability in the european and atlantic regions, URL https://www.ecmwf.int/sites/default/files/elibrary/2012/8609-euro-atlantic-regimes-and-their-teleconnections.pdf.

Charney, J. G. and J. G. DeVore, 1979: Multiple flow equilibria in the atmosphere and blocking. *Journal of the Atmospheric Sciences*, **36 (7)**, 1205–1216, doi:10.1175/1520-0469(1979)036⟨1205:MFEITA⟩2.0.CO;2, URL https://doi.org/10.1175/1520-0469(1979)036<1205:MFEITA>2.0.CO;2.

Charney, J. G. and D. M. Straus, 1980: Form-drag instability, multiple equilibria and propagating planetary waves in baroclinic, orographically forced, planetary wave systems. *Journal of the Atmospheric Sciences*, **37 (6)**, 1157–1176, doi:10.1175/1520-0469(1980)037⟨1157:FDIMEA⟩2.0.CO;2, URL https://doi.org/10.1175/1520-0469(1980)037<1157:FDIMEA>2.0.CO;2.

Christiansen, B., 2007: Atmospheric circulation regimes: Can cluster analysis provide the number? *Journal of Climate*, **20 (10)**, 2229–2250, doi:10.1175/JCLI4107.1, URL https://doi.org/10.1175/JCLI4107.1.

Dee, D. P., et al., 2011: The ERA-Interim reanalysis: configuration and performance of the data assimilation system. *Quarterly Journal Of The Royal Meteorological Society*, **137 (656, A)**, 553–597, doi:{10.1002/qj.828}.

F. Panagiotopoulos, M. Shahgedanova, and D.B. Stephenson, 2002: A review of northern hemisphere winter-time teleconnection patterns. *J. Phys. IV France*, **12 (10)**, 27–47, doi:10.1051/jp4:20020450, URL https://doi.org/10.1051/jp4:20020450.

Ferranti, L. and S. Corti, 2011: New clustering products. *ECMWF Newsletter*, **127**, 6–11.

Ferranti, L., S. Corti, and M. Janousek, 2015: Flow-dependent verification of the ECMWF ensemble over the Euro-Atlantic sector. *Quarterly Journal Of The Royal Meteorological Society*, **141 (688, A)**, 916–924, doi:{10.1002/qj.2411}.

Franzke, C., S. Lee, and S. B. Feldstein, 2004: Is the north atlantic oscillation a breaking wave? *Journal of the Atmospheric Sciences*, **61 (2)**, 145–160, doi:10.1175/1520-0469(2004)061⟨0145:ITNAOA⟩2.0.CO;2, URL `https://doi.org/10.1175/1520-0469(2004)061<0145:ITNAOA>2.0.CO;2`.

Franzke, C., T. Woollings, and O. Martius, 2011: Persistent Circulation Regimes and Preferred Regime Transitions in the North Atlantic. *Journal Of The Atmospheric Sciences*, **68 (12)**, 2809–2825, doi:{10.1175/JAS-D-11-046.1}.

Ghil, M. and K. Mo, 1991: Intraseasonal oscillations in the global atmosphere. part i: Northern hemisphere and tropics. *Journal of the Atmospheric Sciences*, **48 (5)**, 752–779, doi:10.1175/1520-0469(1991)048⟨0752:IOITGA⟩2.0.CO;2, URL `https://doi.org/10.1175/1520-0469(1991)048<0752:IOITGA>2.0.CO;2`.

Ghil, M. and A. Robertson, 2002: *"Waves" vs. "particles" in the atmosphere's phase space: A pathway to long-range forecasting?*, Vol. 99 Suppl 1. National Academy of Sciences, 2493–500 pp., doi:10.1073/pnas.012580899.

Gollan, G. and R. J. Greatbatch, 2017: The relationship between northern hemisphere winter blocking and tropical modes of variability. *Journal of Climate*, **30 (22)**, 9321–9337, doi:10.1175/JCLI-D-16-0742.1, URL `https://doi.org/10.1175/JCLI-D-16-0742.1`.

Grimm, A. M., 2019: Madden-Julian Oscillation impacts on South American summer monsoon season: precipitation anomalies, extreme events, teleconnections, and role in the MJO cycle. *Climate Dynamics*, **53 (1-2)**, 907–932, doi:{10.1007/s00382-019-04622-6}.

Hagos, S., et al., 2010: Estimates of tropical diabatic heating profiles: Commonalities and uncertainties. *Journal of Climate*, **23 (3)**, 542–558, doi:10.1175/2009JCLI3025.1, URL `https://doi.org/10.1175/2009JCLI3025.1`.

Hannachi, A., D. M. Straus, C. L. E. Franzke, S. Corti, and T. Woollings, 2017: Low-frequency nonlinearity and regime behavior in the Northern Hemisphere extratropical atmosphere. *Reviews Of Geophysics*, **55 (1)**, 199–234, doi:{10.1002/2015RG000509}.

Henderson, S. A. and E. D. Maloney, 2018: The impact of the Madden–Julian Oscillation on high-latitude winter blocking during El Niño–Southern Oscillation events. *Journal of Climate*, **31 (13)**, 5293–5318, doi:10.1175/JCLI-D-17-0721.1, URL `https://doi.org/10.1175/JCLI-D-17-0721.1`.

Henderson, S. A., E. D. Maloney, and E. A. Barnes, 2016: The influence of the Madden–Julian Oscillation on northern hemisphere winter blocking. *Journal of Climate*, **29 (12)**, 4597–4616, doi:10.1175/JCLI-D-15-0502.1, URL `https://doi.org/10.1175/JCLI-D-15-0502.1`.

Huang, F., X. Tang, S. Y. Lou, and C. Lu, 2007: Evolution of dipole-type blocking life cycles: Analytical diagnoses and observations. *Journal of the Atmospheric Sciences*, **64 (1)**, 52–73, doi:10.1175/JAS3819.1, URL `https://doi.org/10.1175/JAS3819.1`.

Itoh, H. and M. Kimoto, 1996: Multiple attractors and chaotic itinerancy in a quasi-geostrophic model with realistic topography: Implications for weather regimes and low-frequency variability. *Journal of the Atmospheric Sciences*, **53 (15)**, 2217–2231, doi:10.1175/1520-0469(1996)053⟨2217:MAACII⟩2.0.CO;2, URL `https://doi.org/10.1175/1520-0469(1996)053<2217:MAACII>2.0.CO;2`.

Kimoto, M. and M. Ghil, 1993: Multiple flow regimes in the northern-hemisphere winter .1. methodology and hemispheric regimes. *Journal Of The Atmospheric Sciences*, **50 (16)**, 2625–2643, doi:{10.1175/1520-0469(1993)050⟨2625:MFRITN⟩2.0.CO;2}.

Lin, H., G. Brunet, and J. Derome, 2009: An observed connection between the north atlantic oscillation and the madden–julian oscillation. *Journal of Climate*, **22 (2)**, 364–380, doi:10.1175/2008JCLI2515.1, URL `https://doi.org/10.1175/2008JCLI2515.1`.

Luo, D. and J. Cha, 2012: The North Atlantic Oscillation and the north atlantic jet variability: Precursors to NAO regimes and transitions. *Journal of the Atmospheric Sciences*, **69 (12)**, 3763–3787, doi:10.1175/JAS-D-12-098.1, URL `https://doi.org/10.1175/JAS-D-12-098.1`.

Ma, J. and X. San Liang, 2017: Multiscale dynamical processes underlying the wintertime atlantic blockings. *Journal of the Atmospheric Sciences*, **74 (11)**, 3815–3831, doi:10.1175/JAS-D-16-0295.1, URL https://doi.org/10.1175/JAS-D-16-0295.1.

Madden, R. A. and P. R. Julian, 1971: Detection of a 40–50 day oscillation in the zonal wind in the tropical pacific. *Journal of the Atmospheric Sciences*, **28 (5)**, 702–708, doi:10.1175/1520-0469(1971)028⟨0702:DOADOI⟩2.0.CO;2, URL https://doi.org/10.1175/1520-0469(1971)028<0702:DOADOI>2.0.CO;2.

Messori, G., P. Davini, M. C. Alvarez-Castro, F. S. R. Pausata, P. Yiou, and R. Caballero, 2019: On the low-frequency variability of wintertime Euro-Atlantic planetary wave-breaking. *Climate Dynamics*, **52 (3-4)**, 2431–2450, doi:{10.1007/s00382-018-4373-2}.

Michel, C. and G. Rivière, 2011: The link between Rossby wave breakings and weather regime transitions. *Journal of the Atmospheric Sciences*, **68 (8)**, 1730–1748, doi:10.1175/2011JAS3635.1, URL https://doi.org/10.1175/2011JAS3635.1.

Michelangeli, P., R. Vautard, and B. Legras, 1995: Weather Regimes - Recurrence and Quasi Stationarity. *Journal Of The Atmospheric Sciences*, **52 (8)**, 1237–1256, doi:{10.1175/1520-0469(1995)052⟨1237:WRRAQS⟩2.0.CO;2}.

Michelangeli, P.-A. and R. Vautard, 1998: The dynamics of euro-atlantic blocking onsets. *Quarterly Journal of the Royal Meteorological Society*, **124 (548)**, 1045–1070, doi:10.1002/qj.49712454803, URL https://doi.org/10.1002/qj.49712454803.

Molteni, F., S. Tibaldi, and T. Palmer, 1990: Regimes in the wintertime circulation over northern extratropics .1. observational evidence. *Quarterly Journal Of The Royal Meteorological Society*, **116 (491, A)**, 31–67.

Nakamura, H., M. Nakamura, and J. L. Anderson, 1997: The role of high- and low-frequency dynamics in blocking formation. *Monthly Weather Review*, **125 (9)**, 2074–2093, doi:10.1175/1520-0493(1997)125⟨2074:TROHAL⟩2.0.CO;2, URL https://doi.org/10.1175/1520-0493(1997)125<2074:TROHAL>2.0.CO;2.

Namias, J., 1950: The index cycle and its role in the general circulation. *Journal of Meteorology*, **7 (2)**, 130–139, doi:10.1175/1520-0469(1950)007⟨0130:TICAIR⟩2.0.CO;2, URL `https://doi.org/10.1175/1520-0469(1950)007<0130:TICAIR>2.0.CO;2`.

Plaut, G. and E. Simonnet, 2001: Large-scale circulation classification, weather regimes, and local climate over France, the Alps and Western Europe. *Climate Research*, **17 (3)**, 303–324, doi:{10.3354/cr017303}.

Rayner, N., D. Parker, E. Horton, C. Folland, L. Alexander, D. Rowell, E. Kent, and A. Kaplan, 2003: Global analyses of sea surface temperature, sea ice, and night marine air temperature since the late nineteenth century. *Journal Of Geophysical Research-Atmospheres*, **108 (D14)**, doi:{10.1029/2002JD002670}.

Rex, D. F., 1950: Blocking action in the middle troposphere and its effect upon regional climate. *Tellus*, **2 (4)**, 275–301, doi:10.1111/j.2153-3490.1950.tb00339.x, URL `https://doi.org/10.1111/j.2153-3490.1950.tb00339.x`.

Rivière, G. and I. Orlanski, 2007: Characteristics of the atlantic storm-track eddy activity and its relation with the north atlantic oscillation. *Journal of the Atmospheric Sciences*, **64 (2)**, 241–266, doi:10.1175/JAS3850.1, URL `https://doi.org/10.1175/JAS3850.1`.

Robertson, A. and M. Ghil, 1999: Large-scale weather regimes and local climate over the western United States. *Journal Of Climate*, **12 (6)**, 1796–1813, doi:{10.1175/1520-0442(1999)012⟨1796:LSWRAL⟩2.0.CO;2}.

Sardeshmukh, P. and B. Hoskins, 1988: The generation of global rotational flow by steady idealized tropical divergence. *Journal Of The Atmospheric Sciences*, **45 (7)**, 1228–1251, doi:{10.1175/1520-0469(1988)045⟨1228:TGOGRF⟩2.0.CO;2}.

Song, J., 2016: Understanding anomalous eddy vorticity forcing in North Atlantic Oscillation events. *Journal of the Atmospheric Sciences*, **73 (8)**, 2985–3007, doi:10.1175/JAS-D-15-0253.1, URL `https://doi.org/10.1175/JAS-D-15-0253.1`.

Stan, C., D. Straus, J. S. Frederiksen, H. Lin, E. D. Maloney, and C. Schumacher, 2017: Review of tropicalextratropical teleconnections on intraseasonal time scales. *Reviews of Geophysics*, **55**, doi:10.1002/2016rg000538.

Straus, D., F. Molteni, and C. S, 2017: *The Link between Weather and the Large Scale Circulation, in Nonlinear and Stochastic Climate Dynamics*, 105–135. Cambridge University Press.

Straus, D. M., 1983: On the role of the seasonal cycle. *Journal of the Atmospheric Sciences*, **40 (2)**, 303–313, doi:{10.1175/1520-0469(1983)040⟨0303:OTROTS⟩2.0.CO;2}.

Straus, D. M., 2010: Synoptic-eddy feedbacks and circulation regime analysis. *Monthly Weather Review*, **138 (11)**, 4026–4034, doi:10.1175/2010MWR3333.1, URL https://doi.org/10.1175/2010MWR3333.1.

Straus, D. M., S. Corti, and F. Molteni, 2007: Circulation regimes: Chaotic variability versus sst-forced predictability. *Journal of Climate*, **20 (10)**, 2251–2272, doi:10.1175/JCLI4070.1, URL https://doi.org/10.1175/JCLI4070.1, https://doi.org/10.1175/JCLI4070.1.

Straus, D. M. and R. S. Lindzen, 2000: Planetary-scale baroclinic instability and the mjo. *Journal of the Atmospheric Sciences*, **57 (21)**, 3609–3626, doi:10.1175/1520-0469(2000)057⟨3609:PSBIAT⟩2.0.CO;2, URL https://doi.org/10.1175/1520-0469(2000)057<3609:PSBIAT>2.0.CO;2.

Straus, D. M. and F. Molteni, 2004: Circulation regimes and sst forcing: Results from large gcm ensembles. *Journal of Climate*, **17 (8)**, 1641–1656, doi:10.1175/1520-0442(2004)017⟨1641:CRASFR⟩2.0.CO;2, URL https://doi.org/10.1175/1520-0442(2004)017<1641:CRASFR>2.0.CO;2.

Straus, D. M., E. Swenson, and C.-L. Lappen, 2015: The MJO cycle forcing of the north atlantic circulation: Intervention experiments with the community earth system model.

Journal of the Atmospheric Sciences, **72 (2)**, 660–681, doi:10.1175/JAS-D-14-0145.1, URL `https://doi.org/10.1175/JAS-D-14-0145.1`.

Swenson, E. T. and D. M. Straus, 2015: Transient Tropical Diabatic Heating and the Seasonal-Mean Response to ENSO. *Journal of the Atmospheric Sciences*, **72 (5)**, 1891–1907, doi:10.1175/JAS-D-14-0162.1, URL `https://doi.org/10.1175/JAS-D-14-0162.1`.

Swenson, E. T. and D. M. Straus, 2017: Rossby Wave Breaking and Transient Eddy Forcing during Euro-Atlantic Circulation Regimes. *Journal Of The Atmospheric Sciences*, **74 (6)**, 1735–1755, doi:{10.1175/JAS-D-16-0263.1}.

Takaya, K. and H. Nakamura, 2001: A Formulation of a Phase-Independent Wave-Activity Flux for Stationary and Migratory Quasigeostrophic Eddies on a Zonally Varying Basic Flow. *Journal of the Atmospheric Sciences*, **58 (6)**, 608–627, doi:10.1175/1520-0469(2001)058⟨0608:AFOAPI⟩2.0.CO;2, URL `https://doi.org/10.1175/1520-0469(2001)058<0608:AFOAPI>2.0.CO;2`.

Vautard, R., 1990: Multiple weather regimes over the north-atlantic - analysis of precursors and successors. *Monthly Weather Review*, **118 (10)**, 2056–2081, doi:{10.1175/1520-0493(1990)118⟨2056:MWROTN⟩2.0.CO;2}.

Walker, G. and E. Bliss, 1932: World weather v. *Memoirs of the Royal Meteorological Society*, **36 (4)**, 53–84.

Wallace, J. M. and D. S. Gutzler, 1981: Teleconnections in the geopotential height field during the northern hemisphere winter. *Monthly Weather Review*, **109 (4)**, 784–812, doi:10.1175/1520-0493(1981)109⟨0784:TITGHF⟩2.0.CO;2, URL `https://doi.org/10.1175/1520-0493(1981)109<0784:TITGHF>2.0.CO;2`.

Wheeler, M. and H. Hendon, 2004: An all-season real-time multivariate MJO index: Development of an index for monitoring and prediction. *Monthly Weather Review*, **132 (8)**, 1917–1932, doi:{10.1175/1520-0493(2004)132⟨1917:AARMMI⟩2.0.CO;2}.

Woollings, T., A. Hannachi, and B. Hoskins, 2010: Variability of the north atlantic eddy-driven jet stream. *Quarterly Journal of the Royal Meteorological Society*, **136 (649, B)**, 856–868, doi:{10.1002/qj.625}.

Yadav, P. and D. M. Straus, 2017: Circulation response to fast and slow MJO episodes. *Monthly Weather Review*, **145 (5)**, 1577–1596, doi:10.1175/MWR-D-16-0352.1, URL `https://doi.org/10.1175/MWR-D-16-0352.1`, `https://doi.org/10.1175/MWR-D-16-0352.1`.

Yadav, P., D. M. Straus, and E. Swenson, 2019: The euro-atlantic circulation response to the Madden-Julian Oscillation cycle of tropical heating: Coupled gcm intervention experiments. *Atmosphere-Ocean*.

Zhang, C., 2005: Madden-Julian Oscillation. *Reviews Of Geophysics*, **43 (2)**, doi:{10.1029/2004RG000158}.

Curriculum Vitae

Ralph Getzandanner is a 32 year veteran of the US Air Force Weather Service where he served in numerous positions and locations including multiple combat tours during Operations Desert Storm, Enduring Freedom, and Iraqi Freedom. He has numerous awards to include the Defense Meritorious Service Medal (2 oak leaf clusters) and the Bronze Star. Prior to his retirement, he served as the Weather Career Field Functional Manager for US Air Forces Europe. He was awarded his Bachelor of Science degree from the University of South Carolina in 1992 and a Masters of Science Degree in Atmospheric Science from Creighton University in 1996. In fall of 2014, he came to George Mason University to pursue a Ph.D. degree in Climate Dynamics under the guidance of Dr. David M. Straus.